The Webb Deep-Sky Society

Double Star Section Circular No 29

Contents

Editorial

Micrometric measurements of double stars in 2020 ..... page 1
Jean-François Courtot

Micrometric measures of double stars 2020.10 to 2020.90 ..... page 7
Andreas Alzner

Description of a CCD astrometric double star survey system ..... page 14
Ken Sturrock

Astronomical Association of Queensland 2020 programme: Blue Star Observatory measurement of nine neglected southern multiple stars ..... page 33
Peter N. Culshaw, Diane Hughes, John Hughes, Des Janke & Graeme Jenkinson

Astronomical Association of Queensland 2020 programme: Blue Star Observatory measurement of ten neglected southern multiple stars ..... page 40
Peter N. Culshaw, Diane Hughes, John Hughes, Des Janke & Graeme Jenkinson

CMOS Astrometry of double stars in 2020 ..... page 47
Grant Morris

Double star measurements 2020 ..... page 49
Wilfried Knapp

Observation of neglected double stars - 2 ..... page 61
André Debackère

Observation of double stars with robotic telescopes in 2019/20 ..... page 68
André Debackère

Index of previous Circulars ..... page 72

This circular has been edited and arranged by R.W.Argyle, Director of the Webb Society Double Star Section.
E-mail: `rwa@ast.cam.ac.uk`

On-line copies of Double Star Section Circulars Nos 1 to 28 are available on the following website:
`http://www.webbdeepsky.com/`

In case of difficulty, contact the Webb Society Webmaster, James Whinfrey
E-mail: `james.whinfrey@gmail.com`

For further information about the Webb Society contact:

In the USA and Canada: J. E. Isles, 10575 Darrel Drive, Hanover, Michigan 49241, U.S.A.
E-mail: `j_isles@yahoo.com`

In the UK: D. J. Miles, 10 Rosewood Gardens, Clanfield, Waterlooville, Hampshire, PO8 0LT, England.
E-mail: `donjmiles@googlemail.com`

Editorial

The number of measures included in these Circulars is now 85868.

Observer	WDS code	Pairs	Measures	Method/source
Astro. Assoc. Queensland	AAQ	19	133	CCD imaging
A. Alzner	ALZ	58	128	Lyot Micrometer
J.- F. Courtot	CTT	52	169	RETEL, homemade filar, Lyot micrometer
A. Debackère	DBR	18	19	Internet astrometry
W. Knapp	KPP	152	152	Internet astrometry
G. Morris	GRM	29	106	CMOS astrometry
K. Sturrock	-	123	234	CCD imaging
TOTALS		451	941	

Bob Argyle, 2021 July

Useful sites

The following websites also contain a considerable amount of interesting material for the serious double star observer and no claim is made for the completeness of the list. If anyone knows of any others please contact me:

The Washington Double Star catalogue - the complete reference for visual double stars - updated nightly. The site also contains the Sixth Catalogue of Visual Binary Star Orbits and much more at `http://www.astro.gsu.edu`

Journal for Double Star Observations (`www.jdso.org`)

Etoiles Doubles (in French)
A newly established on-line journal and freely available from `www.etoilesdoubles.org`

Lettre de la Commission des Etoiles Doubles (in French)
A newly established on-line journal. To receive copies contact `wallaert_chatillon@hotmail.com`

El Observador de Estrellas Dobles (in Spanish)
(`www.elobservadordeestrellasdobles.wordpress.com`)

Observatori Astronòmic del Garraf (`www.oagarraf.net`)

Il Bollettino delle Stelle Doppie (in Italian)
(`https://sites.google.com/site/ilbollettinodellestelledoppie/`)

In addition the Stelle Doppie Double Star Database run by Gianluca Sordiglioni allows the WDS catalogue to be quizzed with various search parameters. You can get a user name and password at `stelledoppie.goaction.it`

Acknowledgements

Much of the work presented here has made use of the Washington Double Star Catalogue maintained at the U.S. Naval Observatory. The USNO website remains unavailable at the time of press and users are directed to the mirror website at Georgia State University - see the address above.

MICROMETRIC MEASURES OF DOUBLE STARS IN 2020

Jean−François Courtot, Chaumont, France

Introduction

The measurements presented here have been made during 2020 using two different telescopes: a homemade 205-mm (8-inch) Newtonian and either a Retel filar micrometer at a power of x508 or a Lyot double-image micrometer at x 464, and a 279-mm (11-inch) Schmidt-Cassegrain telescope at x 430 up to x 640 with different homemade filar micrometers[1] (Fig.1). A homemade double-image micrometer (Fig.2) has also been completed and tested with the 11-inch, mostly at x 614 for this series, allowing measurements down to 0".37 (STF1937AB) when conditions allowed.

The measurement procedures have been outlined in previous circular DSSC 23[2]. Further indications on some observed peculiarities with double-image micrometers can also be found in DSSC 24-25[3,4].

Measurements have been arranged as usual in Table 1. Epochs are in Julian years. In last column, "T205" denotes the 205-mm Newtonian telescope, "C11" the 11-inch Schmidt-Cassegrain, "L" is for the Lyot double-image micrometers whilst "F" indicates that a filar micrometer has been used. Table 2 gives a short comment on each measured pair.

As usual also, besides known orbital pairs, some other pairs have been measured. When available, proper motions, parallaxes, luminosity and radial velocities data have been used to investigate the true nature of the observed pairs using Dommanget's criteria[5,6]. The followed procedure can be found in DSSC 28[7]. Most pairs observed for this series which are described in Argyle *et al.*[8], needed astrometric and physical data from this same source as well. Of possible interest here, the case of Albireo, STFA43AB, WDS J19307+2758AB, likely not an orbital pair (Table 3 and Ref. 8, p. 389).

For known observed orbital pairs, residuals O-C with recently computed orbits are to be found in Table 3.

Figure 1: Homemade filar micrometers for the 11-inch telescope

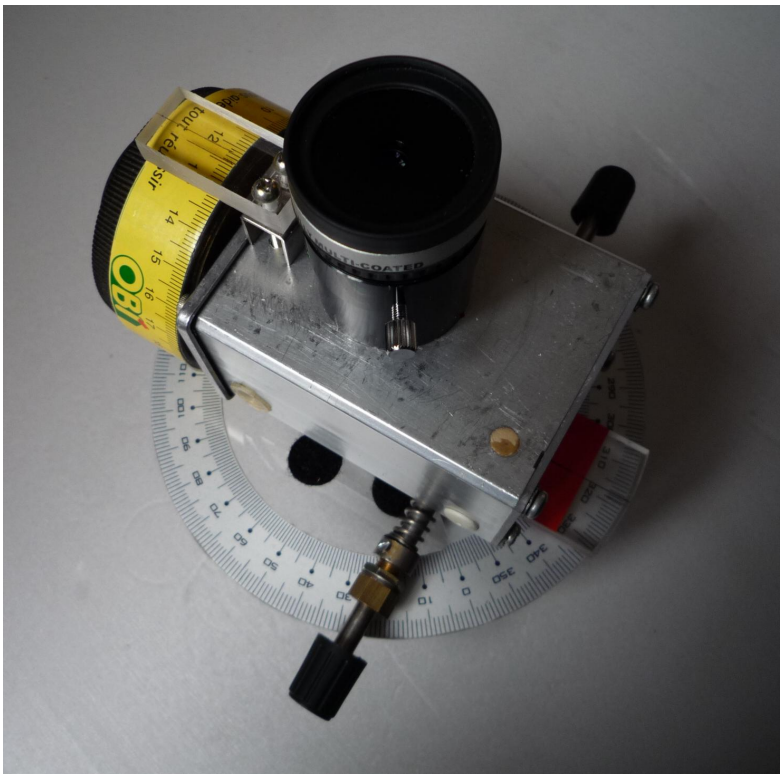

Figure 2: Homemade double-image micrometer

Table1 - Measures

Pair	Comp	RA	Dec	V_a	V_b	PA (°)	Sep (″)	Epoch (Julian)	N	Obs.	Method
STF162	AB	01493	+4754	6.5	7.2	198.8	1.96	2020.052	4	CTT	T205/L
STF162	AC	01493	+4754	6.5	9.2	178.4	20.68	2020.063	2	CTT	T205/F
STF333	AB	02592	+2120	5.2	5.6	209.7	1.39	2020.099	3	CTT	T205/F
STT82	AB	04227	+1303	7.3	8.6	326.9	1.19	2020.056	3	CTT	T205 /L+F
D4	AB	04404	+5328	9.0	10.3	265.6	6.03	2020.099	3	CTT	T205/F
STF668	A-BC	05145	−0812	0.3	6.8	202.4	9.17	2020.121	3	CTT	T205/F
BU1008		06149	+2230	3.5	6.2	257.9	1.80	2020.166	4	CTT	T205/F+L
STF881	AB	06221	+5922	6.1	7.7	148.8	0.66	2020.231	4	CTT	C11/L
STF948	AB	06462	+5927	5.4	6.0	64.8	1.94	2020.213	4	CTT	T205/L+C11/L
STF1110	AB	07346	+3153	1.9	3.0	51.3	5.24	2020.245	4	CTT	T205/F+L+C11/F
STF1110	AC	07346	+3153	1.9	9.8	163.5	71.56	2020.254	5	CTT	T205/F+C11/F
STF1110	BC	07346	+3153	3.0	9.8	168.1	73.81	2020.257	3	CTT	T205/F+C11/F
STF1268		08467	+2846	4.1	6.	307.4	31.28	2020.256	3	CTT	T205/F+C11/F
STF1306	AB	09104	+6708	4.9	8.9	346.3	4.35	2020.291	3	CTT	C11/F
STF1338	AB	09210	+3811	6.7	7.1	314.4	1.21	2020.214	3	CTT	T205/L+C11/L
STF1356		09285	+0903	5.7	7.3	114.1	1.02	2020.269	3	CTT	T205/L+F+C11/L
STF1424	AB	10200	+1950	2.4	3.6	126.9	4.73	2020.275	4	CTT	T205/L+F+C11/F
STF1487		10556	+2445	4.5	6.3	111.5	6.56	2020.303	4	CTT	T205/L+C11/
HO378	AB	11050	+3825	8.3	9.1	233.9	1.06	2020.356	4	CTT	C11 L+F+L
STF1523	AB	11182	+3132	4.3	4.8	151.5	2.31	2020.326	4	CTT	T205/L+F+C11/L+F
STF1527		11190	+1416	7.0	8.0	301.1	0.45	2020.369	3	CTT	C11/L
STF1692	AB	12560	+3819	2.9	5.5	228.7	19.36	2020.401	3	CTT	C11/F+T205/F
STF1695	AB	12563	+5406	6.0	7.8	279.7	3.73	2020.387	4	CTT	C11/F+T205/F
STF1728	AB	13100	+1732	4.9	5.5	194.6	0.46	2020.408	4	CTT	C11/L

BU800	AB	13169	+1701	6.7	9.5	104.1	7.65	2020.417	3	CTT	C11/F
STF1744	AB	13239	+5456	2.2	3.9	153.4	14.61	2020.463	3	CTT	C11/F
STF1768	AB	13375	+3618	5.0	7.0	94.5	1.62	2020.467	4	CTT	C11/F
STF1877	AB	14450	+2704	2.6	4.8	346.6	2.88	2020.480	3	CTT	C11/F
STF1937	AB	15232	+3017	5.6	6.0	287.3	0.37	2020.488	3	CTT	C11/F
STF1938	Ba-Bb	15245	+3723	7.1	7.6	2.1	2.20	2020.506	4	CTT	C11/F
STFA28	AB	15245	+3723	4.3	7.1	170.8	109.17	2020.516	3	CTT	C11/F
STF2032	AB	16147	+3352	5.6	6.5	239.1	7.38	2020.524	4	CTT	C11/F
STF2032	AD	16147	+3352	5.6	10.8	81.9	95.57	2020.526	3	CTT	C11/F
STF2130	AB	17053	+5428	5.7	5.7	358.0	2.49	2020.547	4	CTT	C11/F
STF2140	AB	17146	+1423	3.5	5.4	104.2	4.79	2020.593	4	CTT	C11/F
STF3127	AB	17150	+2450	3.1	8.3	291.4	13.81	2020.601	3	CTT	C11/F+T205/F
STF2264		18015	+2136	4.9	5.2	255.1	6.39	2020.659	4	CTT	C11/F+T205/F
STF2323	AB	18239	+5848	5.1	8.1	347.5	3.55	2020.686	4	CTT	C11/F
STF2323	AC	18239	+5848	5.1	8.0	19.5	88.86	2020.686	4	CTT	C11/F
STF2398	AB	18428	+5938	9.1	10.0	180.8	11.40	2020.659	4	CTT	C11/F+T205/F
STFA43	AB	19307	+2728	3.2	4.7	53.6	34.89	2020.672	4	CTT	C11/F+T205/F
STF2579	AB	19450	+4508	2.9	6.3	212.6	2.74	2020.705	4	CTT	C11/F
STT395		20020	+2456	5.8	6.2	123.8	0.86	2020.703	5	CTT	C11/F+L
STF2637	AB	20099	+2055	6.6	8.9	331.0	11.55	2020.691	3	CTT	C11/F
STF2637	AC	20099	+2055	6.6	7.5	221.6	91.93	2020.692	3	CTT	C11/F
STF2727	AB	20467	+1607	4.4	5.0	265.5	8.88	2020.727	4	CTT	C11/F+T205/F
H 1 48		21137	+6424	7.2	7.3	245.5	0.77	2020.766	4	CTT	C11/F+T205/F+L
STF2822	AB	21441	+2845	4.8	6.2	324.9	1.59	2020.871	4	CTT	T205/L
STF2863	AB	22038	+6438	4.5	6.4	274.4	8.06	2020.898	4	CTT	C11/F+T205/L
SHJ345	AB	22266	−1645	6.3	6.4	93.5	1.23	2020.833	5	CTT	T205/L
STF2909	AB	22288	−0001	4.3	4.5	157.8	2.19	2020.969	4	CTT	T205/F
STF2922	AB	22359	+3938	5.7	6.3	185.5	22.48	2020.920	3	CTT	T205/F

Table 2 - Notes

Pair	ADS	Notes
STF162AB	1438	Retrograde relative motion: 26° in 184 yrs. Separation without any noticeable change. No GAIA−DR2 luminosity data for A component. J. Dommanget's criteria undetermined.
STF162AC	1438	Nearly fixed since W. Struve. Starting from 1836.75 measurement (179°.5 / 20″.36), the effect of DR2 similar proper motions give for 2020.063: 181° / 21″.46 (observed: 178°.4 / 20″.68). No DR2 luminosity data for A. No radial velocity. Similar parallaxes. Dommanget criteria undetermined.
STF333AB	2257	ϵ Ari. Orbital pair. Direct relative motion: 20° in 190 yrs. Getting wider: +0″.8. No complete DR2 data.
STT82AB	3169	Orbital pair. Retrograde relative motion: 264° in 172 yrs. Getting closer. No DR2 luminosity data for B. Relative position from DR2 equatorial coordinates in 2015.5: 342°.5 / 1″.36 (WSI Orbit: 331°.2 / 1″.21).
D4AB	3365	No noticeable motion since Dembowski (1870). Similar DR2 parallaxes and proper motions. Using Dembowski and DR2 somewhat different relative positions, first Dommanget Criterion: 5″.9, the same order than observed separation. No DR2 radial velocity data: second Dommanget Criterion undetermined.
STF668A−BC	3823	Rigel: nearly fixed since W. Struve (1831). No DR2 data for A.
BU1008	4841	η Gem. Retrograde relative motion: 44° in 138 yrs. Getting wider: +0″.8. No DR2 data for secondary. Dommanget's criteria undetermined.

STF881AB	4950	4 Lyn. Orbital pair. Direct relative motion: 58° in 190 yrs.
STF948AB	5400	Orbital pair. Retrograde relative motion: 91° in 188 yrs. Getting slightly wider: +0″.4.
STF1110AB	6175	Castor: long period orbital pair. Retrograde relative motion: 212° in 194 yrs.
STF1110AC	6175	No noticeable rotation since W. Struve (1835). Getting slightly closer: - 1″ . Too small displacement to determine first Dommanget criterion. Barycenter of AB determined using mass-luminosity relation for O-C residuals with Kiyaeva's preliminary orbits.
STF1110BC	6175	Third side of ABC triangle. Using measurements of this series: sinA/a = 0.013 , sinB/b = 0.012 , sinC/c = 0.015.
STF1268	6988	ι Cnc. Nearly fixed since W. Struve (displacement 1″ or so since 1828). If DR2 radial velocities reliable (15.74 & 25.00 km/s), second Dommanget criterion amounts to only: 1″.2 (measured separation: 31″.3) meaning that although parallaxes and proper motions are similar, this pair cannot be a periodic system.
STF1306AB	7203	Long period orbital pair. Retrograde relative motion: 279° in 188 yrs.
STF1338AB	7307	Orbital pair. Direct relative motion: 192° in 191 yrs.
STF1356	7390	ω Leo. Second revolution since W. Struve. Clearly split with gap using the T205 Newtonian.
STF1424AB	7724	γ Leo. Long period orbital pair. Direct relative motion: 23° in 189 yrs. Getting wider: +1″ .
STF1487	7979	54 Leo. Very slow direct relative motion: 8° in 190 years. First Dommanget criterion: 39″ , second criterion: 77″ . Actual measured separation 6″.6, so possibly an orbital pair.
HO378AB	8047	Direct relative motion: 15° in 129 yrs. Getting wider: +0″.7.
STF1523AB	8119	Orbital pair. Retrograde relative motion. Over 3 complete revolutions since W. Struve.
STF1527	8128	Orbital pair, direct relative motion: 291° in 191 yrs. Getting wider. Figure-of-8 shaped, no gap using the C11.
STF1692AB	8706	Very slow retrograde motion: 5° in 243 yrs. Getting closer. Using W. Herschel's 1777 measurement, first Dommanget's criterion: 44″ . Second criterion: 18″ (measured: 19″). Physical or optical status presently undetermined.
STF1695AB	8710	Very slow retrograde relative motion: 9° in 188 yrs. Getting wider: +0″.5.
STF1728AB	8804	Orbital pair. Orbital inclination is near 90° . Presently getting closer. Figure-of-eight shape with no complete gap using the C11.
BU800AB	8841	Retrograde relative motion: 17° in 139 years. Getting wider: +6″.4.
STF1744AB	8891	ζ UMa, Mizar, direct relative motion: 7° in 190 years. Getting slightly wider. Starting from W. Struve's measurement in 1830, first Dommanget criterion: 322″ . Measured separation: 15″ . Possibly an orbital pair.
STF1768AB	8974	Orbital pair. Retrograde relative motion: 341° in 189 years. Getting closer.
STF1877AB	9372	Slow direct relative motion: 26° in 191 years. Getting slightly wider: +0″.2. First Dommanget criterion: 42″ (current measured separation: 2″.9). Possibly a long period orbital pair. A: yellow, B: blue. Important magnitude and colour contrast.
STF1937AB	9617	Single elongated diffraction image using the C11. Orbital pair. 5th revolution since W. Struve (1826). Getting wider.
STF1938BaBb	9626	Long period orbital pair. Retrograde relative motion: 324° in 194 yrs. Getting closer.
STFA28AB	9626	Nearly fixed since W. Struve (1834).
STF2032AB	9979	Long period orbital pair. Direct relative motion: 151° in 193 yrs. Getting wider.
STF2032AD	9979	Optical pair. Starting from W. Struve's 1836 measurement (88°.8/43″.75), the effect of proper motions mentioned in WDS gives for 2020.53: 80°.8/96″.3. Measured: 81°.9/95″.6.
STF2130AB	10345	Long period orbital pair. Retrograde relative motion: 208° in 192 yrs.
STF2140AB	10418	α Her. Very long period orbital pair. Retrograde relative motion: 13° in 191 yrs. No DR2 data for A.
STF3127AB	10424	δ Her. First Dommanget' criterion: 0″.16, in good agreement with second criterion determined after radial velocities: 0″.13. Current measured separation: 13″.8, well beyond the limit for a periodic motion. Optical pair. Residuals from Hartkopf's linear ephemeris: −1°.9 ; −0″.17.
STF2264	10993	Very slow retrograde relative motion: 6° in 191 yrs. Separation without any noticeable change. Starting from Struve' measurement (1829.90: 261°.7/6″.06), first Dommanget criterion: 20″ . Current measured separation: 6″.4, so possibly an orbital pair. Observed colours: A: light blue, B: yellow/orange (gold).
STF2323AB	11336	Orbital pair. Retrograde relative motion: 16° in 197 yrs.
STF2323AC	11336	Nearly fixed since W. Struve (1834).
STF2398AB	11632	Orbital pair. Direct relative motion: 49° in 188 yrs. Getting closer: −1″ .

STFA43AB	12540	Albireo, β Cyg. Starting from Bradley's measurement (1755: 58° /34″.6), first Dommanget criterion: 7″.7. Second Dommanget criterion: 4″.2. Both of the same order and much less than current observed separation (34″.9). So, if used data reliable, STFA43AB cannot be an orbital pair.
STF2579AB	12880	Orbital pair. Retrograde relative motion: 176° in 190 yrs.
STT395	13277	Orbital pair. Direct relative motion: 225° in 176 yrs.
STF2637AB	13442	Slow direct relative motion: 5° in 188 yrs. Separation without any noticeable change. First Dommanget criterion: 52″ . Current measured separation: 12″ . Possibly an orbital pair.
STF2637AC	13442	Apparent relative displacement: 22″ in 188 yrs due to much differing proper motions. First Dommanget criterion: 0″.1. Current measured separation: 92″ . Clearly an optical pair.
STF2727AB	14279	γ Del. Orbital pair. Very slow retrograde relative motion: 13° in 265 yrs (Bradley). Getting closer: −3″ . First Dommanget criterion: 24″ . Second criterion: 81″ . A: golden-yellow, B: pale azure.
H1-48	14783	Orbital pair. Completing its third revolution since Herschel's discovery (1782). Currently getting wider.
STF2822AB	15270	Orbital pair. Direct relative motion: 217° in 240 yrs. Currently getting closer.
STF2863AB	15600	Long period orbital pair. Retrograde relative motion: 14° in 241 years.
SHJ345AB	15934	Long period orbital pair. Direct relative motion: 151° in 197 years. Near periastron.
STF2909AB	15971	ζ Aqr. Long period orbital pair. Retrograde relative motion: 202° in 195 yrs. Getting wider.
STF2922AB	16095	Nearly fixed since W. Struve (1831). Distance reported by Herschel in 1782 probably erroneous (17″.2). From Struve's 1831 measurement (185°.7/22″.47), first Dommanget criterion: 13″.3. Second Dommanget criterion: 77″.5. Presently undetermined status.

Table 3 - Residuals from known orbits

Pair	Comp	ADS	Residual(O-C) PA(°)	Sep (″)	Orbit	Date	Grade	Period (years)
STF333	AB	2257	−0°.4	+0″.08	Rica Romero	2012	4	1216
STT82	AB	3169	+0°.1	+0″.02	W.S.I.	2004	3	241
BU1008		4841	+6°.5	+0″.19	Baize	1980	5	474
STF881	AB	4950	−1°.6	+0″.04	Zirm	2013	4	503
STF948	AB	5400	0°.0	+0″.02	W.S.I.	2006	4	908
STF1110	AB	6175	−0°.6	−0″.15	Docobo	2014	3	460
STF1110	AB-C	6175	−2°.8	0.″00	Kiyaeva	2015	5	18700
			−0°.7	+1″.58				13500
			−3°.6	+2″.16				12800
STF1306	AB	7203	+0°.1	−0″.15	Scardia	2015	4	970
STF1338	AB	7307	−7°.8	+0″.21	Scardia	2002	3	303
STF1356		7390	−1°.0	+0″.10	van Dessel	1976	2	118
			−0°.7	+0″.13	Muterspaugh	2010	2	118
STF1424	AB	7724	+0°.4	+0″.25	Rabe	1958	4	619
			−0°.6	−0″.02	Pulkova Obs	2014	4	554
STF1523	AB	8119	+0°.3	+0″.09	Mason	1995	1	60
STF1527		8128	−1°.1	−0″.01	Tokovinin	2012	3	415
STF1728	AB	8804	+2°.7	0″.00	Muterspaugh	2015	1	26
STF1768	AB	8974	+1°.0	−0″.03	Soderhjelm	1999	3	228
STF1937	AB	9617	−5°.3	+0″.01	Muterspaugh	2010	1	42
STF1938	BaBb	9626	−0°.3	−0″.04	Kiyaeva	2014	2	265
STF2032	AB	9979	0°.0	+0″.12	Raghavan	2009	4	726
STF2130	AB	10345	+0°.1	−0″.12	Prieur	2012	4	812
STF2140	AB	10418	+1°.6	+0″.15	Baize	1978	4	3600
STF2323	AB	11336	−0°.4	−0″.19	Novakovic	2006	5	3963

STF2398	AB	11632	−1°.6	+0″.50	Heintz	1987	4	408
STF2579	AB	12880	−2°.4	−0″.03	Scardia	2012	4	918
STT395		13277	−3°.9	+0″.01	Zirm	2013	4	1201
STF2727	AB	14279	+0°.8	+0″.02	Hale	1994	4	3249
H1-48		14783	+1°.2	−0″.05	Hartkopf	2014	3	82
STF2822	AB	15270	−2°.6	+0″.15	Heintz	1995	4	789
STF2863	AB	15600	+1°.0	−0″.41	Zeller	1965	5	3800
SHJ345	AB	15934	+8°.5	−0″.12	Hale	1994	4	3500
			+0°.7	−0″.01	Tokovinin	2020	4	2000
STF2909	AB	15971	−2°.1	−0″.37	Heintz	1984	4	760
			−0°.2	−0″.19	Scardia	2010	3	487
			+3°.7	−0″.19	Tokovinin	2016	3	540

References

1. Courtot, J.-F., 2017, *Webb Society Deep Sky Observer*, **177**, 16 sq.
2. Courtot, J.-F., 2015, *Webb Society Double Star Circulars*, **23**, 6 sq.
3. Courtot, J.-F., 2016, *Webb Society Double Star Circulars*, **24**, 6-7.
4. Courtot, J.-F., 2017, *Webb Society Double Star Circulars*, **25**, 16.
5. Dommanget, J., *Critère de non-périodicité du mouvement relatif d'un couple stellaire visuel*, *Bulletin Astronomique*, Paris 1955
6. Dommanget, J., Second *Critère de non-périodicité du mouvement relatif d'un couple stellaire visuel*, *Bulletin Astronomique*, Paris 1960.
7. Courtot, J.-F., 2020, *Webb Society Double Star Circulars*, **28**, 4 sq.
8. Argyle, R., Swan, M, James, A., *An Anthology of Visual Double Stars*, Cambridge University Press 2019.

Acknowledgements

Sincere thanks to Bob Argyle for arranging and editing this Circular and to our colleagues at the US Naval Observatory for maintaining the Washington Double Star Catalogue.

This work makes use also of results from the European Space Agency (ESA) space mission Gaia. Gaia data are being processed by the Gaia Data Processing and Analysis Consortium (DPAC). Funding for the DPAC is provided by national institutions, in particular the institutions participating in the Gaia MultiLateral Agreement (MLA).

The Gaia mission website is `https://www.cosmos.esa.int/gaia`.

The Gaia archive website is `https://archives.esac.esa.int/gaia`.

MICROMETER MEASURES OF DOUBLE STARS FROM 2020.10 TO 2020.90

Andreas Alzner, Zeckerner Hauptstrasse 3, 91334 Hemhofen, Germany

E-mail: aalzner@t-online.de

Results and Method

The total number of measurements is 128 of 58 double stars. Seven negative observations of five pairs were obtained. Most of the pairs are in orbital motion and about 50% were closer than 1″.0 at the time of the measurement. All measurements were obtained by using a 32.5-cm f19 Cassegrain sited in Hemhofen (latitude N49° 42′) close to Erlangen, Germany. The telescope was designed and constructed in 1996 by Peter Grosse, employee of Zeiss Jena.

The limit for clearly resolvable stars is 0″.40.

The following micrometer was used: a MECA PRECIS Double Image Micrometer with magnifications of 390x (only in some few cases for faint pairs), 490x, 620x, 690x, 930x. In most cases, the 620x magnification was applied. On each night, the distance and the PA each are set two to ten times (mostly four times). When the distance is less than about 0″.4, the distance is measured as well as estimated, and the final value is the mean value. Mostly, the difference between the two methods does not exceed 0″.05. Residuals were calculated for pairs with known orbits and the corrections for precession were taken into account. The measurements:

1. column: Name of star
2. column: Component
3. column: RA 2000
4. column: DEC 2000
5. column: estimated magnitude difference
6. column: PA(°)
7. column: Separation(″)
8. column: Epoch
9. column: number of nights
10. column: observer
11. column: note indicated

Observer: Andreas Alzner **Method:** 325mm Cassegrain, Double image micrometer

Pair	Comp	RA	Dec	Δm	PA(°)	Sep(″)	Epoch	N	Obs.	
STF73		0055.0	+2338	0.5	335.1	1.18	2020.90	2	ALZ	
MAD2		0100.6	+4719	1.0	0.3	0.88	2020.87	3	ALZ	
STT21		0103.0	+4723	1.1	176.1	1.32	2020.86	2	ALZ	
STF115		0123.4	+5809	0.3	155.7	0.48	2020.89	2	ALZ	
STT34		0149.9	+8053	0.3	293.1	0.54	2020.90	2	ALZ	note
STF186		0155.9	+0151	0.1	77.2	0.66	2020.84	2	ALZ	
STF185		0202.2	+7530	1.2	3.5	1.10	2020.88	1	ALZ	
STF216		0211.4	+6221		round		2020.88	1	ALZ	note
STT77		0415.9	+3142	0?	304.2	0.50	2020.10	1	ALZ	
STT79		0419.9	+1631	1.0	12.7	0.71	2020.10	1	ALZ	
STT82		0422.7	+1503	1.1	323.8	1.16	2020.10	2	ALZ	
STF554		0430.1	+1538	2.0	15.3	1.33	2020.10	1	ALZ	
STT98		0507.9	+0830	0.8	283.4	0.99	2020.11	3	ALZ	
WNC2	A-BC	0523.9	−0052	0.5	158.6	3.12	2020.13	1	ALZ	
STF694		0524.0	+2458	0.2	193.2	1.34	2020.10	1	ALZ	

BU1008		0614.9	+2230	3.0	258.9	1.70	2020.13	1	ALZ	
STT159		0657.3	+5825	1.2	236.7	0.71	2020.10	2	ALZ	
STT170		0717.6	+0918	0.3	282.7	0.60	2020.21	3	ALZ	
STF1110	AB	0734.6	+3153	0.9	53.2	5.36	2020.10	4	ALZ	
STT185		0757.3	+0108	0.0	22.2	0.43	2020.22	2	ALZ	
STF1187		0809.5	+3213	0.8	20.8	3.07	2020.27	2	ALZ	
STF1211		0818.3	+3859	-	161.5	0.37	2020.27	2	ALZ	note
VDK3		0850.7	+0752	0.5	198.9	1.00	2020.27	2	ALZ	
STF1280		0855.4	+7048	0.0	358.7	3.48	2020.28	2	ALZ	
HO369		0951.2	+3629	0.5?	284.4	0.29	2020.28	2	ALZ	
STT229		1048.0	+4107	0.3	255.6	0.66	2020.27	3	ALZ	
STF1523		1118.2	+3132	0.3	150.6	2.24	2020.27	2	ALZ	note
STF1527		1119.0	+1416	0.8	299.6	0.52	2020.28	4	ALZ	
STF1670		1241.7	−0127	0.0	356.5	2.90	2020.31	3	ALZ	
STF1687	AB	1253.3	+2114	2.0	202.8	1.20	2020.35	1	ALZ	
STF1711		1302.9	+1328		round		2020.35	1	ALZ	
COU11		1306.4	+2109	2.0	314.1	1.64	2020.35	1	ALZ	
STT261		1312.0	+3205	0.2	338.4	2.65	2020.35	1	ALZ	
STF1865		1441.1	+1344	-	277.6	0.22:	2020.48	2	ALZ	note
STF1909		1503.8	+4739	-	138:	0.22:	2020.48	1	ALZ	note
STF1937		1523.2	+3017	0.5	291.9	0.34	2020.48	2	ALZ	
STF1938	BC	1524.5	+3723	0.3	2.5	2.26	2020.48	2	ALZ	
STF2384		1838.4	+6708	0.5	306.9	0.36	2020.75	2	ALZ	note
BU648		1857.0	+3254	2.5	231.6	1.24	2020.76	2	ALZ	
KU2		1934.4	+7136		single		2020.75	1	ALZ	note
STF2592		1939.2	+7634	1.9	296.6	0.84	2020.76	2	ALZ	
STF2574		1940.6	+6240	0.3	273.8	0.61	2020.76	2	ALZ	
STT387		1948.7	+1148	0.5	94.4	0.47	2020.76	2	ALZ	
STT395		2002.2	+2456	0.4	127.0	0.77	2020.76	3,2	ALZ	
STF2695		2032.0	+2548	-	257.2	0.32	2020.76	2	ALZ	note
STT413		2047.4	+3629	1.1	359.6	0.98	2020.75	2	ALZ	
STF2737		2059.1	+0418		round		2020.76	2	ALZ	
STF2744		2103.1	+0132	0.4	106.9	1.21	2020.76	2	ALZ	
H 1 48		2113.7	+6424	0.2	246.1	0.80	2020.81	3	ALZ	
STT437		2120.8	+3227	0.3	18.7	2.45	2020.83	3	ALZ	
A764		2122.3	+5734	2	21.1	1.29	2020.80	2	ALZ	
STT442		2133.9	+6148		round		2020.83	2	ALZ	note
STF2822		2144.1	+2845	1.2	323.9	1.57	2020.78	4	ALZ	
STT464		2211.3	+4011	0.5?	189.5	0.36	2020.88	2	ALZ	
STF2924		2233.0	+6955	0.4?	232.5	0.33	2020.83	3	ALZ	note
STF2934		2241.9	+2126	1.2	55.2	1.40	2020.82	4	ALZ	note
STF2944		2247.8	−0414	0.6	307.4	1.85	2020.81	3	ALZ	
STF2950		2251.4	+6142	1.0	272.4	1.09	2020.86	3	ALZ	
STT483		2259.2	+1144	1.2?	30.6	0.43	2020.82	3	ALZ	
STT487		2301.2	+8047	1.1	18.9	0.47	2020.84	3	ALZ	note
STT489		2307.9	+7523	2.4	0.9	1.11	2020.87	3	ALZ	
STF3001		2318.6	+6807	2.6	223.3	3.36	2020.90	2	ALZ	
STF3050		2359.5	+3343	0.1	342.1	2.48	2020.84	3	ALZ	

Notes to individual stars

System	ADS	Notes
STT34	1411	First measurement since 2007. Large residual of 2020 measurement to the orbit given by Hartkopf in 2008 in the WDS catalog. Three orbits have been calculated since 1987: - Baize 1987 - Heintz 1997 - Hartkopf 2008. For all calculations, the early measurements 1843 - 1931 have been placed in the 2nd quadrant. The magnitude difference is reported as about 0.3 mag. Several observers like H. Struve (1889) and P. Fox (1912, 1915) gave the 4th quadrant. Baize favoured a short-period solution (P = 173.2), so the companion is now back at the discovery position. But the measurements in the last 30 years have confirmed the 4th quadrant (the magnitude difference was e.g. clearly visible in the 13-inch during the 2020 measurements, the pair being a rather easy target). Heintz prefers a long-period solution: 1843 - 1931 2nd quadrant, 1974 - 1997 4th quadrant. Hartkopf has chosen another approach, his orbit with a large semiaxis major predicting currently a rapid motion closing in. Since the latter solution is ruled out I have calculated two short period orbits A and B (Baize's approach, but quadrants reversed) and for comparison one long period orbit C following Heintz's solution 1997 (2nd quadrant 1843 - 1931, 4th quadrant 1974 - 2020). Among the three orbits from 1987, 1997 and 2008, Baize's solution from 1987 gives by far the lowest residuals not only for the new 2020 measurement given here but for the majority of all the other measurements. My results are as follows (nodes for epoch 2000): Orbit A (best fit, close to Baize 1987, but quadrants reversed, errors of orbital elements in brackets): P = 176.6(6.6), T = 1937.29(2.54), a = 0.395(0.048), e = 0.854(0.025), i = 44.5(9.0), omega = 105.8(8.7), node = 4.3(12.7). Orbit B (P and a fixed): P = 176.6, T = 1938.50, a = 0.350, e = 0.827, i = 34.2, omega = 292.3, node = 179.5 Orbit C: P=335.3, T=2025.9, a=0.618, e=0.188, i=72.5, omega=205.4, node=109.9 The resulting total masses in solar masses using the revised Hipparcos parallax 5.03±0.68 mas are as follows: - orbit A: 15.5, - orbit B: 10.8, - orbit C: 16.5. The sum of weighted and squared residuals for orbits A and B is about 2 times smaller than that for orbit C, i.e. C gives considerably larger residuals. Moreover, orbital elements of long period solutions are rather uncertain. As the spectral type for STT34 is A0V, the values for the total mass combining the orbital parameters P and a with the Hipparcos parallax are still very high. For Heintz' orbit (1997) a total mass of 14.28 results whereas Hartkopf's solution (2008) reveals a much higher value. Malkov et al (2012) give the same value for the dynamical mass of 14.28 (using Heintz' 1997 orbit and the Hipparcos-parallax), a photometric mass of 4.72 and a spectroscopic mass of 2.24.

Ephemerides for the new orbits A, B and C:

		A		B		C	
	2021.0	294°.1	0″.537	293°.6	0″.542	295°.3	0″.481
	2023.0	294°.9	0″.539	294°.4	0″.544	296°.4	0″.473
	2025.0	295°.7	0″.540	295°.2	0″.545	297°.5	0″.463

STF216	1682	Last positive measurement 2009
STF1211	6721	First positive measurement since 1994. Faint and difficult in the 13-inch. The companion is now back in the 2nd quadrant where it will remain for many years. Measurements with large telescopes are desirable.
STF1523	8119	AB: P = 59.878 (Mason 1995, grade 1) AB: P=59.84 (Heintz 1996, grade 1) Aa-A: P=1.834 (Heintz 1996, grade 9) Residuals were calculated first combining AB (Mason 1995) and Aa-A (Heintz 1996), according to the elements given in the Sixth Catalog of Orbits of Visual Binary Stars and secondly combining AB (Heintz 1996) and Aa-A (Heintz 1996).
STF1865	9343	Stars not separated
STF1909	9494	Stars not separated, measurement uncertain
STF2384	11568	First measurement since 2000. Easier than STF1211. In one of two nights with fine seeing, the stars were clearly separated. Measurements with a large telescope are desirable.
KU2	12690	No trace of the companion, fine seeing. The last measurement is from 2000.
STF2695	13964	Stars not separated
STT442	15103	The last positive measurement was made in 2008
STT464	15707	First positive measurement since 2011
STF2924	16057	Stars only separated during one measurement
STF2934	16185	Triple system. Residuals calculated using ephemeris values given by H. Zirm (private communication)
STT487	16469	First measurement since 2007. Stars at moments separated, but difficult pair because of magnitude difference

Residuals for Micrometer measurements by Andreas Alzner 2020.10 to 2020.90

Pair	ADS	Residual(O-C) PA(°)	Sep(″)	Orbit	Period (yrs)	Date	Grade
STF73	755	−0.4	−0.01	Muterspaugh	167.51	2010	2
MAD1	829	+3.3	+0.13	Ling	925	2012	5
STT21	862	+0.4	+0.14	Heintz	450	1966	5
STF115	1105	−0.3	0.00	Soederhjelm	222	1999	3
STT34	1411	−1.8	+0.01	Baize∗	173.1995	1987	3 ∗
		+1.2	−0.13	Heintz	416	1997	3
		−9.4	+0.31	Hartkopf	195.89	2008	3
		−1.2	0.00	Alzner∗∗	P=176.6,a=0.395	2020	∗∗
STF186	1538	+1.6	+0.04	Josties/Mason	166.4	2018	2
STT77	3082	−2.6	+0.02	Starikova	187.925	1985	3
STT79	3135	−1.8	+0.07	Soederhjelm	89.7	1999	2
STT82	3169	−3.0	−0.01	Mason et al.	241	2004	3
		−1.1	−0.05	Izmailov	252.1919	2019	3
STF554	3264	+0.1	−0.11	Torres	172.5	2019	3
STT98	3711	0.0	0.00	Scardia	197.45	2008	2
		+0.9	+0.01	Izmailov	195.5577	2019	2
BU1008	4841	+3.5	−0.06	Izmailov	1031.1632	2019	5
STT159	5586	+0.1	0.00	Alzner	262	2000	3
STT170	5958	−3.7	+0.02	Scardia	289.2	2018	3
STF1110	6175	+1.1	−0.02	Docobo	459.8	2014	3
STT185	6483	−2.0	+0.03	Mason	58.01	2009	2
STF1187	6623	+1.2	+0.09	Olevic	1385.156	2001	5

STF1211	6721	+4.2	−0.02	Heintz	407	1996	5
VDK3	7044	+2.7	−0.07	Izmailov	223.9709	2019	4
		+2.2	−0.04	Josties/Mason	221.2	2019	4
STF1280	7067	−0.4	−0.07	Heintz	609	1997	3
		+0.5	−0.13	Izmailov	688.512	2019	3
HO369	7541	−2.7	−0.03	Alzner	118.1	2020	3
		−2.9	−0.03	Alzner	1100	2020	4
STT229	7929	+1.6	+0.03	Alzner	335.4	2020	3
STF1523 AB	8119	−0.9	+0.05	Mason/Heintz	see notes		
		−0.4	+0.06	Heintz/Heintz	see notes		
STF1527	8128	−2.0	+0.06	Tokovinin	415	2012	3
STF1670	8630	−0.4	−0.07	Scardia	169.104	2007	2
STF1687	8695	+2.0	+0.01	Izmailov	486.3482	2019	3
STT261	8814	+0.1	+0.02	Izmailov	772.2055	2019	4
STF1865	9343	−0.5	−0.01	Scardia	125.24	2007	2
STF1909	9494	+9.4	−0.02	Zirm	209.8	2011	2
		+17.1	−0.03	Izmailov	214.7628	2019	2
STF1937	9617	−0.8	−0.02	Muterspaugh	41.63	2010	1
STF1938	9626	+0.7	+0.06	Scardia	256.5	2013	2
		+0.2	+0.02	Kiyaeva	265	2014	2
STF2384	11568	+4.0	+0.03	Heintz	133.5	1996	3
BU648	11871	+1.0	−0.04	Izmailov	63.2489	2019	2
STF2574	12803	−4.0	+0.07	Zirm	685.13	2010	4
STT387	12972	−1.3	+0.03	Mason et al.	165	2006	2
STT395	13277	−0.4	+0.04	Izmailov	709.37	2019	4
STF2695	13964	−1.2	−0.12	Alzner	269	2005	3
STT413	14296	−0.4	+0.07	Izmailov	800.7968	2019	4
STF2744	14573	0.0	0.00	Izmailov	642.8168	2019	4
H I 48	14783	+1.9	0.00	Josties/Mason	82.18	2018	3
STT437	14889	0.0	0.00	Izmailov	1218.0962	2019	4
A764	14926	−7.0	+0.34	Heintz	150	1995	5
STF2822	15270	+0.8	+0.06	Izmailov	692.0588	2019	3
STT464	15707	−8.1	+0.01	Ling	1360.2	1999	5
STF2924	16057	−3.4	−0.03	Prieur	218.8	2010	2
STF2934	16185	−0.3	0.00	Zirm	3350,81.0	2013	4,9
STF2944	16270	−0.8	+0.08	Zirm	1160.28	2007	4
		−0.6	+0.02	Izmailov	602.8834	2019	4
STF2950	16317	+1.3	+0.06	Izmailov	817.1898	2019	4
STT483	16428	−0.5	−0.03	Alzner	254.3	2020	3
STT489	16538	−3.2	−0.01	Scardia	162.8	2009	3
		−1.0	−0.03	Izmailov	175.9639	2019	3
STF3001	16666	0.0	−0.08	Izmailov	2198.7243	2019	4
STF3050	17149	−0.5	−0.01	Izmailov	572.999	2019	3

∗ quadrants reversed, (see note)
∗∗ Orbit A, this paper, (see note)

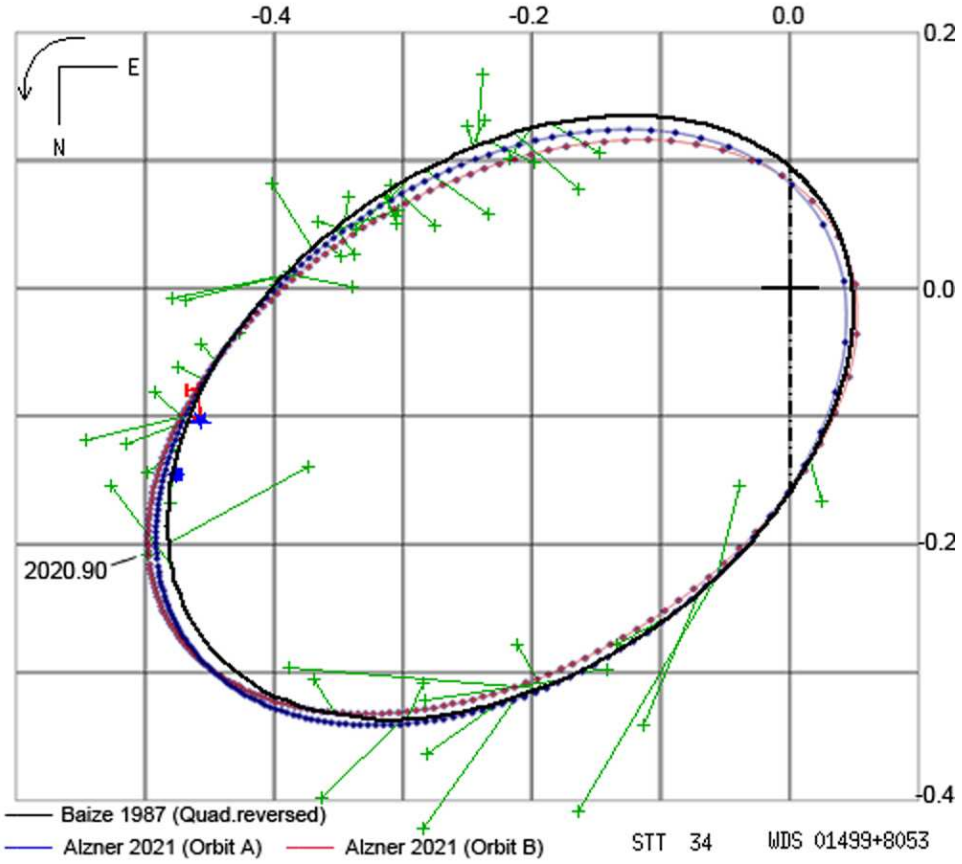

Figure 1: Short period orbits for STT34. (black: Baize 1987, Quadr. reversed, P = 173.2; blue: Alz2021A, P = 176.6, a = 0.395, increments: 1 yr; brown: Alz2021B, P=176.6, a=0.35, increments: 1 yr). Measurements taken from an earlier plot from the Sixth Catalog of Orbits of Visual Binary Stars, U.S. Naval Observatory

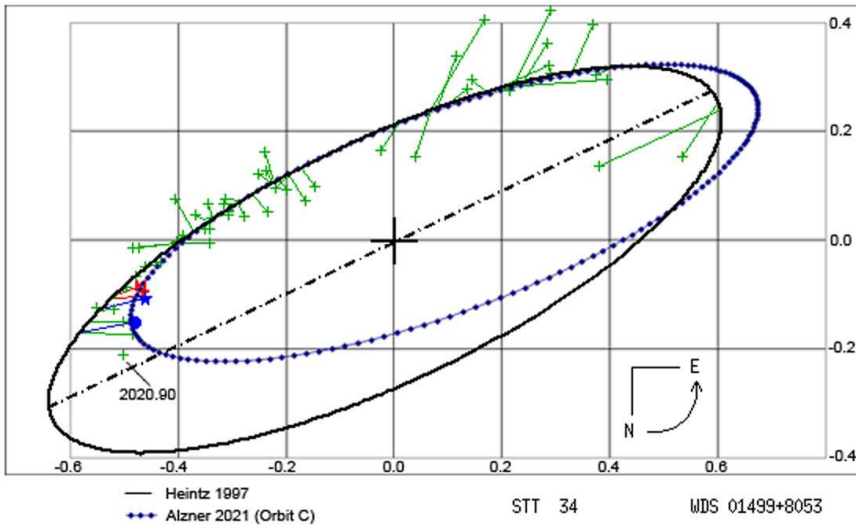

Figure 2: Long period orbits for STT34. (black: Heintz 1997, P = 416; blue: Alz2021C, P = 335.3, increments: 2 yr). Measurements taken from an earlier plot from the Sixth Catalog of Orbits of Visual Binary Stars, U.S. Naval Observatory.

Acknowledgements

Many thanks to R. Argyle for his support and the Webb Society for the opportunity to publish the results. I thank B. D. Mason and W. I. Hartkopf for providing the measurement data for STT34. For the calculation of the residuals mostly the orbital elements given in the 6th Catalog of Orbits of Visual Binary Stars (Hartkopf, Mason & Worley 2021) maintained at the U.S. Naval Observatory were used.

References

Alzner, A., 1998, *A&AS*, **132**, 237-252
Baize, P., 1987, *Astron. Astrophys. Suppl. Ser.* **71**, 177-184
Heintz, W. D., 1996, *A Study of Multiple-Star Systems*, *AJ*, **111**, Number 1, 408-411
Heintz, W. D., 1997 July, *Astrophys. Journal Suppl. Ser.* **111** 335-338
Docobo, J. A., Ling, J. F., Prieto, C., *et al.*, 2007, *Catalogue of Orbits and Ephemerides of Visual Double Stars*, Observatorio Astronomico Ramon Maria Aller. The catalog is available under the Double Star Library.
Hartkopf, W. I., Mason, B. D., & Rafferty, T., 2008, *AJ 135*, **1334**
Hartkopf, W. I., Mason, B. D. & Worley C. E.: *Sixth Catalog of Orbits of Visual Binary Stars.* Astrometry Department, U.S. Naval Observatory.
Malkov, O. Yu.; Tamazian, V. S.; Docobo, J. A.; Chulkov, D. A., 2012, *Dynamical masses of a selected sample of orbital binaries; Astronomy & Astrophysics*, **546**, A69
McAlister, H. A., Hartkopf, W. I., Mason, B. D. & Wycoff, G. L., *Fourth Catalog of Interferometric Measurements of Binary Stars.* Astrometry Department, U.S. Naval Observatory 3450 Massachusetts Ave, NW, Washington, DC 20392.
Zirm, H., private communication

DESCRIPTION OF A CCD ASTROMETRIC DOUBLE STAR SURVEY SYSTEM

Ken Sturrock, Denver, Colorado, USA

E-mail: kenneth.sturrock@gmail.com

Introduction

After years of taking pretty pictures of DSO objects, I wanted to start imaging for more applied purposes. I decided to try my hand at double stars because of the value of their measurements and they are a reasonable match for my equipment and environment. More romantically, I also enjoy the opportunity to be part of a grand tradition.

I primarily image using a Stellarvue SVQ apochromatic refractor with 100mm aperture and 580mm focal length. The imaging camera is a Quantum Scientific Imaging 690 which, along with the SVQ, produces a 1″.3/pixel image scale. This OTA and camera ride atop a Software Bisque Paramount MyT German Equatorial Mount and the entire system is controlled by Software Bisque's The SkyX Professional software (TSX).

In addition to controlling the equipment and providing planetarium features, TSX also contains a built-in plate solving capability, extensive object catalogs as well as a flexible programming interface. My approach was to leverage TSX's various components by means of a set of software routines written in the Python programming language.

To accomplish the goal of measurement, I broke the problem into smaller pieces, and then wrote the software to address each task: selection, acquisition, analysis and reduction of measurements.

Selection

Previous to the imaging session, I create a list of targets using a modified Washington Double Star (WDS) catalog and some custom selection criteria within TSX's 'Observing List' feature. In addition to selecting stars that are appropriate for the imaging system on a given night, I use available options to remove any duplicates, optimize the slew path and export the sorted list as a text file.

Acquisition

A Python program reads a list of targets from the exported text file, verifies that they are well placed in the sky, then slews to and photographs each target pair a number of times. A typical evening's run can slew to two or three hundred targets and shoot over a thousand images.

Analysis

At a later date, I use a second Python program to analyze a collection of images. The analysis process involves plate solving the image, attempting to identify the primary and secondary then measuring their relationship. Results for each image are written to a single text file.

Reduction

A third Python program will examine the results from the analysis process to discard outliers then average the remaining observations of each target. This program will also perform population statistics in an effort to quantify typical deviation from the expected catalog-provided values for the image set. Finally, the program uses the population variation to sort the cleaned and averaged measurements for each star pair

into categories representing 'aligned with expected values', 'deviated from expected values' or 'unreliable measurement'. This last category is determined by comparing the pair's measured separation to the image's resolution.

The software package also includes an additional program, written for the UNIX Bash shell, which converts the UNIX-style comma separated output files into a DOS-style tabular file which is more aesthetic for viewing and printing, especially for Windows users.

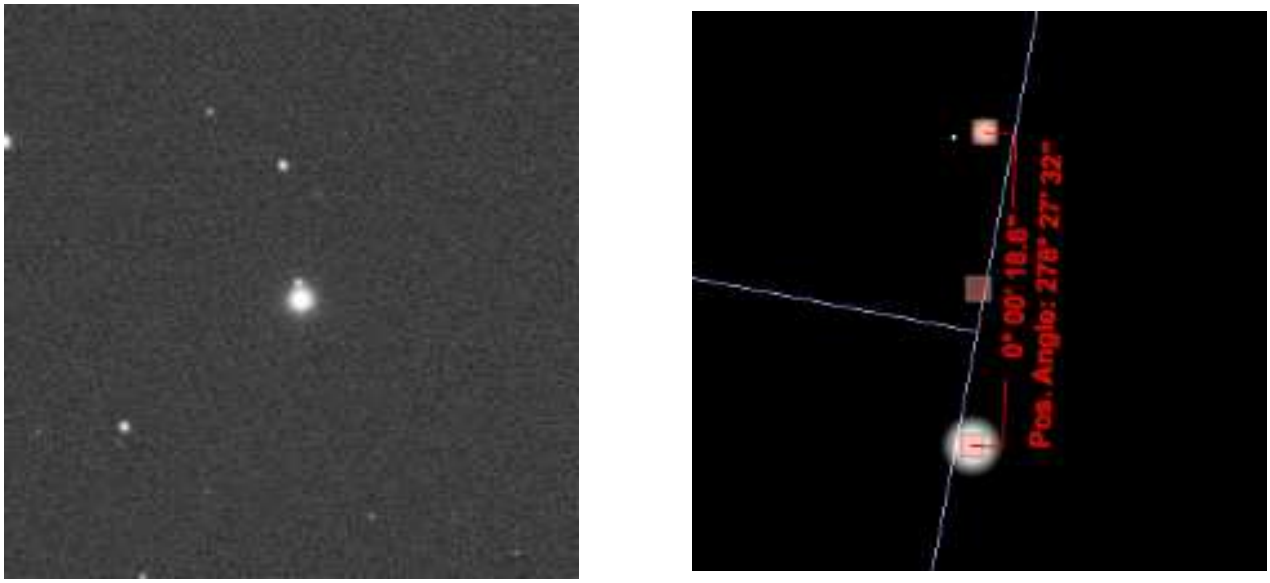

Figure 1: Successful example - ES 77 (left). Screen capture from the TSX (right

Above is a cropped image of ES 77 taken on 2020 May 20. The image scale is 1″.3/pixel. The image PA is 270°.83.

This is a screen capture from TSX showing the PA & separation of the AB pair using a beta copy of the TSX's Gaia catalog.

Acquisition Steps

Here is a portion of the acquisition log concerning WDS ES 77 from the night of 2020 May 20:

[23:09:07] Processing: WDS-2019-C ES 77 AB (40 of 174).
[23:09:10] Slew to WDS-2019-C ES 77 AB starting.
NOTE: Slew in progress
[23:09:21] Arrived at WDS-2019-C ES 77 AB
NOTE: Mount currently at: 55°.27 az., 56°.7 alt.
[23:09:21] Shooting image 1.
[23:09:41] Shooting image 2.
[23:10:01] Shooting image 3.
[23:10:21] Shooting image 4.

The log from the morning of 2020 May 22 documents the acquisition of four more images. The 'WDS-2019-C' nomenclature indicates the use of the 2019 release of SkyX's WDS catalog which was modified by the author to list the components as separate entries.

[02:50:21] Processing: WDS-2019-C ES 77 AB (40 of 174)
[02:50:23] Slew to WDS-2019-C ES 77 AB starting.
NOTE: Slew in progress.
[02:50:34] Arrived at WDS-2019-C ES 77
NOTE: Mount currently at: 329°.09 az., 76°.61 alt.

[02:50:34] Shooting image 1.
[02:50:54] Shooting image 2.
[02:51:14] Shooting image 3.
[02:51:34] Shooting image 4.

Analysis Steps

The analysis log of a single one of these subframes is below. The program verifies the storage location of the image file and identifies the target based upon the metadata which was inserted into the image's FITS header during acquisition. The next step is to perform a plate solve, known within TSX as an 'Image Link'. This is followed by information about the number of significant light sources identified within the image.
Processing image: 285 of 988

NOTE: Directory is /Volumes/Fast_SSD/ks/astronomy/DS_05_21_2020
NOTE: File is SQ_WDS-2019-C_ES___77__AB_Clear_00235219.fit
—
NOTE: Specified image not attached.
NOTE: Opening file.
NOTE: Guessing target with OBJECT keyword.
NOTE: Target may be: WDS-2019-C ES 77 AB

———-
[18:42:30] Finding target X & Y coordinates in image.
—
NOTE: Directory is /Volumes/Fast_SSD/ks/astronomy/DS_05_21_2020
NOTE: File is SQ_WDS-2019-C_ES___77__AB_Clear_00235219.fit
[18:42:30] Attempting Image Link.
—
NOTE: Guessed image scale: 1.31
[18:42:31] Image Link Successful.
NOTE: 173 sources found.

At this point, the program looks up the most recent celestial coordinates for the primary star from the WDS catalog and transforms those to cartesian coordinates relative to the image. It then attempts to find the closest light source to the expected location. The program will then re-transform that location's cartesian coordinates back to celestial coordinates for documentation purposes. The accuracy of these coordinate transformations is impacted by both the image?s resolution as well as the accuracy of the stellar catalogs used by the plate solving function. In this case, I am using a catalog based on the Gaia DR2 release.

—
NOTE: Target: WDS-2019-C ES 77 AB
—
NOTE: Object is a double star.
NOTE: Calculated Coordinates: 1616.719, 1753.056
—
[18:42:33] Closest Source Coordinates: 1616.661, 1753.286 [LS: 103]
—— (j2k) RA: 17h 08m 17s.1 Dec: +50° 50′ 32″.1
(now) RA: 17h 08m 48s.7 Dec: +50° 48′ 56″.6

The next step requires the retrieval of the PA and separation values from TSX's most recent WDS catalog. After reprinting some image and primary information for diagnostic purposes, the program will calculate the expected cartesian coordinates for the secondary and begin a search around that location. If there is a significant light source found by the light source extraction routine within TSX, the program will utilize the calculated centroid of that light source. Otherwise, it will find the nearest and brightest pixel at least 50% more than mean background brightness and utilize the center of that pixel as the secondary's location. Next, the analysis program will transform the secondary's location from cartesian to celestial

coordinates. Obviously, a lower resolution system will tend to have lower accuracy when measuring the location of the secondary. Likewise, a larger separation can be measured more accurately than a smaller separation.

```
[18:42:33] Retrieving catalog information
STATS:
Catalog: My SDBs: WDS 2019-C
WDS: 17083+5051
Components: AB
PA: 276°.70
Separation: 18″.600
Last Obs: 2008
[18:42:33] Measuring primary & secondary relationship.
NOTE: Provided Primary Source: 1616.661, 1753.286
NOTE: Directory is /Volumes/Fast_SSD/ks/astronomy/DS_05_21_2020
NOTE: File is SQ_WDS-2019-C_ES___77__AB_Clear_00235219.fit
NOTE: Reusing previous Image Link information.
NOTE: 173 sources found in: SQ_WDS-2019-C_ES___77__AB_Clear_00235219.fit
NOTE: 173 light sources transferred from SkyX.
NOTE: Image Statistics
Scale: 1″.305/pixel
FWHM: 4″.669
Image (j2k) RA: 17h 07m 22.2s Dec: +50° 48′ 59″.6
Image (now) RA: 17h 07m 53.9s Dec: +50° 47′ 22″.6
Middle (X,Y): 1356.0, 1694.0
Position Angle: 270°.8
Primary (X,Y): 1616.661, 1753.286 [LS: 103]
Primary (j2k) RA: 17h 08m 17.1s Dec: +50° 50′ 32″.1
Primary (now) RA: 17h 08m 48.7s Dec: +50° 48′ 56″.6
NOTE: Using supplied PA & Separation hints.
NOTE: Hinted PA & Sep: 276°.70 & 18″.600
NOTE: Guessed Secondary: 1614.801, 1739.155
[18:42:34] Searching for pixels. Creating a brightness array.
NOTE: Found pixel at: 1614, 1738 with more than 50% over background.
NOTE: Searching for a corresponding LS.
NOTE: No corresponding previously identified light source found.
NOTE: Adding this pixel as LS[173]
NOTE: Refined Secondary: 1614.5, 1738.5 [LS: 173]
Nearest (j2k) RA: 17h 08m 15.1s Dec: +50° 50′ 35″.2
Nearest (now) RA: 17h 08m 46.6s Dec: +50° 48′ 59″.7
```

Naturally, things can and do go wrong. If, for example, the secondary star is too dim or in an unexpected place, it can be overlooked. In other cases, depending on the catalog in use, a separation or even PA measurement may not be available.

As an example, my system was unable to resolve the secondary H component of the WDS BWL 46 system. It is listed within the TSX WDS-2019 database with a PA of 91° .2 and a separation of about 11″ which should be at the very tip of the red arrow in Figure 2, below the star.

If the program cannot find a bright pixel near the expected location, it will search a little farther afield for a significant light source that was identified as such by the light source extraction function. This approach is limited to brighter stars. If both of those directed searches near the expected location fail, the

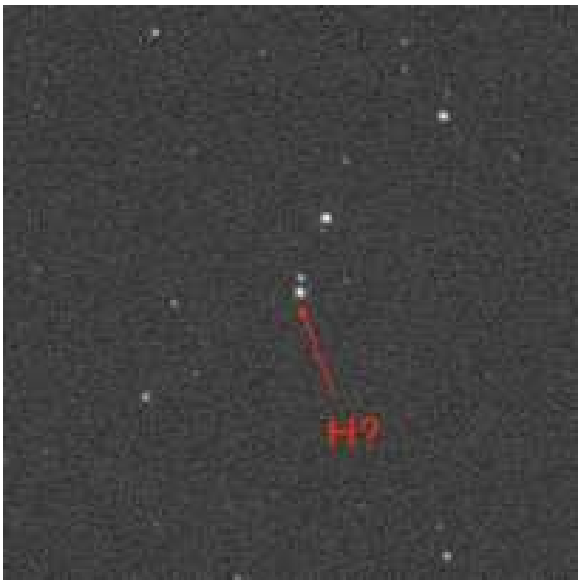

Figure 2: BWL 46 AH

routine will try to use a triangular search area radiating along the PA.

In the case of BWL 46:

NOTE: Guessed Secondary: 1635.401, 1862.884

[18:36:00] Searching for pixels. Creating a brightness array.
NOTE: No corresponding pixels found.
[18:36:00] Pixel search failed.
NOTE: Searching for previously identified light sources.
ERROR: No corresponding light source found.
[18:36:00] Finished measuring relationship.
[18:36:00] Unable to find secondary at the hinted location.
NOTE: Using supplied PA hint with no separation hint.

—

NOTE: Total of 9 light sources found in the search zone.
NOTE: Found Secondary: 1608.807, 2245.603 [LS: 181]
Nearest (j2k) RA: 17h 20m 32.0s Dec: +26° 30′ 35″.2
Nearest (now) RA: 17h 21m 21.8s Dec: +26° 29′ 21″.1

Unfortunately, the star that the routine identified as the H component was not the correct star, and was considerably farther away than the expected catalog location:

—

NOTE: Positional Measurements
Pos. Angle (SkyX now): 87°.0
Pos. Angle (SkyX j2k): 87°.12
Pos. Angle (Geometry): 87°.03
Separation (SkyX now): 511″.87
Separation (SkyX j2k): 511″.88
Separation (Geometry): 511″.76 (392.16 px)

When using the newer WDS catalogs available within TSX, the triangular search routine rarely finds the correct secondary. This failure, however, is not due to the routine's lack of ability but because, if the secondary was prominent, it would have already been found with the first approach. As an example, using an older version of TSX's WDS catalog which lacks separation information, the program was able to make successful use of the 'triangular search area approach' while analyzing an image of BUP 159 (Kochab)

NOTE: Using supplied PA hint with no separation hint.

NOTE: Total of 15 light sources found in the search zone.
NOTE: Found Secondary: 2046.172, 1453.091 [LS: 92]
Nearest (j2k) RA: 14h 50m 25.0s Dec: +74° 12′ 42″.3
Nearest (now) RA: 14h 50m 27.0s Dec: +74° 07′ 54″.3

NOTE: Positional Measurements
Pos. Angle (SkyX now): 341°.32
Pos. Angle (SkyX j2k): 341°.58
Pos. Angle (Geometry): 341°.64
Separation (SkyX now): 213″.32
Separation (SkyX j2k): 213″.32
Separation (Geometry): 213″.34 (163.35 px)

Which agrees closely with TSX's 2019 WDS catalog's secondary measurements (reported in 2010) of PA: 340°.4 with a separation of 214″.13.

In case the triangular approach fails, the final technique involves simply searching for the closest light source near the primary. The reliability of this approach is even lower and, again, suffers from the fact that if the correct secondary were visible, it would have already been found by the previous approaches:

NOTE : No light source found in search zone.

NOTE : No hints provided. Flying blind.

Nearest (X,Y): 1466.559, 1742.26 [LS: 99]
Nearest (j2k) RA: 15h 36m 47.0s Dec: +30° 01′ 51.″0
Nearest (now) RA: 15h 37m 37.6s Dec: +29° 57′ 55″.0

The last step in the image analysis process is to measure the PA and separation between the candidate primary and secondary. Largely for the amusement of the author, this measurement is conducted using several approaches. Finally, a primitive minimum separation limit is provided based upon a gap of one pixel between the measured FWHM radii of the primary & secondary stars.

NOTE : Positional Measurements
Pos. Angle (SkyX now): 279.17
Pos. Angle (SkyX j2k): 279.33
Pos. Angle (Geometry): 279.16
Separation (SkyX now): 19″.5
Separation (SkyX j2k): 19″.5
Separation (Geometry): 19″.5 (14.94 px)

Reliable separation limit: 7″.7

[18:42:34] Finished measuring relationship.

The entries for ES 77 from the analysis spreadsheet, look like this:

A-RA (j2k)	A-Dec (j2k)	B-RA (j2k)	B-Dec (j2k)	Catalog PA	Catalog Sep	Image PA	Image Sep	Rel. Sep. Dist.
17.138086551368215	50.84224102847357	17.137522231108214	50.843119369450875	276.70	18.600	279.16	19.5	7.7
17.1380839295623	50.842227000460596	17.13753443549335	50.843339696213455	276.70	18.600	281.9	19.16	7.62
17.13807976095589	50.842253920688506	17.137531199402616	50.84324831016801	276.70	18.600	280.66	19.04	8.0
17.138089719089518	50.84225168242301	17.137508582347973	50.8432573072287	276.70	18.600	280.18	20.14	7.66
17.13803788433537	50.84260235536424	17.137519833299738	50.8434459886914	276.70	18.600	279.76	17.93	7.7
17.13803994994698	50.842568183761166	17.137510036862622	50.84346961557604	276.70	18.600	280.18	18.36	7.83
17.13803960863975	50.84259208292696	17.13753164851089	50.84341972657366	276.70	18.600	279.76	17.58	7.94
17.13804398351892	50.8426057988273	17.137546015676445	50.84307783888801	276.70	18.600	275.72	17.07	7.87

The columns represent: The discoverer code, the coordinate-based name, the primary and secondary coordinates in J2000 equinox, the catalog PA & separation values, the PA & separation values and a 'realistic measurable separation distance' based upon the above described FWHM of the primary & secondary within each image.

Reduction Steps

The final task is to run the reduction program. The first step performed is to examine the observations for each target that were contained in the CSV spreadsheet produced by the analysis program. The program then rejects observations whose values exceed 1.5 sigma of the population of observations for that target in either separation or PA.

The separation measurements are examined twice (for large-scale and small-scale differences) in order to screen out precisely the kind of 'far afield' errors generated by the triangular zone search area routine when a secondary is not found where it was expected. The in the following example, measurements for ES 77 AB contained a single outlier, and it was a small-scale difference: The separation was slightly short:

```
[19:37:48]  Processing 20 of 172 targets.
------------
NOTE:       Observations:
            WDS-2019-C ES 77 AB 279.16 19.5
            WDS-2019-C ES 77 AB 281.9 19.16
            WDS-2019-C ES 77 AB 280.66 19.04
            WDS-2019-C ES 77 AB 280.18 20.14
            WDS-2019-C ES 77 AB 279.76 17.93
            WDS-2019-C ES 77 AB 280.18 18.36
            WDS-2019-C ES 77 AB 279.76 17.58
            WDS-2019-C ES 77 AB 275.72 17.07
[19:37:48]  Small-scale outlier rejection:
            Observation 0 accepted.
            Observation 1 accepted.
            Observation 2 accepted.
            Observation 3 accepted.
            Observation 4 accepted.
            Observation 5 accepted.
            Observation 6 accepted.
            Observation 7 rejected as an outlier (S).
------------
NOTE:       Component: AB
NOTE:       Used 7 observations.
```

The remaining values are median averaged and reported out with catalog values for comparison.

```
------------
NOTE:   Med. PA: 280.18
NOTE:   Med. Sep: 19.04
NOTE:   Cat PA: 276.7
NOTE:   Cat Sep: 18.6
```

Measurements may suffer from a variety of problems on any given night. In this case, if there are only two nights of observations, then the program may not be able to statistically reject outliers because the measurement differences may be evenly split. It is always better to have images acquired over several sessions.

Although using cleaned and averaged measurements will usually produce more reliable results, there are unfortunate occasions when the reduced measurement is less accurate than one of the original measurements. As expected, more observations will help.

Finally, after cleaning & averaging all of the measurements, the reduction program will categorize the reduced measurements based on the difference between the median measurements and the expected values from the catalog. With the assumption that most measurements will be close to accurate, star

pairs whose averaged measurements fall within the standard deviation are considered to be 'aligned with catalog expectations' while those who fall outside of this range are considered to be 'deviants'. Again, a two-stage approach is followed to mitigate the large-scale separation errors caused by missed secondaries.

———-
[19:37:49] Observation vs. Catalog Difference Distribution Statistics
———-
NOTE: First Stage Separation Difference Distribution
NOTE: Median: 0.9
NOTE: Standard Deviation: 107.65

NOTE : Second Stage Separation Difference Distribution
NOTE: Median: 0.8
NOTE: Standard Deviation: 16.56

NOTE : First Stage Position Angle Difference Distribution
NOTE: Median: 1.1
NOTE: Standard Deviation: 26.37
———-
[19:37:49] 135 stars were measured reliably.
[19:37:49] 35 stars were measured but not considered reliable due to resolution.
[19:37:49] 2 stars could not be measured at all.

An example of the final CVS spreadsheet looks like this:

Pair		RA(A)	Dec(A)	RA(B)	Dec(B)	N	PA Std Dev	Sep Std Dev	Cat PA	Cat Sep	Median PA	Median Sep	PA Diff.
HJL1081	AB	13.620137	52.59315	13.614895	52.62781	7	0.14	0.06	305.8	212.305	305.81	212.36	0.0
KZA73	AE	13.624272	36.29524	13.629908	36.21768	2	0.02	0.06	138.9	369.527	138.52	371.68	0.4
STF1774	AB	13.673015	50.51993	13.673373	50.51653	3	0.14	0.04	134.5	18.142	134.53	17.36	0.0
STF1772	AD	13.677869	19.95600	13.678061	20.01379	3	0.04	0.24	1.4	208.36	2.64	207.93	1.2
HJ2682	AB	13.677877	76.84397	13.675848	76.84545	7	0.16	0.03	281.7	25.663	291.95	25.48	0.2
SHY633	AC	13.783178	38.54276	13.738888	38.79776	2	0.00	0.04	296.2	2081.52	296.24	2080.05	0.0

Where the first column is the discoverer name, the second column is the coordinate-based name the third column represents the components, the fourth through seventh columns represent the primary and secondary coordinates in J2000 equinox. Column eight represents the number of observations kept and averaged, columns nine & ten show the standard deviation of the kept values which were averaged. Columns 11 and 12 represent the catalog values used for comparison. Columns 13 and 14 show the reduced values for PA and separation. Columns 15 and 16 show the difference between the cataloged and measured values.

I attempted to image 174 targets on the nights of 2020, May 20 and 21. Of those, one star was not successfully acquired. Of the remaining 173 star pairs, 135 were reliably reduced. Thirty five stars were deemed unreliable because the separation was less than the calculated reliable separation limit. Two stars could not be analyzed and one star could not be reduced due to excessive variation between the measurements. Of the 135 star pairs which were considered reliable, 116 were considered aligned with catalog expectations (See Table 1) while 19 star pairs were classified as deviant from catalog expectations. While much satisfaction is found when your measurements align with expectations, it can sometimes be more interesting to ask "what went wrong?". In that spirit, an examination of the nineteen deviants follows.

Deviant Measurement Analysis

TOK 569 AC

This star pair's C component (PA: 274.8 Sep: 1252.7) was not resolvable with my equipment. The program incorrectly chose a neighboring star

TOK 294 AB

Although it appears in TSX's Gaia star catalog, the 20th magnitude B component is not visible in the acquired images, so the program latched onto a much more prominent star almost three arcminutes away.

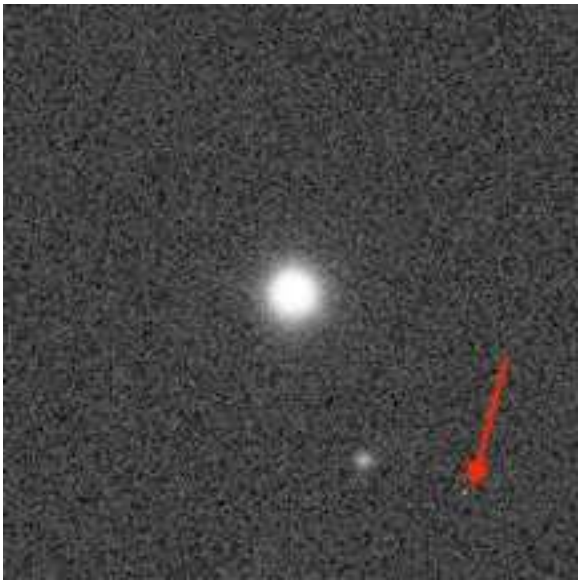

Figure 3: PIN 8 AB

PIN 8 AB

In the case of PIN 8 AB, the secondary (tip of red arrow) is visible in the image but is smaller than the system's resolution and dimmer than the program's threshold. Instead the program selected the more prominent star to the left.

SHY 645 AB

While the pointing of the mount and OTA are refined by the use of TPOINT software a number of months had passed since I adjusted my polar alignment and TPOINT model. My backyard pier and mount appear to have shifted slightly because the stars of interest no longer appear dead center in the image. In this case, the primary star was shifted towards the top of the image and the widely spaced secondary was off the edge of the plate.

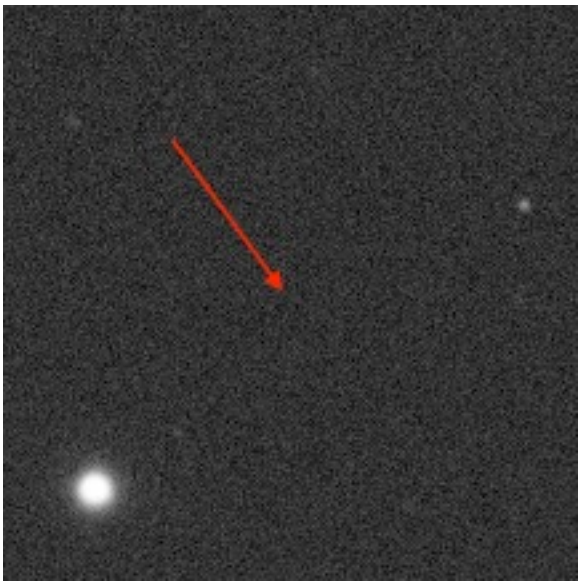

Figure 4: PIN 2

PIN 2 AB

This is another example of the approximately 19th magnitude B component (located at the tip of the arrow in the image to the left) not appearing in the 10 second exposure through my four-inch refractor.

Instead, the program latched on the star located near the right-hand edge of the cropped image.
KZA 97 AB-D

This is an example of discordant measurements evenly split between two sessions. Unfortunately the set of incorrect measurements showed better internal consistency than the correct measurements. This helped frame the standard deviation in their favor and the less consistent, but more accurate measurements were rejected. More observations, or better conditions during acquisition, would probably allow the routine to choose the accurate measurements.
KIR 4 AB-E

Yet another example of a secondary (17th magnitude) located approximately mid-frame that is not visible. As a result, the program mistakenly selected the star to the lower right.

Figure 5: KIR 4 AB-E

[19:37:48] Processing 31 of 172 targets.

NOTE: Observations:
WDS-2019-C KZA 97 AB-D 324°.12 314″.52
WDS-2019-C KZA 97 AB-D 324°.12 314″.69
WDS-2019-C KZA 97 AB-D 324°.13 314″.48
WDS-2019-C KZA 97 AB-D 324°.14 314″.44
WDS-2019-C KZA 97 AB-D 319°.32 117″.54
WDS-2019-C KZA 97 AB-D 319°.45 117″.5
WDS-2019-C KZA 97 AB-D 319°.35 116″.44
WDS-2019-C KZA 97 AB-D 319°.25 116″.79

[19:37:48] Large-scale outlier rejection:
Observation 6 rejected as an outlier (S).
Observation 7 rejected as an outlier (S).
[19:37:48] Small-scale outlier rejection:
Observation 0 accepted.
Observation 1 accepted.
Observation 2 accepted.
Observation 3 accepted.
Observation 4 rejected as an outlier (S).
Observation 5 rejected as an outlier (S).

———-
NOTE: Component: AB-D
NOTE: Used 4 observations.
———-
NOTE: Med. PA: 324°.12
NOTE: Med. Sep: 314″.5

NOTE Cat PA: 318°.8
NOTE: Cat Sep: 118″.3

STT 298 AB-D

This failure represents another dim secondary. The script found a brighter, but wrong, star.

DEA 52 AB

Here is another example of discordant measurements separated over two nights. Unlike KZA 97, however, in this case neither set of measurements resembled the catalog values for the secondary. Images from neither night reveal any sign of a secondary rising out of the background. On the night of May 20, both the search around the expected location as well as the triangular search failed. The program defaulted to selecting the light source that was closest to the identified primary's location. On the night of the 21st, the framing was different within the FOV and the program found a candidate secondary using the triangular search area method. That secondary was still wrong.

HJ 1277 AC

In this case, the secondary star was close to the minimum brightness threshold and, due to varying conditions, was rejected as too dim in favor of a brighter artifact:

[19:37:49] Processing 158 of 172 targets.
———-
NOTE: Observations:

WDS-2019-C HJ 1277 AC 271°.56 56″.88
WDS-2019-C HJ 1277 AC 270°.9 55″.4
WDS-2019-C HJ 1277 AC 270°.35 54″.79
WDS-2019-C HJ 1277 AC 271°.23 51″.93
WDS-2019-C HJ 1277 AC 275°.07 69″.55
WDS-2019-C HJ 1277 AC 267°.33 145″.82
WDS-2019-C HJ 1277 AC 267°.39 145″.19
WDS-2019-C HJ 1277 AC 267°.3 145″.41

[19:37:49] Large-scale outlier rejection:
Observation 5 rejected as an outlier (S).
Observation 6 rejected as an outlier (S).
Observation 7 rejected as an outlier (S).
[19:37:49] Small-scale outlier rejection:
Observation 0 accepted.
Observation 1 accepted.
Observation 2 accepted.
Observation 3 accepted.
Observation 4 rejected as an outlier (S).
———-
NOTE: Component: AC
NOTE: Used 4 observations.
———-
NOTE: Med. PA: 271°.06
NOTE: Med. Sep: 55″.09

NOTE : Cat PA: 266°.7
NOTE: Cat Sep: 142″.939

STT 584 This set of measurements were sorted as deviant from the expected catalog measure. Yet, the sizes of the errors are not particularly large and, upon examination the secondary measurements are probably

accurate.

[19:37:48] Processing 6 of 172 targets.
———-
NOTE: Observations:

WDS-2019-C STT 584 AB 327°.17 338″.28
WDS-2019-C STT 584 AB 327°.18 337″.9
WDS-2019-C STT 584 AB 327°.15 337″.98
WDS-2019-C STT 584 AB 327°.17 338″.11
[19:37:48] Small-scale outlier rejection:
Observation 0 rejected as an outlier (S).
Observation 1 accepted.
Observation 2 rejected as an outlier (P).
Observation 3 accepted.
———-
NOTE: Component: AB
NOTE: Used 2 observations.
———-
NOTE: Med. PA: 327°.17
NOTE: Med. Sep: 338″.0

NOTE Cat PA: 325°.7
NOTE: Cat Sep: 313″.785

Of course, system resolution may be a factor but the catalog comparison values were measured in 2001 and the system has historically shown significant change. Moreover, using the TSX PA angular separation & position angle tool, measurements made against the beta release Gaia catalog appear closer to the analysis program's measurements than the 2001 catalog measurements.

Figure 6: STT 584 AB

The red arrow in this image depicts the WDS catalog position for the STT 584 B component. The star to the upper right is the probable current location.

This diagram from TSX's PA & Separation Tool shows the approximate placement of the B component based on Gaia data. Note that the tool anchor is offset due to over-lapping star depictions on the chart.
KUI 69 AB

Another example of a secondary that was indiscernible by the analysis program on the 20th but was recognized on the 21st. When averaged, the PA from the second day are 2.5 degrees less than the catalog PA reported in 2015. The averaged second-day separation is 1″.4 less than the 2015 catalog separation.

Figure 7: STT 584 AB - diagram from TSX PA and separation tool

Additional measurements would have probably resulted in agreement with the catalog.

DEA 55 AB

Visible as a single, slightly brighter, pixel - the (reportedly 13 magnitude) B component was too dim compared to the background for the analysis program to register it.

STT 305 AC

This target presented a double mystery. There is no sign of a light source anywhere close to the location indicated for the C component according to the measurements taken in the year 1847, which are the most recent in the TSX's WDS database. The analysis program searched through a triangular search area centered on the 1847 PA and located an incorrect star over thirty times too far away.

After examining the TSX Gaia DR2 database, the only star that seems plausible for the C component is located at PA 210° with a separation of about 25″ . If correct, this is approximately 23″ away from the location measured in 1847.

LDS 1844 AB

The images for this pair show a dim smudge adjacent to the expected location based on the 2010 measurements. Unfortunately, the smudge was considered too dim by the analysis program for it to be considered valid.

SKF 242 AB

The B component for this system is barely visible as a single ghostly pixel. Due to its dimness, it was noted in only two of eight images. When it was found, under-sampling and close proximity to the primary made precise measurement difficult.

TOK 177 AB

The B component was too dim to be found in the image.

BWL 46 AH

As documented above, the H component was too dim to locate within the image.

SDR 1 AB-D

A final discordant pair. The very slight extra blur seen in the right-hand image from May 20 subtly dimmed the D component, (directly below the primary), compared to the slightly brighter background versus the image on the left from May 21. As a result, for the May 21 images, the analysis program found the proper secondary and measured it at PA 256°.9 with a separation of 23″.2 compared to a catalog PA of 251°.7 and a separation of 23″.8. For the images from May 20, the program ignored the pixels and chose the wrong secondary star.

The image on the right demonstrates enough extra atmospheric (or focus) blur to prevent the analysis

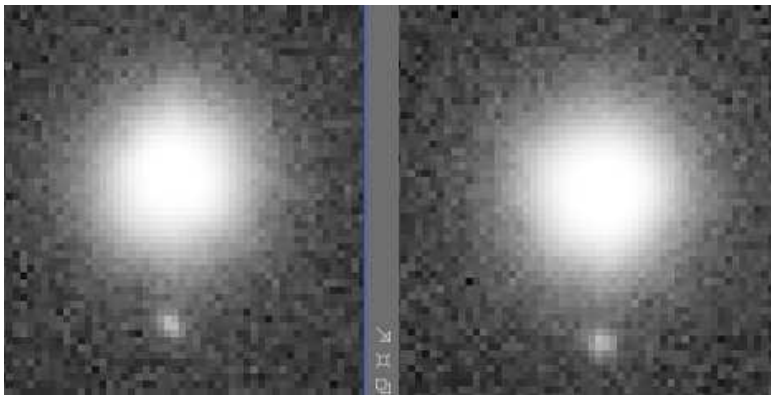

Figure 8: SDR 1 AB-D

program from recognizing the secondary directly below the primary.

Table 1: Measures made on the nights of 2020, May 21 and 22

Catalogue	J2000	Comp.	N.	PA Std. Dev.	Sep. Std. Dev.	Cat. PA	Cat. Sep.	Median PA	Median Sep.	$\Delta\theta$	$\Delta\rho$
HJL1081	13372+5236	AB	7	0.14	0.06	305.8	212.505	305.81	212.36	0.0	0.1
KZA 73	13375+3618	AE	2	0.02	0.06	138.9	369.527	138.52	371.68	0.4	2.2
STF1774	13404+5031	AB	3	0.14	0.04	134.5	18.142	134.53	17.36	0.0	0.8
STF1772	13407+1957	AD	3	0.04	0.24	1.4	208.36	2.64	207.93	1.2	0.4
HJ 2682	13407+7651	AB	7	0.16	0.03	281.7	25.663	281.95	25.48	0.2	0.2
SHY 633	13470+3833	AC	2	0.0	0.04	296.2	2081.52	296.24	2080.05	0.0	1.5
HJL1082	13514+3441	AB	6	0.09	0.12	64.7	169.188	64.82	169.91	0.1	0.7
SKF1494	13533+4211	AC	2	0.02	0.01	137.3	143.033	137.19	143.09	0.1	0.1
SHJ 169	13547+1824	AB	4	0.07	0.23	85.0	114.033	85.1	115.7	0.1	1.7
STF1830	14161+5643	CE	3	0.04	0.04	244.6	138.04	244.68	138.32	0.1	0.3
STFA 26	14162+5122	AB	3	0.05	0.02	33.1	38.947	33.12	39.11	0.0	0.2
ENG 51	14193+1300	AB	7	0.07	0.14	219.1	163.66	219.26	164.12	0.2	0.5
WAL 65	14199+6747	AC	4	0.85	0.43	238.9	144.855	239.41	144.75	0.5	0.1
HJL1086	14242+0549	AB	2	0.0	0.03	273.6	158.9	273.69	158.07	0.1	0.8
HJL1087	14265+1914	AB	6	0.14	0.49	253.9	224.4	254.97	223.95	1.1	0.5
J 2733	14275+7542	AB	7	0.67	0.7	127.0	23.709	127.6	24.61	0.6	0.9
SKF 911	14298+0050	AB	3	0.03	0.03	330.9	5.679	0.92	49	0.0	0.2
GUI 15	14298+3147	AC	7	0.08	0.19	121.4	106.914	121.27	107.0	0.1	0.1
HJ 2728	14318+3022	AB	4	0.14	0.1	343.4	33.84	344.5	32.47	1.1	1.4
KUI 68 S	14342+3232	AB	2	0.03	0.03	316.6	27.778	316.15	27.62	0.5	0.2
STT 582	14347+2945	AC	2	0.01	0.05	101.4	222.644	102.5	221.16	1.1	1.5
STF1864	14407+1625	AC	3	0.01	0.06	163.7	128.76	164.06	127.39	0.4	1.4
H 6 104	14411+1344	AB-C	7	0.21	0.13	258.9	103.758	259.75	104.61	0.9	0.9
STF1882	14441+6106	AB	2	0.02	0.07	359.7	11.44	0.14	11.36	0.4	0.1
STF1877	14450+2704	AC	3	0.02	0.04	254.6	175.524	254.45	174.07	0.2	1.5
STF1889	14495+5122	AB	2	0.06	0.03	92.5	15.119	92.5	15.3	0.0	0.2
HJ 5489	14500+2837	AC	7	0.23	0.06	21.3	110.378	21.43	110.28	0.1	0.1
BUP 159	14507+7409	AB	3	0.04	0.12	340.5	214.13	341.72	213.11	1.2	1.0
ARN 12	14514+1906	AF	7	0.14	0.71	37.0	337.475	38.75	334.49	1.8	3.0
HU 908	14531+7811	AC	4	1.24	0.49	140.0	112.992	141.02	113.14	1.0	0.1

HJ 1259	14554+0647	AB	8	0.25	0.37	79.6	32.83	79.24	32.87	0.4	0.0
S 666	14568+7454	AB	6	0.25	0.06	32.5	167.8	31.25	170.44	1.2	2.6
SOZ 24	14572-0421	AB	3	0.33	0.06	296.6	22.772	294.53	19.42	2.1	3.4
ARN 13	14576-0010	AC	7	0.49	0.79	173.5	267.61	173.56	267.11	0.1	0.5
STT 291	15006+4717	AB	3	0.01	0.02	169.7	35.91	155.38	35.6	14.	0.3
STF1899	15016-0310	AB	3	0.13	0.05	66.9	28.257	67.13	28.62	0.2	0.4
BU 348	15018-0008	AC	6	1.95	0.36	217.2	31.224	219.53	30.78	2.3	0.4
DRS 57	15073+1827	AC	5	0.02	0.1	321.3	110.341	321.5	110.08	0.2	0.3
ENG 52	15073+2452	AC	7	0.09	0.09	18.0	247.86	12.15	257.87	5.8	10.0
STF1918	15078+6307	AB	3	0.05	0.07	19.1	18.89	19.73	17.8	0.6	1.1
STF1919	15127+1917	AB	2	0.03	0.0	10.6	23.36	10.76	23.26	0.2	0.1
STT 292	15141+3147	AB	2	0.01	0.02	157.8	117.618	157.62	117.9	0.2	0.3
STFA 27	15155+3319	AB	3	0.02	0.01	78.1	105.026	77.89	105.54	0.2	0.5
AMM 6	15160+0048	AC	5	1.22	0.83	38.3	11.677	36.35	8.37	1.9	3.3
STF1930	15193+0146	AC	2	0.03	0.01	17.2	151.1	16.94	152.43	0.3	1.3
ENG 53	15201+2937	AB	7	0.14	0.15	342.3	142.16	342.72	144.32	0.4	2.2
LEP 74	15208+3129	AB	6	0.06	0.05	325.5	1580.963	325.72	1580.77	0.2	0.2
STFA 28	15245+3723	AB	3	0.03	0.08	170.8	108.158	170.46	108.07	0.3	0.1
BUP 162	15249+5858	AB	8	0.44	1.21	49.6	253.682	50.79	253.2	1.2	0.5
HJL1090	15263+3420	AB	8	0.14	0.35	312.3	155.05	312.55	152.81	0.2	2.2
GIC 128	15289+5727	AD	5	0.1	0.08	130.6	185.255	130.42	185.32	0.2	0.1
STF1972	15292+8027	AC	3	0.02	0.09	101.1	186.398	100.82	187.94	0.3	1.5
BU 944	15294+4743	AB	7	3.41	1.56	127.1	11.0	127.31	9.37	0.2	1.6
STT 300	15402+1203	AB	3	0.35	0.08	260.9	15.04	260.33	14.49	0.6	0.5
BU 1451	15416+1940	AB-D	7	0.06	0.45	109.9	152.844	109.37	153.7	0.5	0.9
TOK 302	15419+1828	AC	2	0.01	0.09	273.9	248.996	273.97	248.84	0.1	0.2
A 2230	15440+0231	AD	4	0.11	0.28	284.9	172.39	285.86	173.51	1.0	1.1
STF1970	15462+1525	AB	2	0.04	0.05	263.6	29.997	263.09	29.5	0.5	0.5
SOZ 15	15473-0016	AB	2	0.14	0.04	272.2	14.192	278.71	10.69	6.5	3.5
LAF 55	15482+0134	AI	3	2.03	0.18	209.5	12.26	198.77	8.05	10.	4.2
STF1984	15511+5254	AC	2	0.0	0.05	97.5	172.49	96.81	173.67	0.7	1.2
BUP 163	15512+3539	AB	6	0.16	0.14	208.1	109.18	208.78	106.07	0.7	3.1
STT 304	16009+3911	AB	3	1.89	0.11	172.6	10.422	166.3	10.55	6.3	0.1
S 676	16010+3318	AB	7	0.17	0.08	46.5	141.71	45.15	145.95	1.3	4.2
STF2007	16060+1319	AC	3	0.64	0.03	137.0	162.727	138.28	162.62	1.3	0.1
GWP2598	16074+1320	AB	7	0.22	0.2	350.3	27.758	350.47	27.61	0.2	0.1
STF2010	16081+1703	AB	2	0.02	0.19	12.0	27.1	20.23	24.01	8.2	3.1
ES 2651	16090+5756	AB	7	1.71	1.4	139.7	12.282	138.77	13.38	0.9	1.1
STF2024	16118+4222	AB	3	0.13	0.04	44.0	22.8	44.47	23.65	0.5	0.8
STF2032	16147+3352	AC	3	0.04	0.08	92.9	26.2	88.76	29.91	4.1	3.7
SHJ 223	16167+2909	AD	7	0.14	0.05	50.0	123.265	50.17	123.15	0.2	0.1
BUP 167	16221+3054	AB	7	0.17	0.31	62.3	188.173	63.45	188.84	1.2	0.7
STFA 29	16224+3348	AD	2	0.02	0.01	153.3	277.11	153.05	277.19	0.2	0.1
H 6 18	16224+3348	BD	7	0.28	0.08	15.9	100.007	15.89	98.69	0.0	1.3
H 5 38	16229+3220	AB	8	0.33	0.06	16.3	31.122	16.33	30.98	0.0	0.1
SMY9002	16240+6131	AF	7	0.2	0.12	17.9	364.586	18.23	362.92	0.3	1.7
BU 625	16254+1402	AD	7	0.03	0.23	271.8	129.465	271.88	129.39	0.1	0.1
BUP 170	16302+2129	AB	6	0.07	0.88	274.7	245.23	276.02	245.86	1.3	0.6
STF2055	16309+0159	AD	2	0.0	0.06	247.0	308.1	247.1	307.74	0.1	0.4
STF2063	16318+4536	AB	2	0.08	0.03	197.4	16.34	194.73	16.22	2.7	0.1
WEB 6	16354+1703	AB	7	0.13	0.81	359.8	155.53	0.63	155.27	0.8	0.3

STFA 30	16362+5255	CD	2	0.01	0.03	122.5	123.924	122.53	125.47	0.0	1.5
STF2082	16387+4856	AB	3	0.11	0.04	92.5	27.21	91.68	28.05	0.8	0.8
STF2074	16406+0413	BC	3	0.05	0.1	316.0	25.888	315.93	25.96	0.1	0.1
STF2093	16429+3855	AB	2	0.0	0.04	265.2	116.72	266.32	117.25	1.1	0.5
KU 1	16431+7731	AC	2	0.02	0.09	13.0	103.511	14.68	101.57	1.7	1.9
STT 585	16450+0605	AC	3	0.01	0.06	252.7	128.219	253.14	126.46	0.4	1.8
ENG 58	16469+0215	AB	6	0.03	0.13	218.0	148.84	217.24	149.07	0.8	0.2
STF2096	16472+0204	AC	3	0.03	0.11	193.0	214.068	193.03	214.15	0.0	0.1
BUP 174	16478+0515	AB	3	0.05	0.03	80.1	121.21	79.97	121.44	0.1	0.2
BU 627	16492+4559	AE	3	0.01	0.03	269.8	7.197	9.93	0	0.1	0.2
STF2103	16496+1316	AC	11	2.34	0.77	247.3	14.768	247.71	13.89	3.6	0.9
STF2110	16550+2544	AB	8	0.09	0.06	91.5	17.877	91.6	17.98	0.1	0.1
H 4 122	17016+1457	AB	6	0.16	0.13	237.5	18.892	237.12	18.59	0.	0.3
STFA 33	17037+1336	BD	8	0.0	0.05	272.3	154.534	272.63	154.49	0.3	0.0
STFA 33	17037+1336	AD	5	0.02	0.21	137.7	177.718	137.71	177.84	0.0	0.1
BU 822	17039+1941	AC	3	0.1	0.04	196.5	114.0	196.46	114.69	0.0	0.7
FOX 281	17047+1936	AC	5	0.02	0.06	133.1	106.763	133.13	106.86	0.0	0.1
BU 1088	17053+5428	BC	2	1.42	0.0	185.7	13.57	178.26	11.05	7.4	2.5
HO 412	17080+3556	AB-C	7	0.44	1.49	132.3	20.242	131.78	19.56	0.5	0.7
ES 77	17083+5051	AB	7	0.81	0.84	276.7	18.6	280.18	19.04	3.5	0.4
SHY 713	17111+2414	AB	7	0.69	0.62	74.2	195.505	74.2	195.5	0.0	0.0
KUI 78	17117+4945	AC	4	0.8	0.75	107.0	27.93	108.15	28.45	1.2	0.5
B 2826	17125+1035	AB	3	0.56	0.1	33.7	30.471	28.87	32.08	4.8	1.6
AGC 16	17146+1423	AC	2	0.41	0.1	297.4	19.91	298.27	16.09	0.9	3.8
STF3127	17150+2450	AD	2	0.01	0.02	93.1	191.58	90.14	191.5	3.0	0.1
WAL 79	17161+6043	AC	3	0.04	0.07	79.4	137.29	80.91	133.73	1.5	3.6
ARN 14	17207+3228	AF	3	0.0	0.02	104.0	383.15	101.17	373.52	2.8	9.6
GUI 41	17209+2430	AD	7	0.54	0.61	221.8	222.082	221.82	222.04	0.0	0.0
STF2161	17237+3709	AC	2	0.02	0.02	222.1	117.683	221.87	118.56	0.2	0.9
STT 329	17245+3657	AB	4	0.04	0.02	12.0	33.5	12.45	33.13	0.4	0.4
KUI 81	17259+1655	AC	6	0.63	0.25	218.1	23.233	217.67	22.91	0.4	0.3
BU 1090	17304+5218	AC	3	0.02	0.18	155.4	118.365	155.81	118.11	0.4	0.3
BU 1458	17320+6808	AB	4	0.5	0.45	342.1	154.89	342.67	154.69	0.6	0.2
STF2184	17344+1310	AC	2	0.0	0.1	293.1	128.047	293.19	128.37	0.1	0.3
STFA 34	17346+0935	AD	3	0.02	0.01	212.9	126.77	213.07	127.0	0.2	0.2

Table 2: Measures made on the nights of 2020, June 22 to 26

Catalogue	J2000	Comp.	N.	σ_θ	σ_ρ	Cat. PA	Cat. Sep.	Median PA	Median Sep.	$\Delta\theta$	$\Delta\rho$
HJL1081	13372+5236	AB	11	0.01	0.09	305.8	212.505	305.97	212.44	0.2	0.1
KZA 73	13375+3618	AE	11	0.02	0.16	138.9	369.527	138.7	371.59	0.2	2.1
STF1774	13404+5031	AB	9	0.22	0.1	134.5	18.142	135.19	17.34	0.7	0.8
STF1772	13407+1957	AD	7	0.02	0.14	1.4	208.36	1.38	208.66	0.0	0.3
HJ 2682	13407+7651	AB	13	0.11	0.06	281.7	25.663	281.77	25.47	0.1	0.2
HJL1082	13514+3441	AB	9	0.03	0.12	64.7	169.188	64.83	169.72	0.1	0.5
SHJ 169	13547+1824	AB	9	0.12	0.29	85.0	114.033	84.54	114.89	0.5	0.9
DRS 14	14016+0133	AE	5	1.99	0.43	175.0	14.9	177.99	12.5	3.0	2.4
STF1830	14161+5643	CE	11	0.06	0.13	244.6	138.04	244.84	138.23	0.2	0.2
STFA 26	14162+5122	AB	9	0.08	0.06	33.1	38.947	33.07	39.0	0.0	0.1

ENG 51	14193+1300	AB	8	0.01	0.1	219.1	163.66	219.22	164.21	0.1	0.6
WAL 65	14199+6747	AC	7	0.03	0.06	238.9	144.855	238.75	144.39	0.2	0.5
HJL1086	14242+0549	AB	10	0.02	0.1	273.6	158.9	273.69	158.46	0.1	0.4
HJL1087	14265+1914	AB	8	0.13	0.77	253.9	224.4	254.71	223.75	0.8	0.7
HJ 2733	14275+7542	AB	12	1.21	0.52	127.0	23.709	127.98	24.95	1.0	1.2
SKF 911	14298+0050	AB	6	0.03	0.13	330.9	135.679	330.89	135.38	0.0	0.3
GUI 15	14298+3147	AC	9	0.03	0.04	121.4	106.914	121.36	107.22	0.0	0.3
HJ 2728	14318+3022	AB	9	0.46	0.42	343.4	33.84	344.58	31.87	1.2	2.0
STT 582	14347+2945	AC	10	0.02	0.14	101.4	222.644	102.6	221.02	1.2	1.6
STF1864	14407+1625	AC	9	0.04	0.06	163.7	128.76	164.24	127.4	0.5	1.4
H 6 104	14411+1344	AB-C	7	0.04	0.1	258.9	103.758	259.36	104.26	0.5	0.5
STF1882	14441+6106	AB	5	0.16	0.05	359.7	11.44	359.89	11.31	0.2	0.1
STF1877	14450+2704	AC	10	0.23	0.36	254.6	175.524	254.2	174.52	0.4	1.0
STF1889	14495+5122	AB	8	0.12	0.02	92.5	15.119	92.98	15.12	0.5	0.0
HJ 5489	14500+2837	AC	9	0.03	0.07	21.3	110.378	21.37	110.28	0.1	0.1
BUP 159	14507+7409	AB	15	0.26	0.51	340.5	214.13	341.1	212.3	0.6	1.8
ARN 12	14514+1906	AF	10	0.08	0.92	37.0	337.475	38.61	335.39	1.6	2.1
HU 908	14531+7811	AC	10	0.46	0.24	140.0	112.992	141.31	112.61	1.3	0.4
HJ 1259	14554+0647	AB	8	0.08	0.05	79.6	32.83	79.41	32.98	0.2	0.1
S 666	14568+7454	AB	10	0.24	0.19	32.5	167.8	33.8	167.6	1.3	0.2
SOZ 24	14572-0421	AB	7	1.33	0.28	296.6	22.772	293.32	19.39	3.3	3.4
ARN 13	14576-0010	AC	10	0.04	0.22	173.5	267.61	174.55	265.69	1.1	1.9
STT 291	15006+4717	AB	7	0.06	0.04	169.7	35.91	155.75	35.68	13.	0.2
BU 348	15018-0008	AC	7	1.46	0.07	217.2	31.224	220.67	30.77	3.5	0.5
DRS 57	15073+1827	AC	8	0.03	0.06	321.3	110.341	321.38	109.97	0.1	0.4
ENG 52	15073+2452	AC	9	0.01	0.08	18.0	247.86	12.16	257.64	5.8	9.8
STF1918	15078+6307	AB	9	0.13	0.04	19.1	18.89	19.98	17.8	0.9	1.1
STF1919	15127+1917	AB	11	0.06	0.04	10.6	23.36	10.64	23.15	0.0	0.2
STT 292	15141+3147	AB	8	0.02	0.06	157.8	117.618	157.73	117.95	0.1	0.3
STFA 27	15155+3319	AB	11	0.03	0.15	78.1	105.026	78.01	105.28	0.1	0.3
AMM 6	15160+0048	AC	9	1.78	0.39	38.3	11.677	37.39	8.5	0.9	3.2
STF1930	15193+0146	AC	9	0.03	0.16	17.2	151.1	16.87	152.23	0.3	1.1
ENG 53	15201+2937	AB	11	0.02	0.06	342.3	142.16	342.95	144.07	0.6	1.9
LEP 74	15208+3129	AB	8	0.01	0.32	325.5	1580.963	325.68	1580.2	0.2	0.8
STFA 28	15245+3723	AB	11	0.06	0.13	170.8	108.158	170.63	108.22	0.2	0.1
BUP 162	15249+5858	AB	19	0.25	0.54	49.6	253.682	50.99	252.84	1.4	0.8
HJL1090	15263+3420	AB	11	0.03	0.11	312.3	155.05	312.62	152.6	0.3	2.5
GIC 128	15289+5727	AD	12	0.19	0.2	130.6	185.255	131.75	185.41	1.2	0.2
STF1972	15292+8027	AC	8	0.03	0.19	101.1	186.398	100.83	188.11	0.3	1.7
BU 944	15294+4743	AB	17	2.75	1.2	127.1	11.0	127.92	9.29	0.8	1.7
KZA 97	15318+4054	AB-D	9	0.21	0.33	318.8	118.3	319.14	117.31	0.3	1.0
STT 300	15402+1203	AB	8	0.3	0.06	260.9	15.04	260.41	14.62	0.5	0.4
BU 1451	15416+1940	AB-D	14	0.05	0.35	109.9	152.844	109.41	152.77	0.5	0.1
TOK 302	15419+1828	AC	9	0.01	0.1	273.9	248.996	274.07	249.16	0.2	0.2
A 2230	15440+0231	AD	7	0.13	0.28	284.9	172.39	285.94	173.58	1.0	1.2
HJ 1277	15443+0626	AC	8	0.21	0.41	266.7	142.939	267.05	146.2	0.4	3.3
STF1970	15462+1525	AB	10	0.19	0.16	263.6	29.997	262.94	29.89	0.7	0.1
SOZ 15	15473-0016	AB	10	4.42	0.41	272.2	14.192	267.42	12.43	4.8	1.8
LAF 55	15482+0134	AI	9	1.71	0.24	209.5	12.26	207.47	10.03	2.0	2.2
STF1984	15511+5254	AC	8	0.02	0.1	97.5	172.49	97.02	173.51	0.5	1.0
BUP 163	15512+3539	AB	20	0.25	0.11	208.1	109.18	209.15	106.29	1.1	2.9

STT 304	16009+3911	AB	9	2.95	0.87	172.6	10.422	169.99	10.58	2.6	0.2
S 676	16010+3318	AB	9	0.17	0.86	46.5	141.71	47.28	141.43	0.8	0.3
KUI 69	16038+0459	AB	7	0.47	0.45	275.0	29.214	273.2	28.3	1.8	0.9
STF2007	16060+1319	AC	10	0.04	0.12	137.0	162.727	137.03	162.65	0.0	0.1
GWP2598	16074+1320	AB	11	0.16	0.04	350.3	27.758	349.99	27.82	0.3	0.1
STF2010	16081+1703	AB	11	0.08	0.09	12.0	27.1	13.87	26.81	1.9	0.3
ES 2651	16090+5756	AB	13	1.2	1.21	139.7	12.282	139.24	10.6	0.5	1.7
STF2024	16118+4222	AB	11	0.11	0.04	44.0	22.8	44.3	23.6	0.3	0.8
STF2032	16147+3352	AC	9	0.28	0.5	92.9	26.2	89.05	29.91	3.9	3.7
SHJ 223	16167+2909	AD	9	0.04	0.08	50.0	123.265	50.18	123.12	0.2	0.1
BUP 167	16221+3054	AB	19	0.08	0.31	62.3	188.173	63.38	188.69	1.1	0.5
STFA 29	16224+3348	AD	9	0.01	0.11	153.3	277.11	153.22	277.22	0.1	0.1
H 6 18	16224+3348	BD	12	0.11	0.04	15.9	100.007	15.97	98.73	0.1	1.3
H 5 38	16229+3220	AB	14	0.1	0.05	16.3	31.122	16.0	31.01	0.3	0.1
SMY9002	16240+6131	AF	10	0.03	0.18	17.9	364.586	18.06	362.44	0.2	2.1
SKF 242	16243+5520	AB	9	2.26	0.29	122.8	18.495	126.04	15.02	3.2	3.5
BU 625	16254+1402	AD	21	0.09	0.41	271.8	129.465	271.94	129.99	0.1	0.5
BUP 170	16302+2129	AB	18	0.1	0.81	274.7	245.23	276.03	245.79	1.3	0.6
STF2055	16309+0159	AD	9	0.01	0.12	247.0	308.1	247.08	308.11	0.1	0.0
STF2063	16318+4536	AB	11	0.18	0.06	197.4	16.34	195.14	16.26	2.3	0.1
WEB 6	16354+1703	AB	6	0.09	0.36	359.8	155.53	0.64	155.25	0.8	0.3
STFA 30	16362+5255	CD	8	0.01	0.04	122.5	123.924	122.78	125.48	0.3	1.6
STF2082	16387+4856	AB	10	0.06	0.05	92.5	27.21	92.18	28.05	0.3	0.8
STF2074	16406+0413	BC	9	0.1	0.06	316.0	25.888	316.12	25.7	0.1	0.2
STF2093	16429+3855	AB	9	0.05	0.1	265.2	116.72	265.98	116.43	0.8	0.3
KU 1	16431+7731	AC	3	0.02	0.02	13.0	103.511	13.01	102.45	0.0	1.1
STT 585	16450+0605	AC	9	0.03	0.09	252.7	128.219	253.17	126.36	0.5	1.9
ENG 58	16469+0215	AB	10	0.04	0.12	218.0	148.84	217.28	149.06	0.7	0.2
STF2096	16472+0204	AC	10	0.02	0.18	193.0	214.068	192.94	214.31	0.1	0.2
BUP 174	16478+0515	AB	19	0.09	0.15	80.1	121.21	79.9	121.04	0.2	0.2
BU 627	16492+4559	AE	22	0.11	0.26	269.8	147.197	270.08	147.55	0.3	0.4
STF2103	16496+1316	AC	11	2.34	0.77	247.3	14.768	243.71	13.89	3.6	0.9
STF2110	16550+2544	AB	8	0.09	0.06	91.5	17.877	91.6	17.98	0.1	0.1
TOK 177	16586+1527	AB	6	1.5	0.49	58.9	17.726	65.72	13.7	6.8	4.0
H 4 122	17016+1457	AB	12	0.33	0.1	237.5	18.892	238.06	18.87	0.6	0.0
STFA 33	17037+1336	BD	8	0.0	0.05	272.3	154.534	272.63	154.49	0.3	0.0
STFA 33	17037+1336	AD	8	0.02	0.21	137.7	177.718	137.71	177.84	0.0	0.1
BU 822	17039+1941	AC	21	0.15	0.05	196.5	114.0	196.67	114.79	0.2	0.8
FOX 281	17047+1936	AC	18	0.02	0.2	133.1	106.763	133.18	106.69	0.1	0.1
BU 1088	17053+5428	BC	16	1.48	0.45	185.7	13.57	178.63	10.98	7.1	2.6
HO 412	17080+3556	AB-C	9	0.34	0.73	132.3	20.242	131.57	19.31	0.7	0.9
ES 77	17083+5051	AB	16	0.81	0.39	276.7	18.6	278.61	18.45	1.9	0.2
SHY 713	17111+2414	AB	8	0.41	0.12	74.2	195.505	74.26	195.47	0.1	0.0
KUI 78	17117+4945	AC	12	0.95	0.88	107.0	27.93	106.41	26.66	0.6	1.3
B 2826	17125+1035	AB	15	2.08	0.27	33.7	30.471	31.06	31.62	2.6	1.1
AGC 16	17146+1423	AC	20	2.98	0.3	297.4	19.91	295.79	16.56	1.6	3.4
STF3127	17150+2450	AD	8	0.04	0.14	93.1	191.58	90.47	193.17	2.6	1.6
WAL 79	17161+6043	AC	9	0.12	0.29	79.4	137.29	80.54	134.2	1.1	3.1
ARN 14	17207+3228	AF	18	0.02	0.27	104.0	383.15	101.15	373.99	2.8	9.2
GUI 41	17209+2430	AD	9	0.13	0.78	221.8	222.082	222.66	221.68	0.9	0.4
STF2161	17237+3709	AC	9	0.05	0.15	222.1	117.683	221.39	118.36	0.7	0.7

STT 329	17245+3657	AB	9	0.08	0.04	12.0	33.5	12.43	33.0	0.4	0.5
KUI 81	17259+1655	AC	9	0.37	0.16	218.1	23.233	218.91	23.49	0.8	0.3
BU 1090	17304+5218	AC	22	0.25	0.65	155.4	118.365	155.5	118.72	0.1	0.4
BU 1458	17320+6808	AB	20	0.16	0.22	342.1	154.89	342.32	154.88	0.2	0.0
STF2184	17344+1310	AC	9	0.02	0.08	293.1	128.047	293.24	127.82	0.1	0.2
SDR 1	17350+6153	AB-D	9	1.6	0.51	251.7	23.86	258.61	20.01	6.9	3.8

Conclusion

The described automated approach to double star surveys shows promise for analyzing systems which are chosen appropriately for the equipment. Despite occasional mis-categorizations, the system may prove beneficial by screening out star pairs demonstrating expected values and, thereby, allowing the astronomer to investigate the unexpected measurements more carefully.

I would like to thank Rick McAlister, Thomas Bisque and Robert Argyle for their assistance and thoughts concerning this project. I would also like to thank Software Bisque for producing such capable astronomy mounts and flexible software. This project makes use of Washington Double Star measurements collected and published by the US Naval Observatory.

ASTRONOMICAL ASSOCIATION OF QUEENSLAND 2020 PROGRAMME: BLUE STAR OBSERVATORY MEASUREMENT OF NINE NEGLECTED SOUTHERN MULTIPLE STARS

Peter N. Culshaw, Diane Hughes, John Hughes, Des Janke, Graeme Jenkinson,
Astronomical Association of Queensland, Australia.
E-mail: bluestars@iprimus.com.au

Abstract

This paper presents some results from our 2020 programme of photographic measurements of southern multiple stars. All results were obtained using an Atik 460EX mono CCD camera used in conjunction with an equatorially mounted 400-mm F4.5 Newtonian reflector. Fellow AAQ members Culshaw, Hughes and Hughes provided invaluable assistance with image processing using Losse's REDUC software.

System		Last listed measure			New measure			Comment
		PA °	Sep.″	Epoch	PA°	Sep.″	Epoch∗	
BRT2806		349	4.0	1894	205.72	5.643	2020.274	Large decrease in PA. Possible cataloguing error.
JSP914	AC	184	2.7	1929	188.05	7.96	2020.285	Clear increase in both axes.
RST4501	AB	125	3.5	1929	128.08	3.92	2020.282	Modest change in PA.
B1225		10	0.5	1931	180.12	3.03	2020.452	Possible incorrect original N-S alignment.
B1226		257	3.4	1998	257.43	3.41	2020.452	No movement evident.
BRT3169		247	3.3	1892	218.27	2.31	2020.320	Significant change in PA.
BRT2075		217	4.5	1918	164.13	2.28	2020.323	Large decrease in PA.
DON786		151	2.8	1970	161.13	3.44	2020.80	Consistent increase in PA.
RSS438		162	5.7	1975	160.24	5.79	2020.802	Small decrease in PA.

∗ Epochs of new measures given in Besselian years as the average of the observations making up the measure.

The mean 95% confidence intervals for the new measures were ±0°.839 in PA and±0″.106 in separation. The results were as follows:

Introduction

These latest results are part of an ongoing programme commenced in 2008 by the Double Star Section of the Astronomical Association of Queensland. The target stars were selected from the Washington Double Star Catalogue and were observed in Queensland, Australia from a latitude of approximately 27° S.

Method

Nightly sets of one hundred images were obtained with the equipment described above, after which the images were stacked using Atik DAWN software and then analysed using the astrometric double star program REDUC[1]. Approximately ten stacked images of each target were taken per night for seven nights and the results averaged to obtain measures of separation and position angle with sufficient confidence.

Full details of the method are given in Napier-Munn and Jenkinson[2]. Subsequent work on the errors inherent in the method is described in Napier-Munn and Jenkinson[3]. As proficiency has grown in the use of this equipment with the 400-mm reflector, close doubles with considerable magnitude difference between the components have been successfully measured.

Fellow AAQ members Culshaw, Hughes and Hughes provided invaluable assistance with image processing using Losse's REDUC software, and Janke with processing the original FITS image files into JPEG photographs.

Results

For all of the systems shown below the information is first reproduced, showing the epoch 2000 position, magnitudes, separation, PA, and the last recorded measurement. The new measurements are then given in tabular form, including the mean and standard deviation and 95% confidence limits. Any uncertainties between the images and the last recorded measurements are discussed. Finally a conclusion is given as to whether any movement of the component stars has occurred in PA or separation, based on the P-value for the t-test comparing the new mean values with the catalogued value ($P < 0.05$ is considered as evidence of change).

As detailed in the tabulated results above, BRT2806, BRT3169 and BRT2075 show considerable differences in PA between the original Barton measures and our 2020 results.

BRT2806 Shows possible incorrect original cataloging of co-ordinates which shows a single star to the east (right) of the imaged pair as the original target.

B1225 A possible reversed North-South alignment in the original measure may explain the difference.

Please note that all attached images are aligned with North to the bottom and East to the right.

Figure 1: BRT 2806 in Crux

Date	No. images	PA(°)	Sep″
29 March 2020	10	205.63	5.66
30 March 2020	10	205.54	5.64
01 April 2020	10	205.77	5.690
04 April 2020	10	205.69	5.647
05 April 2020	10	205.69	5.635
06 April 2020	10	205.80	5.638
22 April 2020	10	205.94	5.58
Mean		205.723	5.643
Standard deviation		0.129	0.033
95% CI		±0.119	0.031
P(t) movement		0.000	0.000

Table 2: Individual measures of BRT 2806

BRT2806 Crux RA. 12 04 29 DEC. -57 24 52 Last Measure 1894 MAG. 11.9 & 13.1 PA. 349° SEP. 4″.0
COMMENTS: Large decrease in PA since original measure 126 years ago. Possible incorrect cataloguing of original co-ordinates.

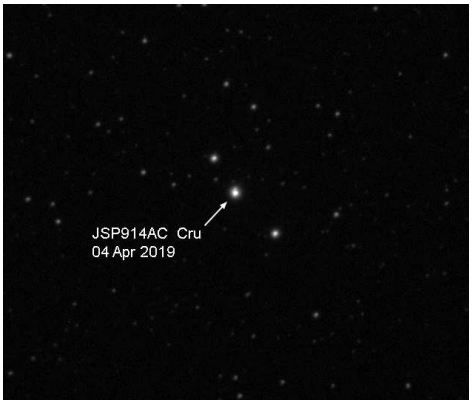

Figure 2: JSP 914 AC in Crux

Date	No. images	PA(°)	Sep″
01 Apr 2020	10	188.34	7.875
04 Apr 2020	10	187.57	7.788
05 Apr 2020	10	188.40	8.011
06 Apr 2020	10	188.47	7.977
08 Apr 2020	10	187.25	8.022
17 Apr 2020	10	188.05	8.011
27 Apr 2020	10	188.25	8.066
Mean		188.047	7.964
Standard deviation		0.464	0.098
95% CI		±0.429	0.090
P(t) movement		0.000	0.000

Table 3: Individual measures of JSP 914 AC

JSP914 AC Crux RA. 12 16.2 DEC. -60 32 Last Measure 1929 MAG. 9.78 & 14.00 PA. 184° SEP. 2″.7
COMMENTS: Clear changes in both PA & separation over 91 years.

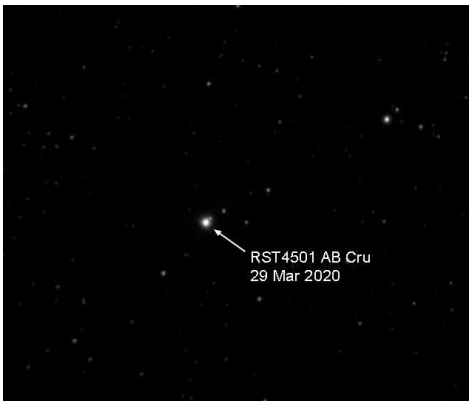

Figure 3: RST 4501 in Crux

Date	No. images	PA(°)	Sep″
29 Mar 2020	10	128.31	3.88
01 Apr 2020	10	125.38	3.923
04 Apr 2020	10	127.33	3.901
05 Apr 2020	10	129.75	3.986
06 Apr 2020	10	128.12	3.943
23 Apr 2020	10	130.50	3.805
24 Apr 2020	10	127.14	4.024
Mean		128.076	3.923
Standard deviation		1.705	0.072
95% CI		± 1.577	0.066
P(t) movement		0.003	0.000

Table 4: Individual measures of RST 4501

RST4501AB Crux RA. 12 31.1 DEC. -59 32 Last Measure 1929 MAG. 8.86 & 13.5 PA. 125° SEP. 3″.5
COMMENTS: Modest increase in PA since initial measure.

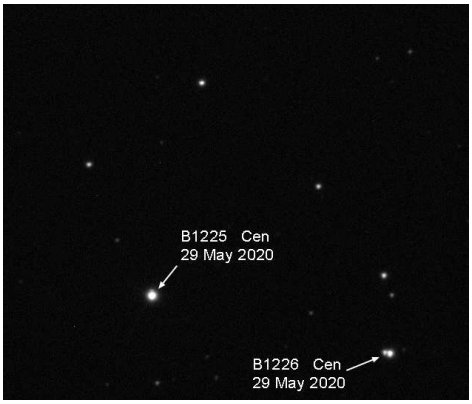

Figure 4: B 1225 in Centaurus

Date	No. images	PA(°)	Sep″
26 May 2020	10	179.80	2.922
28 May 2020	10	0.00	0.000
29 May 2020	10	180.34	3.128
30 May 2020	10	180.69	3.162
31 May 2020	10	179.78	3.030
22 Jun 2020	10	0.00	0.000
23 Jun 2020	10	180.00	2.902
Mean		180.122	3.029
Standard deviation		0.389	0.117
95% CI		±0.483	0.146
P(t) movement		0.000	0.000

Table 5: Individual measures of B 1225

B1225 Centaurus RA. 13 19.4 DEC. -42 01 Last Measure 1931 MAG. 9.9 & 11.6 PA. 10° SEP. 0″.5
COMMENTS: Possible incorrect North - South alignment on original recorded PA may explain large difference between measures. Two nights results not included due to poor quality images.

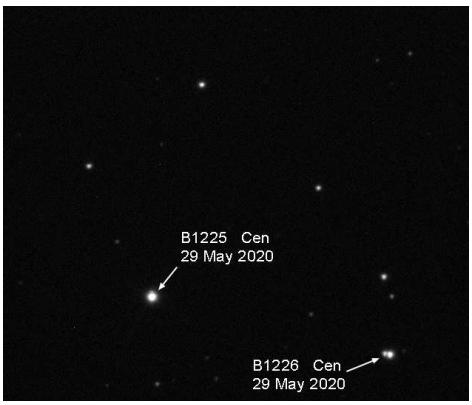

Figure 5: B 1226 in Centaurus

Date	No. images	PA(°)	Sep″
26 May 2020	10	257.24	3.47
08 May 2020	10	?	?
29 May 2020	10	256.81	3.392
30 May 2020	10	257.81	3.468
31 May 2020	10	257.16	3.022
22 Jun 2020	10	258.47	3.723
23 Jun 2020	10	257.07	3.354
Mean		257.427	3.405
Standard deviation		0.608	0.227
95% CI		±0.638	0.239
P(t) movement		0.000	0.000

Table 6: Individual measures of B 1226

B1226 Centaurus RA. 13 20.5 DEC. -42 06 Last Measure 1998 MAG. 11.2 & 12.7 PA.257° SEP. 3″.4
COMMENTS: No probable movement over 22 years. One night's results not included due to poor quality images.

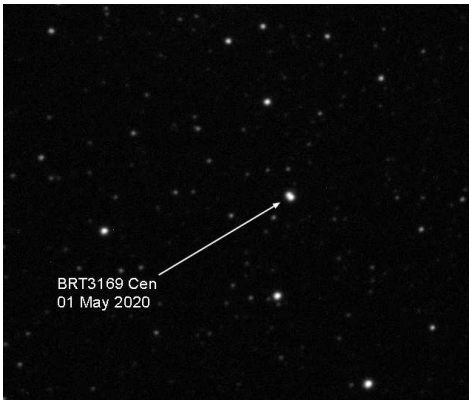

Figure 6: BRT 3169 in Centaurus

Date	No. images	PA(°)	Sep″
23 Apr 2020	10	218.46	2.414
24 Apr 2020	10	217.67	2.307
25 Apr 2020	10	217.77	2.174
26 Apr 2020	10	217.90	2.173
28 Apr 2020	10	217.42	2.328
29 Apl 2020	10	219.44	2.361
01 May 2020	10	219.24	2.431
Mean		218.271	2.313
Standard deviation		0.797	0.105
95% CI		±0.737	0.097
P(t) movement		0.000	0.000

Table 7: Individual measures of BRT 3169

BRT3169 Centaurus RA. 13 28.3 DEC. -58 43 Last Measure 1892 MAG. 11.99 & 12.46 PA. 247° SEP. 3″.3
COMMENTS: Significant change in position angle over 128 years - slight decrease in separation.

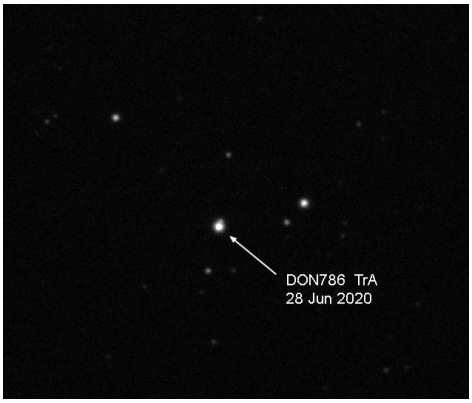

Figure 7: DON 786 in Triangulum Australe

Date	No. images	PA(°)	Sep″
26 Jun 2020	10	157.62	3.624
28 Jun 2020	10	161.59	3.536
29 Jun 2020	10	162.66	3.309
16 Jul 2020	10	161.95	3.421
18 Jul 2020	10	161.38	3.423
19 Jul 2020	10	159.62	3.408
20 Jul 2020	10	163.12	3.339
Mean		161.134	3.437
Standard deviation		1.908	0.110
95% CI		±1.765	0.101
P(t) movement		0.000	0.000

Table 8: Individual measures of DON 786

DON 786 Triangulum Australe RA. 16 16.0 DEC. -67 08 Last Measure 1970 MAG. 9.62 & 13.9PA. 151° SEP. 2″.8
COMMENTS: Increase in PA appears consistent with both previous measures. Separation increasing again after reduction from 1929 to 1970.

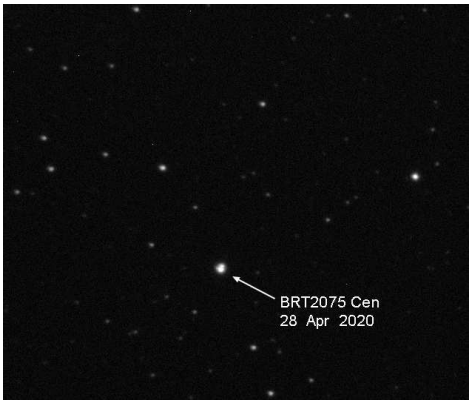

Figure 8: BRT 2075 in Centaurus

Date	No. images	PA(°)	Sep″
24 Apr 2020	10	165.31	2.117
25 Apr 2020	10	164.94	2.203
26 Apr 2020	10	163.72	2.316
28 Apr 2020	10	164.08	2.363
29 Apr 2020	10	163.43	2.438
01 May 2020	10	164.89	2.167
02 May 2020	10	162.51	2.357
Mean		164.126	2.280
Standard deviation		0.993	0.119
95% CI		±0.918	0.110
P(t) movement		0.000	0.000

Table 9: Individual measures of BRT 2075

BRT2075 Centaurus RA. 14 00.3 DEC. -53 50 Last Measure 1918 MAG. 10.4 & 10.8 PA. 217° SEP. 4″.5
COMMENTS: Large decrease in PA since original measurement.

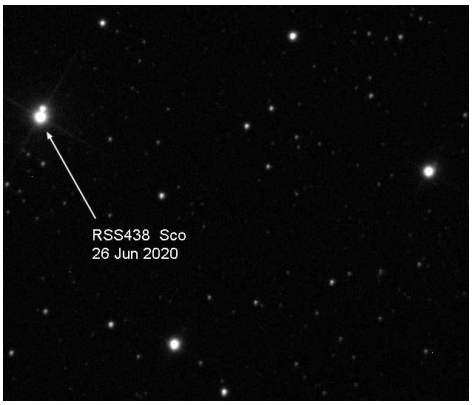

Figure 9: RSS 438 in Scorpius

Date	No. images	PA(°)	Sep″
26 Jun 2020	10	160.72	5.852
28 Jun 2020	10	160.14	5.814
29 Jun 2020	10	159.89	5.861
16 Jul 2020	10	161.74	5.63
18 Jul 2020	10	158.52	5.785
19 Jul 2020	10	160.39	5.741
20 Jul 2020	10	160.31	5.859
Mean		160.244	5.792
Standard deviation		0.966	0.084
95% CI		±0.893	0.078
P(t) movement		0.003	0.028

Table 10: Individual measures of BRT 2021

RSS438 Scorpius RA. 17 20.8 DEC. -40 23 Last Measure 1975 MAG. 9.3 & n/a PA. 162° SEP. 5″.7
COMMENTS: Small decrease in PA evident.

Acknowledgements

This research has made use of the Washington Double Star Catalogue maintained at the U.S. Naval Observatory. The Edward Corbould Research Fund administered by the Astronomical Association of Queensland for granting of funds to upgrade imaging camera and observatory computer to suit.

References

1. Losse, F. REDUC software, V4.5.1. `http://www.astrosurf.com/hfosaf/uk/tdownload.htm`
2. Napier-Munn, T.J. and Jenkinson, G., 2009. Measurement of some neglected southern multiple stars in Pavo.// *Webb Society Double Star Section Circulars*, **17**, 6-12.
3. Napier-Munn, T.J and Jenkinson G., 2014. Analysis of errors in the measurement of double stars using imaging// and the REDUC software. *Journal of Double star Observations* **10** No.3.
4. Argyle, R.W. (ed.), 2012. *Observing and Measuring Visual Double Stars* (2nd edition). Springer.

ASTRONOMICAL ASSOCIATION OF QUEENSLAND 2020 PROGRAMME: BLUE STAR OBSERVATORY MEASUREMENT OF TEN NEGLECTED SOUTHERN MULTIPLE STARS

Peter N. Culshaw, Diane Hughes, John Hughes, Des Janke, Graeme Jenkinson,
Astronomical Association of Queensland, Australia.

E-mail: bluestars@iprimus.com.au

Abstract

This paper presents the final results of our photographic measurements of southern multiple stars from 2017 - 2019. All results were obtained using an Atik 460EX mono CCD camera used in conjunction with an equatorially mounted 400-mm F4.5 Newtonian reflector. Fellow AAQ members Culshaw, Hughes and Hughes provided invaluable assistance with image processing using Losse's REDUC software. The mean 95% confidence intervals for the new measures were ±0°.539 in PA and ±0″.125 in separation. The results were as follows:

System	Last listed measure			New measure			Comment
	PA °	Sep.″	Epoch	PA°	Sep.″	Epoch∗	
HU1406	189	2.8	1922	186.75	2.65	2018.996	Slight decrease in both axes.
JSP562	205	3.3	1965	205.97	3.17	2019.274	Little probable movement.
B805	260	4.4	2000	257.71	4.61	2019.274	Some movement in PA.
B1241	189	3.6	1929	186.00	3.28	2018.338	Definite movement in PA.
RSS331	254	8.2	1976	255.77	7.90	2017.395	Slight increase in PA.
RSS449	257	11.2	1975	253.51	10.99	2018.453	Decrease in both axes.
J1755	105	4.0	1941	95.15	3.947	2018.543	Significant change in PA.
HU1195	321	2.1	1921	23.34	6.47	2019.699	Questionable large change in PA.
GLP19AC	36	11.5	1910	290.55	21.35	2018.702	Questionable large change in both axes.
SCA122	113	48.4	1986	201.14	36.40	2018.666	Considerable change in both axes.

Epochs of new measures given in Besselian years as the average of the observations making up the measure.

Introduction

These results are part of an ongoing programme commenced in 2008 by the Double Star Section of the Astronomical Association of Queensland. The target stars were selected from the Washington Double Star Catalogue (WDSC) and were observed in Queensland, Australia from a latitude of approximately -27° South.

Method

Nightly sets of one hundred images were obtained with the equipment described above, after which the images were stacked using Atik DAWN software and then analysed using the astrometric double star program REDUC[1]. Approximately ten stacked images of each target were taken per night for seven nights and the results averaged to obtain measures of separation and position angle with sufficient confidence.

Full details of the method are given in Napier-Munn and Jenkinson[2]. Subsequent work on the errors inherent in the method is described in Napier-Munn and Jenkinson[3]. As proficiency has grown in the use of this equipment with the 400-mm reflector, close doubles with considerable magnitude difference between the components have been successfully measured.

Fellow AAQ members Culshaw, Hughes and Hughes provided invaluable assistance with image processing using Losse's REDUC software, and Janke with processing the original FITS image files into JPEG photographs.

Results

For all of the systems shown below the WDSC information is first reproduced, showing the epoch 2000 position, magnitudes, separation, PA, and the last recorded measurement. The new measurements are then given in tabular form, including the mean and standard deviation and 95% confidence limits. Any uncertainties between the images and the last recorded measurements are discussed. Finally a conclusion is given as to whether any movement of the component stars has occurred in PA or separation, based on the P-value for the t-test comparing the new mean values with the catalogued value ($P < 0.05$ is considered as evidence of change).

JSP562	location coordinates differ from actual position as per imaged field of view.
HU1195	shows a very large decrease in PA over 98 years. Given the relatively small separation (2″.1) measured in 1921, perhaps the secondary measured at that time may have moved closer to the primary and not be separable with the 400-mm reflector.
J1755	location coordinates also differ from actual position as per imaged field of view.
SCA122	shows considerable change in both axes over only 32 years.
GLP19AC	no probable 'C' component found in the area of original measurement. Very large changes in both axes over 108 years.

Please note that all attached images are aligned with North to the bottom and East to the right.

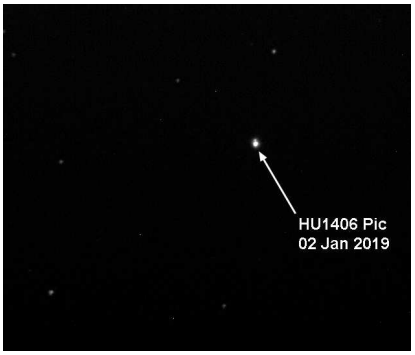

Figure 1: HU 1406 in Pictor

Date	No. images	PA°	Sep″
28 Dec 2018	10	185.72	2.65
29 Dec 2018	10	187.06	2.626
30 Dec 2018	10	187.37	2.622
31 Dec 2018	10	186.68	2.711
01 Jan 2019	10	186.21	2.71
02 Jan 2019	10	186.89	2.534
04 Jan 2019	10	187.3	2.675
Mean		186.747	2.647
Standard deviation		0.600	0.061
95% CI		±0.555	0.057
P(t) movement		0.000	0.001

Table 2: Individual measures of HU 1406

HU1406 Pictor RA. 06 15.4 DEC. -56 09 Last Measure 1922 MAG. 9.78 & 13.6 PA. 189° SEP. 2″.8
COMMENTS: Slight decreases in both axes.

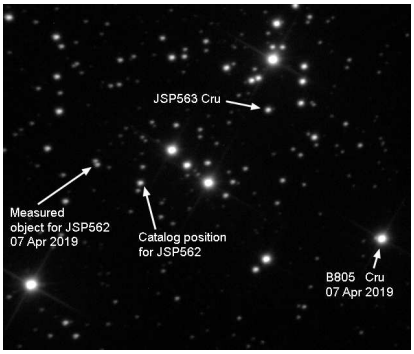

Figure 2: JSP 562 in Crux

Date	No. images	PA°	Sep″
4 Apr 2019	10	205.57	3.283
5 Apr 2019	10	206.22	3.211
6 Apr 2019	10	205.76	3.093
7 Apr 2019	10	205.97	3.000
12 Apr 2019	10	206.28	3.224
15 Apr 2019	10	?	?
17 Apr 2019	10	205.99	3.193
Mean		205.965	3.167
Standard deviation		0.269	0.103
95% CI		±0.283	0.108
P(t) movement		0.000	0.000

Table 3: Individual measures of JSP 562

JSP562 Crux RA. 12 53.5 DEC. -60 21 Last Measure 1965 MAG. 10.3 & 10.4 PA. 205° SEP. 3″.3
COMMENTS: Little probable movement over the last 55 years. Poor quality 15 April images not included.

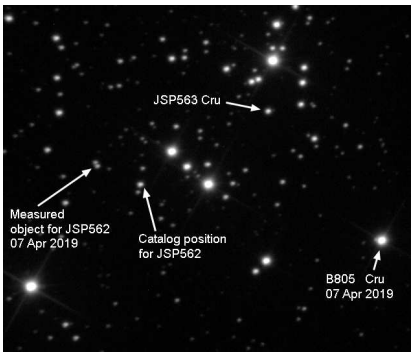

Figure 3: B 805 in Crux

Date	No. images	PA°	Sep″
04 Apr 2019	10	255.24	4.440
05 Apr 2019	10	259.34	4.581
06 Apr 2019	10	257.90	4.898
07 Apr 2019	10	257.36	4.604
12 Apr 2019	10	258.17	4.668
15 Apr 2019	10	?	?
17 Apr 2019	10	258.24	4.453
Mean		257.708	4.607
Standard deviation		1.372	0.168
95% CI		±1.440	0.176
P(t) movement		0.009	0.029

Table 4: Individual measures of B 805

B805 Crux RA. 12 54.0 DEC. -60 20 Last Measure 2000 MAG. 6.77 & 13.2 PA. 260° SEP. 4″.4
COMMENTS: Some movement evident in PA over 19 years. 15 April poor quality images not used

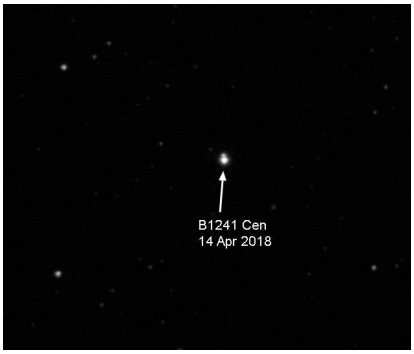

Figure 4: B 1241 in Centaurus

Date	No. images	PA°	Sep″
14 Apr 2018	10	186.43	3.249
09 May 2018	10	185.38	3.538
11 May 2018	10	185.41	3.259
13 May 2018	10	186.59	3.235
15 May 2018	10	185.42	3.265
16 May 2018	10	186.01	3.119
21 May 2018	10	186.76	3.265
Mean		186.00	3.276
Standard deviation		0.603	0.127
95% CI		±0.557	0.117
P(t) movement		0.000	0.000

Table 5: Individual measures of B 1241

B1241 Centaurus RA. 14 15.4 DEC. -50 46 Last Measure 1929 MAG. 10.0 & 13.0 PA. 189° SEP. 3″.6
COMMENTS: Definite movement in PA. Not evident for separation.

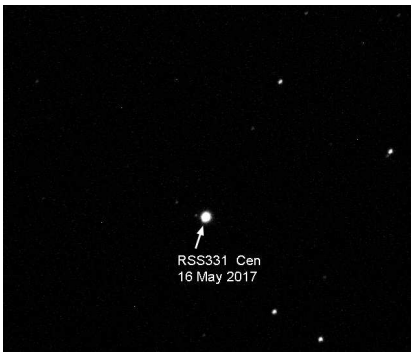

Figure 5: RSS 331 in Centaurus

Date	No. images	PA°	s Sep″
16 May 2017	10	256.16	8.111
24 May 2017	10	255.80	7.939
25 May 2017	10	255.86	7.834
26 May 2017	10	255.77	7.793
27 May 2017	10	255.97	7.873
30 May 2017	10	255.05	7.856
02 Jun 2017	10	255.75	7.861
Mean		255.766	7.895
Standard deviation		0.346	0.105
95% CI		±0.320	0.097
P(t) movement		0.000	0.000

Table 6: Individual measures of RSS 331

RSS331 Centaurus RA. 14 22.7 DEC. -30 36 Last Measure 1976 MAG. 9.89 & 17.0 PA. 254° SEP. 8″.2
COMMENTS: Slight increase in PA. Little probable change in separation.

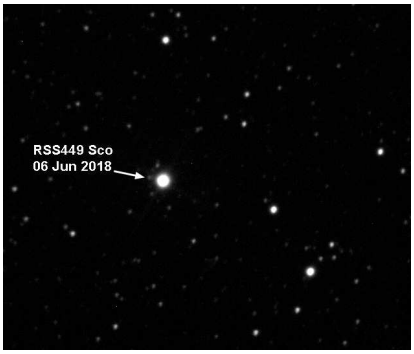

Figure 6: RSS 449 in Scorpius

Date	No. images	PA°	Sep″
06 Jun 2018	10	253.21	10.509
12 Jun 2018	10	253.58	11.208
15 Jun 2018	10	253.65	10.616
16 Jun 2018	10	253.23	10.775
17 Jun 2018	10	253.88	10.905
19 Jun 2018	10	253.47	10.575
22 Jun 2018	10	253.15	10.297
Mean		253.453	10.698
Standard deviation		0.270	0.296
95% CI		±0.250	0.274
P(t) movement		0.000	0.000

Table 7: Individual measures of RSS 449

RSS449 Scorpius RA. 17 34.1 DEC. -41 39 Last Measure 1975 MAG. 8.1 & 15.3 PA. 257° SEP. 11″.2
COMMENTS: Decreases in both PA and separation evident.

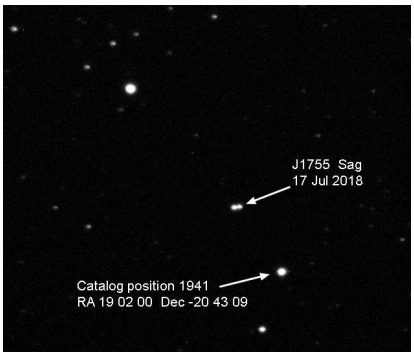

Figure 7: J1755 in Sagittarius

Date	No. images	PA°	Sep″
13 Jul 2018	10	95.82	3.934
14 Jul 2018	10	95.30	4.057
15 Jul 2018	10	95.17	4.019
16 Jul 2018	10	94.47	3.798
17 Jul 2018	10	95.17	3.724
18 Jul 2018	10	94.93	4.015
22 Jul 2018	10	95.19	4.08
Mean		95.15	3.947
Standard deviation		0.405	0.136
95% CI ±		0.375	0.126
P(t) movement		0.000	0.000

Table 8: Individual measures of J 1755

J1755 Sagittarius RA. 19 02.0 Dec -20 43 Last measure 1941 MAG 10.23 & 10.4 PA. 105° SEP. 4″.0 Date
COMMENTS: Significant change in PA. No probable movement in separation.

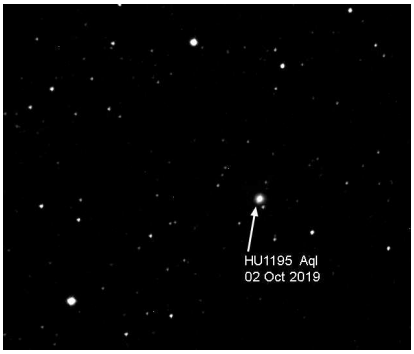

Figure 8: HU 1195 in Aquila

Date	No. images	PA°	Sep″
24 Aug 2019	10	24.32	6.615
04 Sep 2019	10	21.76	6.259
18 Sep 2019	10	23.17	6.363
23 Sep 2019	10	24.31	6.353
29 Sep 2019	10		
02 Oct 2019	10	23.06	6.603
03 Oct 2019	10	23.43	6.622
Mean		23.342	6.469
Standard deviation		0.950	0.162
95% CI		±0.997	0.170
P(t) movement		0.000	0.000

Table 9: Individual measures of HU 1195

HU1195 in Aquila. RA. 19 43.6 DEC. +13 42 Last Measured 1921 MAG. 8.53 & 14.30 PA. 321° Sep. 2″.1
COMMENTS Poor quality images on 29 September not used. Very large movement in PA over 98 years.

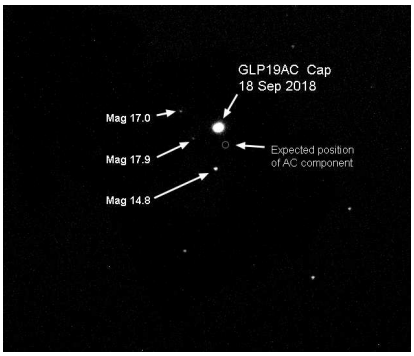

Figure 9: GLA 19AC in Capricornus

Date	No. images	PA°	Sep″
01 Sep 2018	10	290.22	21.278
08 Sep 2018	10	290.55	21.381
12 Sep 2018	10	290.80	21.338
16 Sep 2018	10	290.74	21.301
18 Sep 2018	10	290.72	21.350
23 Sep 2018	10	290.69	21.411
28 Sep 2018	10	290.10	21.399
Mean		290.546	21.351
Standard deviation		0.276	0.050
95% CI		±0.256	0.046
P(t) movement		0.000	0.000

Table 10: Individual measures of GLP 19AC

GLP19AC Capricornus RA. 21 43.4 DEC. -14 10 Last Measure 1910 MAG. 10.54 & 14.10 PA. 36?° SEP. 11″.5
COMMENTS: No 'C' component sighted in area of original measurement.

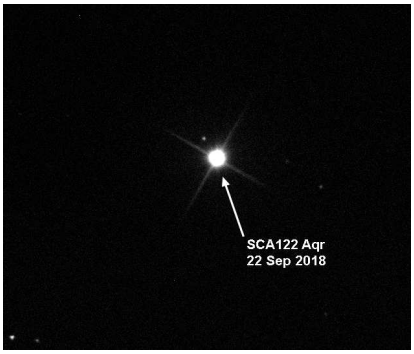

Figure 10: SCA 122 in Aquarius

Date	No. images	PA°	Sep″
10 Aug 2018	10	209.90	36.325
08 Sep 2018	10	210.22	36.371
12 Sep 2018	10	210.35	36.586
16 Sep 2018	10	210.28	36.465
18 Sep 2018	10	210.57	36.536
22 Sep 2018	10	210.26	36.461
23 Sep 2018	10	209.43	36.020
Mean		210.144	36.395
Standard deviation		0.372	0.188
95% CI		±0.344	0.174
P(t) movement		0.000	0.000

Table 11: Individual measures of SCA 122

SCA 122 Aquarius RA. 22 10.6 DEC. -04 16 Last Measure 1986 MAG. 6.01 & 12.0 PA. 113° SEP. 48″.4
COMMENTS: Considerable change in both axes since the original 1986 measure.

Acknowledgements

This research has made use of the Washington Double Star Catalogue maintained at the U.S. Naval Observatory. The Edward Corbould Research Fund administered by the Astronomical Association of Queensland for granting of funds to upgrade imaging camera and observatory computer to suit.

References

1) Losse, F. REDUC software, V4.5.1. `http://www.astrosurf.com/hfosaf/uk/tdownload.htm`
2) Napier-Munn, T.J. and Jenkinson, G., 2009. *Measurement of some neglected southern multiple stars in Pavo. Webb Society Double Star Section Circular* **17**, 6-12.
3) Napier-Munn, T.J and Jenkinson G., 2014. *Analysis of errors in the measurement of double stars using imaging and the Reduc software, Journal of Double star Observations* **10** No.3.
Argyle, R.W.(ed.), 2012, *Observing and Measuring Visual Double Stars* 2nd edition. Springer.

CMOS ASTROMETRY OF DOUBLE STARS IN 2020

Grant L. Morris, Greeley, Colorado, USA

E-mail: glmorri@aol.com

Introduction

This paper presents astrometric measurements which were made in September and November of 2020 in Greeley, Colorado USA. The equipment and procedures used were the same as described in Morris[1] with the exception of a different telescope and mount. The scale and orientation of the imaging camera was derived for each observing session with a binary pair selected for long-term stability of position angle and separation.

An 11-inch SCT (C11) mounted on an equatorial mount (Losmandy GM8) was combined with a motorized Crayford focuser, and a flip-mirror for switching between a finding and centering eyepiece or the remainder of the optical train. This consisted of a 3X Barlow and a ZWO ASI 120 monochrome CMOS camera. This optical train and camera produced a pixel scale of approximately 0″.0701 per pixel. The ZWO ASI 120 camera has a peak spectral sensitivity of nearly 80% at 540 nm. All observed binaries were close enough to the zenith at the observing site (40° 24′ 36″ N 104° 41′ 54″ W) that no corrector for atmospheric dispersion was used.

Image Acquisition and Reduction

Acquisition and Reduction procedure and considerations have been described previously[1].

Results

Table 1. Calibration double stars

Pair	Comp	RA	Dec	Va	Vb	PA	Sep	Epoch	N	Obs
STF2445	AB	19046	+2320	7.25	8.57	262.42	12.41	2020.668	4	GRM
STF2551	AB	19374	+2249	9.69	10.53	42.10	6.77	2020.671	3	GRM
STF2577	AB	19452	+2055	8.43	9.56	261.58	5.96	2020.698	4	GRM
STF2762	AB	21086	+3012	5.7	8.1	303.11	3.34	2020.846	4	GRM

PA (position angle) is in degrees(°), and Sep (separation) is in arc seconds(″). Epoch identifies the night when that star was used to calibrate the measurements in Table 2. N is the number of acquisition sequences. Any differences between PA and Sep values used for calibration and values preferred by the reader may be properly treated as constant error and applied to values in Table 2.

Table 2. Measures of double stars

Pair	Comp	RA	Dec	Va	Vb	PA	Sep	Epoch	N	Obs
STF2455	AB	19069	+2210	7.42	9.44	25.6	9.89	2020.668	4	GRM
STF2457		19071	+2235	7.46	9.52	200.6	10.24	2020.698	4	GRM
STF2459		19074	+2558	9.12	10.07	232.3	13.83	2020.698	3	GRM
STF2499		19186	+2157	8.82	9.12	324.0	2.65	2020.698	3	GRM
WSI22		19249	+2126	10.32	10.47	271.6	15.11	2020.668	3	GRM
STF3111		19251	+2150	9.92	10.16	116.3	2.45	2020.671	4	GRM

STF2521	AB	19265	+1953	5.82	10.5	31.3	28.96	2020.698	3	GRM
STF2525	AB	19266	+2719	8.19	8.39	289.0	2.28	2020.668	6	GRM
STF2523	AB	19268	+2110	7.95	8.05	148.3	6.40	2020.668	3	GRM
STF3132	AB	19282	+2013	10.1	11.8	39.4	7.79	2020.698	5	GRM
STF2548		19365	+2500	8.47	9.85	99.9	9.31	2020.668	2	GRM
STF2584		19484	+2212	9.14	9.2	293.2	1.93	2020.671	3	GRM
STF2586	AB	19486	+2458	7.56	9.28	225.9	3.83	2020.698	3	GRM
STT388	AB	19524	+2551	8.32	8.45	138.2	3.89	2020.671	3	GRM
DJU4		19535	+2405	4.63	7.37	247.8	1.53	2020.671	4	GRM
STT395		20020	+2456	5.83	6.19	128.8	0.73	2020.846	4	GRM
STF2631		20072	+2106	8.13	9.12	338.6	4.68	2020.698	5	GRM
STF2655	AB	20141	+2213	7.89	7.95	3.0	6.17	2020.671	4	GRM
STT402		20145	+2451	7.46	10.73	33.4	15.32	2020.698	4	GRM
STF2698		20338	+2808	8.66	9.09	304.6	4.50	2020.668	3	GRM
WFC257		20396	+2018	8.6	10	317.2	6.73	2020.698	3	GRM
STF2716	AB	20410	+3218	5.75	8.1	45.3	2.77	2020.846	4	GRM
STF2724		20445	+2356	8.97	9	151.0	2.59	2020.668	3	GRM
STF2727	AB	20467	+1607	4.36	5.03	266.0	8.82	2020.846	4	GRM
STT413	AB	20474	+3629	4.73	6.26	1.1	0.90	2020.846	4	GRM
STF2761		21074	+2429	9.29	9.76	111.4	5.64	2020.698	3	GRM
STF2769	AB	21105	+2227	6.65	7.42	300.5	18.12	2020.668	5	GRM
STF2822	AB	21441	+2845	4.75	6.18	323.5	1.59	2020.846	3	GRM
BU694	AB	22029	+4439	5.71	7.76	8.0	1.00	2020.846	4	GRM

PA (position angle) is in degrees (°), and Sep (separation) is in arc seconds(″). N is the number of acquisition sequences.

Table 3. Residuals from known orbits.

Pair	ADS	Residual(O−C) PA(°)	Sep (″)	Orbit	Period (yrs)	Date	Grade
STF2525	12447	0.0	+0.05	Izmailov *et al.*	510	2019	3
STT395	13277	+1.0	−0.12	Zirm	1201	2013a	4
DJU4		+0.8	+0.15	Cvetkovic *et al.*	615	2008	5
STF2727	14279	+1.3	−0.03	Hale	3249	1994	4
STT413	14296	+1.0	−0.00	Izmailov *et al.*	801	2019	4
STF2822	15270	+0.3	+0.08	Izmailov *et al.*	692	2019	3

Acknowledgements

Sincere thanks to Bob Argyle for arranging and editing this Circular. Thanks also to Florent Losse and Richard Harshaw for their providing the excellent REDUC and SPECKLETOOLBOX software. This paper made extensive use of the Washington Double Star Catalogue maintained at the U.S. Naval Observatory.

References

1. Morris, G. 2020, *Webb Society Double Star Circulars*, **28**, 19-22.

DOUBLE STAR MEASUREMENTS 2020

Wilfried R.A. Knapp, Vienna, Austria

E-mail: wilfried.knapp@gmail.com

Abstract

The WDS catalog contains currently (January 2021) about 154,000 objects. About 50,000 of these come with a magnitude for the primary with single digit precision indicating rather an estimation than a precise measurement and over 16,000 objects are listed with magnitudes in the blue or red band (WDS note codes $B/K/R/I$) thus in need of a measurement in the V band. After eliminating all objects not suited for resolution with the tools currently available to me (too close, too faint, too bright) about 26,000 objects remained as targets of interest for this project. The selection criterion for the objects for a specific imaging session is then at a given point of time simply the currently highest given altitude to eliminate atmospheric effects as far as possible – so this is then a more or less random selection out of the mentioned 26,000 objects. This report covers about 100 such objects (including several KPP objects also in need of photometry) with images taken 2020 with V-filter to allow for visual magnitude measurement by differential photometry. Several WDS objects that happen to be near the selected targets in the captured images are additionally listed and some objects are listed twice when they are covered by a second imaging session.

Introduction

This report covers photometric and astrometric results from CCD images taken during the year 2020 with iTelescope iT24. Imaging sessions scheduled for the late summer failed due to the horrible wildfires in California so the number of objects is ∼100 a bit smaller than intended. However, the imaging conditions for the spring and early summer sessions were overall quite favourable.

With few exceptions, one single image was taken for all selected objects with V-filter and 20 seconds exposure time. The images were plate solved with Astrometrica using the GAIA DR2 catalog (henceforth DR2) with reference stars in the V range of 8.5 to 16.5 for RA/Dec coordinates and the URAT1 catalog for photometry in the visual band. The objects were then located in the center of the image and astrometry/photometry was done by the rather comfortable Astrometrica procedure with point and click at the components delivering RA/Dec coordinates and Vmag measurements based on all reference stars used for plate solving. The error range of the reported visual magnitudes is calculated from the average V error of the image and the signal to noise ratio of the components. Separation and position angle of the components are calculated from the given RA/Dec coordinates with an error range derived from the RA/Dec position errors. Pairs assumed to be potentially physicals are checked if EDR3 parallaxes and proper motion data support this proposition.

Results of image processing

The measurement results are given in table 1 below with the following structure:

WDS	WDS/WDSS ID
Disc	WDS discoverer designation (blank for WDSS objects)
C	Components (AB if blank)
RA/Dec	Positions for primary and secondary in HH:MM:SS.sss/DD.MM.SS.ss format
ΔRA/ΔDec	Plate solving errors for RA and Dec in arcseconds
Sep	Calculated separation in arcseconds
Err Sep	Separation error
PA	Calculated position angle in degrees
Err PA	Position angle error
Mag	Vmags for both components measured by differential photometry
Err Mag	Magnitude errors
SNR	Signal to noise ratio for both components
ΔV	Plate solving error in V
Date	Julian observation epoch
Notes	Additional comments listed below table 1

WDS	Disc.	C	RA	Dec	ΔRA	ΔDec	Sep	Err. Sep	PA	Err PA	Mag	Err Mag	SNR	ΔV	Date	Not.
08365+3024	KPP179		08 36 30.485	30 23 38.72	0.08	0.07	3.29192	0.10630	48.993	1.850	14.538	0.085	38.15	0.08	2020.31685	4
			08 36 30.677	30 23 40.88							14.954	0.089	26.84			
08445+2827	STF1266		08 44 27.167	28 27 12.49	0.10	0.11	23.26256	0.14866	64.949	0.366	8.660	0.100	275.69	0.10	2020.28932	4
			08 44 28.765	28 27 22.34							9.896	0.100	197.12			
08445+2827	STF1266		08 44 27.158	28 27 12.16	0.08	0.09	23.45606	0.12042	64.251	0.294	8.670	0.080	191.64	0.08	2020.31686	4
			08 44 28.760	28 27 22.35							9.938	0.080	206.40			
08446+2827	KPP3760		08 44 38.379	28 26 37.70	0.10	0.11	3.39739	0.14866	228.526	2.506	12.083	0.100	115.01	0.10	2020.28932	4
			08 44 38.186	28 26 35.45							13.950	0.106	30.97			
08446+2827	KPP3760		08 44 38.367	28 26 37.70	0.08	0.09	3.62551	0.12042	227.914	1.902	12.198	0.081	106.09	0.08	2020.31686	4
			08 44 38.163	28 26 35.27							13.920	0.083	50.09			
08523+3600	KPP182		08 52 20.280	36 00 28.31	0.10	0.11	3.61470	0.14866	52.709	2.355	12.091	0.111	88.99	0.11	2020.28932	4
			08 52 20.517	36 00 30.50							12.870	0.112	56.94			
08523+3600	KPP182		08 52 20.254	36 00 28.15	0.10	0.10	3.77982	0.14142	50.975	2.143	12.016	0.121	66.44	0.12	2020.31686	4
			08 52 20.496	36 00 30.53							12.867	0.126	27.50			
08553+3145	KPP1818		08 55 19.651	31 44 33.41	0.07	0.07	13.97982	0.09899	42.543	0.406	12.652	0.080	130.24	0.08	2020.31695	4
			08 55 20.392	31 44 43.71							14.679	0.082	57.75			
08587+4050	KPP185		08 58 42.757	40 49 32.29	0.07	0.13	4.54957	0.14765	215.367	1.859	12.058	0.122	44.37	0.12	2020.28933	1,6

		08 58 42.525	40 49 28.58							13.461	0.151	11.26				
08587+4050	KPP185	08 58 42.767	40 49 32.27	0.06	0.07	4.43713	0.09220	214.426	1.190	11.992	0.121	87.07	0.12	2020.31687	6	
		08 58 42.546	40 49 28.61							13.179	0.127	24.96				
09030+2805	KPP2405	09 02 58.168	28 05 11.30	0.05	0.06	20.76608	0.07810	10.167	0.215	10.225	0.050	310.31	0.05	2020.31697	4	
		09 02 58.445	28 05 31.74							14.799	0.055	45.23				
09087+4620	KPP1497	09 08 40.277	46 20 22.64	0.04	0.03	11.23693	0.05000	38.534	0.255	11.970	0.060	210.75	0.06	2020.31692	4	
		09 08 40.953	46 20 31.43							14.062	0.061	83.09				
09088+2342	KPP1532	09 08 49.214	23 41 51.82	0.03	0.03	11.56917	0.04243	271.535	0.210	13.376	0.051	119.03	0.05	2020.31693	4	
		09 08 48.372	23 41 52.13							14.978	0.054	52.42				
09150+4311	KPP1607	09 14 57.967	43 11 07.39	0.04	0.04	12.17981	0.05657	74.865	0.266	10.598	0.060	331.34	0.06	2020.31694	4	
		09 14 59.042	43 11 10.57							14.694	0.063	60.04				
09203+3944	KPP1775	09 20 16.911	39 43 55.18	0.09	0.09	13.66616	0.12728	204.858	0.534	12.711	0.051	118.94	0.05	2020.31695	4	
		09 20 16.413	39 43 42.78							14.502	0.053	57.20				
09226+3321	KPP190	09 22 38.397	33 21 07.04	0.09	0.09	4.76279	0.12728	326.465	1.531	12.034	0.091	70.85	0.09	2020.28934	6	
		09 22 38.187	33 21 11.01							12.636	0.093	44.10				
09226+3321	KPP190	09 22 38.422	33 21 07.38	0.08	0.06	4.58799	0.10000	321.088	1.249	12.058	0.112	55.76	0.11	2020.31687	6	
		09 22 38.192	33 21 10.95							12.877	0.112	48.05				
09229+4647	KPP3219	09 22 51.203	46 46 57.83	0.09	0.07	3.62964	0.11402	24.226	1.799	11.516	0.100	188.07	0.10	2020.31685	1,4	
		09 22 51.348	46 47 01.14							14.870	0.116	17.98				
09292+4318	STF1352	09 29 12.092	43 17 38.96	0.06	0.07	21.74319	0.09220	353.194	0.243	10.434	0.070	282.44	0.07	2020.31694		
		09 29 11.856	43 18 00.55							11.551	0.070	194.53				
09292+4318	SIN44 AC	09 29 12.092	43 17 38.96	0.06	0.07	72.95454	0.09220	122.522	0.072	10.434	0.070	282.44	0.07	2020.31694		
		09 29 17.726	43 16 59.74							13.804	0.071	86.13				
09296+4312	KPP1670	09 29 33.804	43 12 22.17	0.06	0.07	12.85287	0.09220	296.177	0.411	13.668	0.071	90.79	0.07	2020.31694	4	
		09 29 32.749	43 12 27.84							14.942	0.073	48.68				
09358+4040	KPP2470	09 35 48.056	40 40 17.25	0.05	0.06	22.03694	0.07810	12.674	0.203	10.265	0.080	279.15	0.08	2020.31698	4	
		09 35 48.481	40 40 38.75							14.434	0.083	52.88				
09415+2727	KPP583	09 41 30.737	27 27 13.32	0.06	0.11	5.64116	0.12530	95.289	1.272	10.778	0.104	37.97	0.10	2020.28934	4	
		09 41 31.159	27 27 12.80							12.919	0.103	40.63				
09415+2727	KPP583	09 41 30.703	27 27 14.01	0.05	0.04	5.39812	0.06403	92.973	0.680	10.617	0.070	229.60	0.07	2020.31689	4	
		09 41 31.108	27 27 13.73							13.105	0.074	45.12				
09521+4315	KPP946	09 52 07.716	43 15 24.81	0.03	0.03	7.76666	0.04243	5.569	0.313	13.505	0.041	115.73	0.04	2020.31691	4	
		09 52 07.785	43 15 32.54							13.588	0.041	109.16				
09574+4658	KPP1996	09 57 21.087	46 58 21.18	0.03	0.03	15.83232	0.04243	300.560	0.154	10.937	0.070	292.13	0.07	2020.31696	4	
		09 57 19.755	46 58 29.23							13.010	0.070	140.02				
09578+4335	KPP750	09 57 47.787	43 35 19.93	0.03	0.03	6.53758	0.04243	218.307	0.372	12.201	0.050	194.66	0.05	2020.31690	6	
		09 57 47.414	43 35 14.80							13.487	0.051	104.01				
10176+3449	KPP1519	10 17 35.654	34 48 34.35	0.02	0.03	11.44862	0.03606	291.146	0.180	10.504	0.060	371.51	0.06	2020.31692	6	
		10 17 34.787	34 48 38.48							14.705	0.062	66.32				
10246+4158	KPP1890	10 24 33.968	41 58 29.38	0.03	0.03	14.78560	0.04243	12.413	0.164	13.301	0.051	123.50	0.05	2020.31696	4	
		10 24 34.253	41 58 43.82							14.353	0.052	75.39				
10280+2741	KPP3816	10 27 57.238	27 41 10.18	0.03	0.03	11.70553	0.04243	333.879	0.208	9.412	0.070	461.10	0.07	2020.31693	4	
		10 27 56.850	27 41 20.69							13.521	0.071	109.16				
10410+3349	KPP2301	10 40 57.696	33 48 55.09	0.02	0.03	19.41953	0.03606	67.728	0.106	14.261	0.071	74.24	0.07	2020.31697	4	
		10 40 59.138	33 49 02.45							14.855	0.072	57.99				

10456+3907	KPP1212	10 45 34.298	39 07 24.17	0.02	0.02	9.37059	0.02828	140.978	0.173	10.440	0.110	343.70	0.11	2020.31691	4
		10 45 34.805	39 07 16.89							14.494	0.111	67.84			
13208+3748	UC2520 AB	13 20 46.506	37 48 27.72	0.03	0.05	4.04657	0.05831	224.423	0.826	13.131	0.071	93.71	0.07	2020.36627	4
		13 20 46.267	37 48 24.83							13.729	0.072	61.07			
13208+3748	PAL4 AC	13 20 46.506	37 48 27.72	0.03	0.05	5.50710	0.05831	21.326	0.607	13.131	0.071	93.71	0.07	2020.36627	
		13 20 46.675	37 48 32.85							14.192	0.072	69.61			
13211+3548	KZA50	13 21 04.031	35 48 32.73	0.02	0.02	25.08074	0.02828	254.316	0.065	10.663	0.040	345.77	0.04	2020.36623	
		13 21 02.046	35 48 25.95							12.269	0.040	205.96			
13235+3534	KZA60	13 23 30.255	35 34 45.03	0.03	0.03	11.47937	0.04243	211.383	0.212	12.845	0.070	148.79	0.07	2020.36625	4
		13 23 29.765	35 34 35.23							13.313	0.071	123.15			
13245+4112	NI31	13 24 29.668	41 11 49.43	0.03	0.03	15.06673	0.04243	328.525	0.161	11.600	0.060	246.60	0.06	2020.36629	7
		13 24 28.971	41 12 02.28							14.550	0.062	67.03			
13303+4024	BVD232	13 30 17.764	40 23 59.00	0.04	0.03	17.09086	0.05000	46.151	0.168	16.571	0.096	19.66	0.08	2020.36636	1
		13 30 18.843	40 24 10.84							16.963	0.108	14.49			
13304+4010	LDS5782	13 30 25.048	40 09 18.34	0.04	0.03	6.71700	0.05000	210.459	0.426	15.838	0.060	32.69	0.05	2020.36636	1,4
		13 30 24.751	40 09 12.55							16.873	0.088	14.40			
13329+4143	LDS4375	13 32 52.293	41 42 49.26	0.04	0.03	6.64912	0.05000	355.654	0.431	11.252	0.070	264.38	0.07	2020.36627	4
		13 32 52.248	41 42 55.89							14.597	0.072	58.49			
13367+3555	KZA72 AB	13 36 44.644	35 39 50.98	0.03	0.05	28.71951	0.05831	96.598	0.116	10.593	0.080	298.92	0.08	2020.36629	
		13 36 46.985	35 39 47.68							10.867	0.080	250.20			
13367+3555	KZA72 AC	13 36 44.644	35 39 50.98	0.03	0.05	50.17134	0.05831	208.573	0.067	10.593	0.080	298.92	0.08	2020.36629	
		13 36 42.675	35 39 06.92							10.797	0.080	248.17			
13365+3543	DAM342	13 36 30.185	35 42 34.55	0.03	0.05	6.03918	0.05831	287.838	0.553	12.951	0.080	128.68	0.08	2020.36629	
		13 36 29.713	35 42 36.40							15.335	0.086	33.20			
13268+3249	UC2539	13 26 50.805	32 49 01.72	0.03	0.03	48.14609	0.04243	237.920	0.050	14.461	0.053	65.59	0.05	2020.36631	6
		13 26 47.569	32 48 36.15							15.750	0.060	32.99			
13383+3314	UC2574	13 38 15.655	33 14 18.52	0.02	0.03	26.01369	0.03606	235.511	0.079	11.766	0.060	213.16	0.06	2020.36638	1,6
		13 38 13.946	33 14 03.79							17.421	0.096	13.97			
13403+3549	UC2583	13 40 14.857	35 49 00.89	0.02	0.03	18.06788	0.03606	125.453	0.114	14.997	0.036	51.79	0.03	2020.36632	4
		13 40 16.067	35 48 50.41							16.094	0.051	25.53			
13413+3422	SKF41 AB	13 41 18.057	34 21 53.62	0.03	0.03	2.41576	0.04243	234.583	1.006	15.750	0.050	35.37	0.04	2020.36632	6
		13 41 17.898	34 21 52.22							15.463	0.048	41.52			
13413+3422	SKF41 AC	13 41 18.057	34 21 53.62	0.03	0.03	20.81711	0.04243	297.152	0.117	15.750	0.050	35.37	0.04	2020.36632	6
		13 41 16.561	34 22 03.12							16.620	0.066	20.16			
13419+3209	TOB131	13 41 51.123	32 09 13.65	0.02	0.04	10.02886	0.04472	190.211	0.255	12.971	0.071	122.13	0.07	2020.36628	
		13 41 50.983	32 09 03.78							15.146	0.073	48.12			
13426+3701	UC2594	13 42 35.901	37 01 26.63	0.02	0.02	19.18347	0.02828	294.122	0.084	11.889	0.090	205.94	0.09	2020.36631	6
		13 42 34.439	37 01 34.47							15.691	0.094	39.26			
13455+3643	UC2606	13 45 27.063	36 43 30.68	0.03	0.03	8.10352	0.04243	39.310	0.300	16.442	0.084	23.33	0.07	2020.36634	4
		13 45 27.490	36 43 36.95							16.552	0.087	20.70			
13459+4157	SLW926	13 45 51.111	41 57 20.47	0.04	0.05	21.74657	0.06403	98.515	0.169	16.738	0.081	14.93	0.04	2020.36634	4,5
		13 45 53.039	41 57 17.25							16.784	0.071	17.91			
13465+3443	CBL597	13 46 32.657	34 43 19.66	0.03	0.03	5.71899	0.04243	176.787	0.425	14.330	0.052	75.36	0.05	2020.36630	2,3,4
		13 46 32.683	34 43 13.95							17.826	0.155	6.92			
13481+3345	LDS4408	13 48 00.883	33 44 29.47	0.02	0.03	69.18559	0.03606	189.432	0.030	13.980	0.071	90.45	0.07	2020.36637	4

		13 47 59.974	33 43 21.22							16.632	0.087	20.75			
13481+3345	LDS4408	13 48 00.883	33 44 29.47	0.02	0.03	168.05474	0.03606	90.283	0.012	13.980	0.071	90.45	0.07	2020.36637	1
		13 48 14.356	33 44 28.64							17.079	0.124	10.14			
13512+3103	CBL598	13 51 09.967	31 03 05.69	0.04	0.05	67.90017	0.06403	119.690	0.054	10.116	0.050	307.36	0.05	2020.36630	
		13 51 14.557	31 02 32.06							15.433	0.057	37.95			
14025+3743	CBR101	14 02 27.164	37 42 54.02	0.03	0.05	12.73674	0.05831	79.093	0.262	16.866	0.091	15.51	0.06	2020.36637	5,6
		14 02 28.218	37 42 56.43							16.764	0.092	15.08			
14037+3846	ALI1091	14 03 43.396	38 46 34.53	0.04	0.03	10.26998	0.05000	187.590	0.279	12.948	0.060	154.04	0.06	2020.36626	
		14 03 43.280	38 46 24.35							13.105	0.060	140.40			
14086+3543	CBR102	14 08 37.298	35 43 15.16	0.03	0.03	18.90436	0.04243	134.457	0.129	13.532	0.041	113.13	0.04	2020.36635	1,4
		14 08 38.406	35 43 01.92							16.682	0.072	17.82			
14123+3646	HJ542	14 12 21.136	36 46 13.41	0.03	0.04	12.34079	0.05000	66.656	0.232	12.978	0.041	155.45	0.04	2020.36624	4
		14 12 22.079	36 46 18.30							12.559	0.040	179.25			
15216+3922	CBL487	15 21 34.849	39 21 59.48	0.03	0.04	25.05210	0.05000	40.394	0.114	13.222	0.041	129.80	0.04	2020.45115	
		15 21 36.249	39 22 18.56							16.551	0.067	19.69			
15301+3232	UC3016	15 30 02.994	32 32 11.90	0.03	0.02	22.56283	0.03606	243.663	0.092	11.951	0.030	232.48	0.03	2020.45110	4
		15 30 01.395	32 32 01.89							13.826	0.032	97.57			
15309+4145	KZA92 AB	15 30 49.350	41 44 58.62	0.09	0.11	15.28294	0.14213	278.959	0.533	13.684	0.071	94.10	0.07	2020.45114	
		15 30 48.001	41 45 01.00							14.296	0.072	68.02			
15309+4145	KZA92 AC	15 30 49.350	41 44 58.62	0.09	0.11	26.05524	0.14213	332.973	0.313	13.684	0.071	94.10	0.07	2020.45114	
		15 30 48.292	41 45 21.83							14.563	0.072	61.76			
15322+4005	KZA99	15 32 11.032	40 04 41.86	0.02	0.03	27.08894	0.03606	337.794	0.076	10.058	0.080	354.53	0.08	2020.45110	
		15 32 10.140	40 05 06.94							15.060	0.083	47.30			
15322+4005	KZA99	15 32 11.030	40 04 41.88	0.03	0.04	27.07101	0.05000	337.831	0.106	10.089	0.060	355.64	0.06	2020.45111	
		15 32 10.140	40 05 06.95							15.004	0.063	52.83			
15323+4003	KZA100 AB	15 32 20.610	40 02 51.79	0.02	0.03	19.72448	0.03606	45.968	0.105	12.135	0.080	189.85	0.08	2020.45110	
		15 32 21.845	40 03 05.50							14.573	0.082	65.24			
15323+4003	KZA100 AB	15 32 20.609	40 02 51.79	0.03	0.04	19.74100	0.05000	46.014	0.145	12.158	0.060	201.83	0.06	2020.45111	
		15 32 21.846	40 03 05.50							14.552	0.062	66.34			
15323+4003	TOB133 AC	15 32 20.610	40 02 51.79	0.02	0.03	16.43026	0.03606	286.913	0.126	12.135	0.080	189.85	0.08	2020.45110	
		15 32 19.241	40 02 56.57							15.911	0.086	32.80			
15323+4003	TOB133 AC	15 32 20.609	40 02 51.79	0.03	0.04	16.55524	0.05000	287.506	0.173	12.158	0.060	201.83	0.06	2020.45111	
		15 32 19.234	40 02 56.77							15.735	0.069	31.60			
15340+4110	KZA101	15 33 57.871	41 09 40.03	0.04	0.04	9.37838	0.05657	204.850	0.346	13.729	0.051	103.32	0.05	2020.45115	4
		15 33 57.522	41 09 31.52							14.047	0.052	83.47			
15355+4145	KZA103	15 35 25.017	41 45 25.34	0.04	0.04	17.23195	0.05657	64.936	0.188	14.722	0.053	63.44	0.05	2020.45116	
		15 35 26.412	41 45 32.64							15.152	0.055	47.97			
15351+4150	E1553	15 35 06.348	41 48 44.68	0.04	0.04	2.47565	0.05657	153.732	1.309	11.242	0.050	163.03	0.05	2020.45116	4
		15 35 06.446	41 48 42.46							11.420	0.051	137.70			
15377+4055	SLW1117	15 37 43.849	40 54 45.83	0.03	0.05	13.21044	0.05831	283.750	0.253	16.448	0.072	20.21	0.05	2020.45119	1,4
		15 37 42.717	40 54 48.97							17.037	0.090	14.07			
15405+4242	BVD243	15 40 32.056	42 41 58.16	0.07	0.10	10.03801	0.12207	101.901	0.697	12.649	0.070	152.58	0.07	2020.45113	2
		15 40 32.947	42 41 56.09							17.423	0.125	9.95			
15419+3313	KPP744	15 41 56.647	33 12 58.80	0.04	0.05	6.56157	0.06403	38.851	0.559	12.324	0.060	182.60	0.06	2020.45112	4
		15 41 56.975	33 13 03.91							13.962	0.061	85.65			

15445+4256	GIC135	15 44 31.255	42 56 49.36	0.04	0.05	12.56674	0.06403	125.739	0.292	14.344	0.043	69.05	0.04	2020.45116	
		15 44 32.184	42 56 42.02							15.535	0.048	41.02			
15461+3840	KPP707	15 46 05.991	38 40 01.94	0.05	0.05	6.31212	0.07071	319.643	0.642	12.806	0.051	147.94	0.05	2020.45114	4
		15 46 05.642	38 40 06.75							14.114	0.052	73.12			
15518+3211	LDS4596	15 51 52.062	32 11 15.43	0.04	0.07	114.79089	0.08062	39.961	0.040	12.767	0.070	142.91	0.07	2020.45114	6
		15 51 57.870	32 12 43.42							16.366	0.085	21.87			
15523+4129	GRV1212	15 52 16.495	41 29 18.62	0.04	0.04	20.17786	0.05657	136.063	0.161	16.046	0.065	25.83	0.05	2020.45117	4
		15 52 17.741	41 29 04.09							16.058	0.064	27.08			
15524+3303	KPP2107	15 52 21.927	33 03 20.43	0.04	0.03	17.01443	0.05000	264.029	0.168	10.541	0.060	295.36	0.06	2020.45108	4
		15 52 20.581	33 03 18.66							13.127	0.061	131.03			
15532+3341	UC3077	15 53 11.828	33 40 47.56	0.04	0.04	33.83703	0.05657	95.784	0.096	15.881	0.068	32.87	0.06	2020.45118	10
		15 53 14.525	33 40 44.15							16.451	0.074	24.82			
15547+3048	UC3088	15 54 41.423	30 48 00.11	0.04	0.05	10.99749	0.06403	44.381	0.334	15.054	0.073	54.29	0.07	2020.45117	4
		15 54 42.020	30 48 07.97							17.515	0.118	10.88			
15568+3816	UC3090	15 56 45.614	38 16 02.47	0.07	0.08	94.19524	0.10630	325.799	0.065	12.515	0.070	158.89	0.07	2020.45113	4
		15 56 41.118	38 17 20.38							15.864	0.078	30.63			
15578+3735	UC3094	15 57 50.196	37 34 51.50	0.04	0.04	60.43215	0.05657	70.322	0.054	15.936	0.107	27.44	0.10	2020.45118	1,4
		15 57 54.983	37 35 11.85							17.433	0.138	10.92			
16032+4213	VKI25	16 03 10.424	42 13 01.51	0.03	0.04	6.11759	0.05000	162.674	0.468	12.038	0.060	194.25	0.06	2020.45108	4
		16 03 10.588	42 12 55.67							13.696	0.061	91.62			
16032+4215	OSO67	16 03 12.939	42 14 39.21	0.03	0.04	26.74832	0.05000	321.212	0.107	9.830	0.060	376.08	0.06	2020.45108	6,7
		16 03 11.430	42 15 00.06							16.619	0.079	20.85			
16037+3709	UC3111	16 03 42.642	37 08 57.47	0.04	0.04	9.53959	0.05657	15.334	0.340	10.318	0.060	284.91	0.06	2020.45108	4
		16 03 42.853	37 09 06.67							13.736	0.061	92.84			
16077+4024	UC3121	16 07 44.748	40 23 31.05	0.05	0.05	47.74603	0.07071	24.724	0.085	12.346	0.050	188.82	0.05	2020.45111	1,6
		16 07 46.496	40 24 14.42							16.531	0.076	18.68			
16072+3536	KPP2512	16 07 11.052	35 35 38.72	0.03	0.04	22.57975	0.05000	296.061	0.127	11.377	0.070	257.75	0.07	2020.45109	4
		16 07 09.389	35 35 48.64							14.336	0.071	75.30			
16120+3803	LDS4649	16 12 00.028	38 02 27.63	0.07	0.08	154.83502	0.10630	68.962	0.039	15.744	0.077	33.59	0.07	2020.45119	6
		16 12 12.262	38 03 23.22							15.961	0.081	25.62			
18163+3846	KPP1820	18 16 19.817	38 45 35.62	0.10	0.11	14.14391	0.14866	295.549	0.602	13.221	0.111	98.50	0.11	2020.54439	4
		18 16 18.726	38 45 41.72							13.456	0.111	88.98			
18165+3451	DAM105	18 16 31.525	34 50 54.89	0.06	0.07	6.96299	0.09220	145.669	0.759	12.077	0.110	184.89	0.11	2020.54434	
		18 16 31.844	34 50 49.14							14.321	0.111	60.69			
18180+3846	GIC151	18 18 03.572	38 46 11.47	0.10	0.11	9.81771	0.14866	276.551	0.868	11.906	0.080	164.48	0.08	2020.54435	4
		18 18 02.738	38 46 12.59							13.622	0.081	93.92			
18183+3920	ALI1101	18 18 21.693	39 20 05.97	0.11	0.10	7.58567	0.14866	176.317	1.123	10.937	0.120	193.35	0.12	2020.54438	4
		18 18 21.735	39 19 58.40							11.847	0.120	116.32			
18189+3918	MLB1078	18 18 56.592	39 18 32.72	0.11	0.10	6.57812	0.14866	316.101	1.295	12.644	0.121	91.81	0.12	2020.54438	4
		18 18 56.199	39 18 37.46							12.768	0.121	88.17			
18208+3547	DAM107	18 20 50.013	35 46 56.33	0.07	0.07	7.73000	0.09899	305.056	0.734	9.987	0.100	299.71	0.10	2020.54428	
		18 20 49.493	35 47 00.77							14.003	0.102	58.75			
18210+3923	DAM108	18 20 57.188	39 22 44.85	0.08	0.09	5.64842	0.12042	115.144	1.221	11.786	0.090	133.56	0.09	2020.54436	
		18 20 57.629	39 22 42.45							13.157	0.093	50.00			
18213+3920	HJ1321	18 21 20.447	39 19 23.14	0.08	0.09	9.48007	0.12042	74.960	0.728	9.997	0.090	197.19	0.09	2020.54436	

			18 21 21.236	39 19 25.60							11.714	0.090	161.15				
18269+4031	ES1653		18 26 58.201	40 30 37.59	0.07	0.09	10.20825	0.11402	190.102	0.640	11.229	0.120	232.09	0.12	2020.54433		
			18 26 58.044	40 30 27.54							12.182	0.120	155.12				
18270+3500	CBL77		18 27 02.206	34 59 43.87	0.06	0.08	39.24769	0.10000	68.460	0.146	9.878	0.110	310.29	0.11	2020.54427		
			18 27 05.177	34 59 58.28							13.912	0.111	81.81				
18272+3847	MLB854		18 27 18.560	38 47 35.55	0.10	0.11	6.79940	0.14866	9.301	1.253	12.167	0.081	101.98	0.08	2020.54436		
			18 27 18.654	38 47 42.26							12.615	0.081	85.17				
18299+3633	ALI377		18 29 55.621	36 33 17.39	0.11	0.12	7.23247	0.16279	278.908	1.289	11.645	0.110	134.43	0.11	2020.54438		
			18 29 55.028	36 33 18.51							11.768	0.110	139.88				
18343+3832	SLE210		18 34 20.769	38 31 56.99	0.10	0.09	9.57096	0.13454	236.733	0.805	12.832	0.100	109.28	0.10	2020.54437		
			18 34 20.087	38 31 51.74							13.324	0.101	82.39				
18348+3939	SLE215		18 34 46.625	39 39 18.31	0.12	0.11	4.29801	0.16279	88.267	2.169	13.696	0.112	46.15	0.11	2020.54439		
			18 34 46.997	39 39 18.44							13.740	0.112	49.63				
18367+3911	DAM678	AB-C	18 35 53.048	39 10 41.80	0.08	0.09	12.26979	0.12042	163.426	0.562	11.121	0.090	222.42	0.09	2020.54433		
			18 35 53.349	39 10 30.04							13.737	0.091	89.50				
18362+3858	ES2571		18 36 12.328	38 58 30.37	0.07	0.09	6.71437	0.11402	70.874	0.973	12.573	0.051	143.26	0.05	2020.54430		
			18 36 12.872	38 58 32.57							12.861	0.051	118.20				
18366+3859	MLB755		18 36 35.965	38 58 34.91	0.07	0.09	9.28212	0.11402	100.365	0.704	13.394	0.051	102.92	0.05	2020.54430		
			18 36 36.748	38 58 33.24							13.615	0.051	97.53				
18367+3841	H459		18 36 40.572	38 41 29.13	0.05	0.07	29.75445	0.08602	298.286	0.166	9.930	0.090	322.44	0.09	2020.54428		
			18 36 38.334	38 41 43.23							11.879	0.090	184.50				
18380+3652	KPP1213		18 38 00.292	36 51 34.53	0.06	0.08	9.44857	0.10000	171.306	0.606	10.701	0.090	286.70	0.09	2020.54432	4	
			18 38 00.411	36 51 25.19							13.016	0.090	137.29				
18381+3935	BU50	AB	18 38 06.088	39 35 10.93	0.09	0.10	22.24703	0.13454	3.307	0.346	9.444	0.005	219.59	0.10	2020.54429		
			18 38 06.199	39 35 33.14							13.662	0.101	81.53				
18381+3935	BU50	AC	18 38 06.088	39 35 10.93	0.09	0.10	74.31514	0.13454	328.124	0.104	9.444	0.100	219.59	0.10	2020.54429		
			18 38 02.693	39 36 14.04							11.742	0.100	156.85				
18381+3935	BU50	AD	18 38 06.088	39 35 10.93	0.09	0.10	68.12118	0.13454	326.565	0.113	9.444	0.100	219.59	0.10	2020.54429		
			18 38 02.841	39 36 07.78							13.219	0.101	74.03				
18381+3935	BU50	CD	18 38 02.693	39 36 14.04	0.09	0.10	6.48948	0.13454	164.718	1.188	11.742	0.100	156.85	0.10	2020.54429		
			18 38 02.841	39 36 07.78							13.219	0.101	74.03				
18385+3837	SLE230	AB	18 38 28.665	38 42 23.09	0.06	0.08	9.03656	0.10000	218.825	0.634	13.078	0.071	123.97	0.07	2020.54431	9	
			18 38 28.181	38 42 16.05							12.769	0.070	144.04				
18385+3837	SLE230	AC	18 38 28.665	38 42 23.09	0.06	0.08	39.10400	0.10000	158.211	0.147	13.078	0.071	123.97	0.07	2020.54431	9	
			18 38 29.905	38 41 46.78							12.101	0.070	173.28				
18389+3658	AL378		18 38 49.354	36 58 07.64	0.09	0.07	12.41750	0.11402	32.781	0.526	11.540	0.090	205.51	0.09	2020.54435		
			18 38 49.915	36 58 18.08							11.874	0.090	184.21				
18393+3517	HJ1335		18 39 21.105	35 18 30.62	0.07	0.07	16.67976	0.09899	6.870	0.340	10.627	0.100	270.63	0.10	2020.54432		
			18 39 21.268	35 18 47.18							12.375	0.100	167.54				
18416+3503	GRV237		18 41 40.321	35 03 24.14	0.11	0.11	57.78840	0.15556	175.625	0.154	12.571	0.130	103.62	0.13	2020.54437		
			18 41 40.680	35 02 26.52							13.668	0.131	73.59				
18420+3505	SEI570		18 41 55.193	35 04 18.26	0.11	0.11	9.38356	0.15556	130.870	0.950	11.512	0.130	119.12	0.13	2020.54437		
			18 41 55.771	35 04 12.12							12.573	0.130	109.53				
18445+3733	ES2482		18 44 31.091	37 34 40.78	0.06	0.08	12.38312	0.10000	160.600	0.463	11.589	0.140	200.81	0.14	2020.54434		
			18 44 31.437	37 34 29.10							12.849	0.140	133.07				

18449+3651	ES2483		18 44 52.132	36 52 09.49	0.07	0.08	5.74860	0.10630	89.203	1.059	12.722	0.100	135.04	0.10	2020.54429	
			18 44 52.611	36 52 09.57							14.467	0.102	51.12			
20535+3645	SEI1296		20 53 31.704	36 44 36.23	0.06	0.06	10.51748	0.08485	277.759	0.462	9.420	0.120	325.86	0.12	2020.64286	
			20 53 30.837	36 44 37.65							12.324	0.121	97.91			
20533+3639	SEI1293		20 53 16.979	36 38 24.17	0.06	0.06	14.16081	0.08485	52.707	0.343	9.460	0.120	321.62	0.12	2020.64286	
			20 53 17.915	36 38 32.75							10.678	0.120	205.16			
20552+3755	SEI1312		20 55 09.912	37 54 08.60	0.06	0.06	8.17030	0.08485	284.604	0.595	11.347	0.130	159.48	0.13	2020.64287	
			20 55 09.244	37 54 10.66							12.621	0.131	87.81			
20569+3818	KPP1144		20 56 52.909	38 18 11.32	0.06	0.07	8.94316	0.09220	247.516	0.591	11.672	0.140	143.10	0.14	2020.64285	4
			20 56 52.207	38 18 07.90							12.543	0.140	97.64			
20577+3711	SEI1331		20 57 43.895	37 11 20.39	0.07	0.07	26.58093	0.09899	48.538	0.213	12.273	0.130	103.81	0.13	2020.64283	
			20 57 45.562	37 11 37.99							13.096	0.131	68.20			
20575+3717	DAM221		20 57 29.683	37 17 04.11	0.07	0.07	5.89804	0.09899	59.314	0.962	10.593	0.130	186.95	0.13	2020.64283	
			20 57 30.108	37 17 07.12							12.955	0.132	50.85			
20582+3715	DAM223		20 58 11.045	37 14 47.00	0.06	0.06	4.82776	0.08485	35.711	1.007	12.763	0.141	70.37	0.14	2020.64284	
			20 58 11.281	37 14 50.92							12.712	0.141	74.14			
20590+3655	SEI1347		20 59 05.255	36 55 10.86	0.09	0.08	18.58960	0.12042	125.179	0.371	12.919	0.062	75.28	0.06	2020.64287	
			20 59 06.522	36 55 00.15							12.990	0.062	79.22			
20595+3646	SEI1354		20 59 33.378	36 45 27.17	0.07	0.07	26.39365	0.09899	324.960	0.215	10.554	0.120	214.07	0.12	2020.64288	
			20 59 32.117	36 45 48.78							11.215	0.120	168.59			
20599+3612	SEI1359		20 59 53.733	36 12 06.57	0.06	0.07	16.54532	0.09220	108.136	0.319	12.518	0.141	75.18	0.14	2020.64288	
			20 59 55.032	36 12 01.42							12.647	0.141	74.88			
21002+3547	POP81		21 00 09.586	35 42 49.98	0.05	0.06	5.86682	0.07810	203.749	0.763	12.432	0.140	97.60	0.14	2020.64286	
			21 00 09.392	35 42 44.61							13.166	0.141	61.38			
21003+3543	SEI1361		21 00 14.169	35 43 22.58	0.05	0.06	20.75452	0.07810	281.000	0.216	10.220	0.140	255.33	0.14	2020.64286	
			21 00 12.496	35 43 26.54							11.802	0.140	134.42			
21010+3647	SEI1367		21 01 00.810	36 46 01.46	0.06	0.07	20.57872	0.09220	247.395	0.257	12.295	0.130	104.05	0.13	2020.64289	4
			21 00 59.229	36 45 53.55							12.816	0.131	83.55			
21013+3554	SEI1368	AB	21 01 15.993	35 53 32.59	0.08	0.08	13.27987	0.11314	56.757	0.488	11.990	0.140	100.95	0.14	2020.64289	
			21 01 16.907	35 53 39.87							12.136	0.141	90.07			
21028+3534	BTG6	AC	21 02 45.861	35 33 35.91	0.09	0.09	10.57885	0.12728	235.447	0.689	11.270	0.160	122.46	0.16	2020.64290	
			21 02 45.147	35 33 29.91							12.253	0.161	77.76			
21028+3534	BTG6	BC	21 02 45.861	35 33 35.91	0.09	0.09	15.92048	0.12728	273.673	0.458	11.270	0.160	122.46	0.16	2020.64290	
			21 02 44.559	35 33 36.93							14.055	0.163	32.76			
21028+3534	SEI1375	BD	21 02 46.056	35 33 29.86	0.09	0.09	6.50113	0.12728	338.530	1.122	11.674	0.160	93.89	0.16	2020.64290	
			21 02 45.861	35 33 35.91							11.270	0.160	122.46			
21028+3534	SEI1376		21 02 46.056	35 33 29.86	0.09	0.09	11.09252	0.12728	270.258	0.657	11.674	0.160	93.89	0.16	2020.64290	
			21 02 45.147	35 33 29.91							12.253	0.161	77.76			
21036+3701	SEI1382		21 03 35.731	37 01 12.41	0.07	0.07	6.03091	0.09899	156.723	0.940	13.146	0.141	58.07	0.14	2020.64290	
			21 03 35.930	37 01 06.87							13.181	0.141	55.21			
21042+3542	SEI1387		21 04 12.423	35 41 23.02	0.07	0.07	9.06939	0.09899	133.388	0.625	12.044	0.131	93.64	0.13	2020.64291	
			21 04 12.964	35 41 16.79							12.280	0.131	89.03			
21050+3559	SEI1395		21 05 02.069	35 59 15.39	0.06	0.06	21.12569	0.08485	133.046	0.230	11.322	0.150	144.91	0.15	2020.64291	
			21 05 03.341	35 59 00.97							11.894	0.150	104.91			
21058+3610	SEI1398		21 05 48.971	36 10 23.16	0.08	0.09	30.47958	0.12042	36.124	0.226	12.031	0.100	108.72	0.10	2020.64292	

			21 05 50.455	36 10 47.78							12.552	0.101	85.54				
21061+3558	SEI1401		21 06 06.437	35 58 08.68	0.09	0.10	10.51262	0.13454	333.158	0.733	12.529	0.111	77.99	0.11	2020.64292		
			21 06 06.046	35 58 18.06							12.956	0.111	62.27				
21064+3643	SEI1403		21 06 24.584	36 42 59.41	0.07	0.07	11.41195	0.09899	123.328	0.497	11.639	0.150	115.10	0.15	2020.64293		
			21 06 25.377	36 42 53.14							12.570	0.151	76.00				
21066+3645	SEI1404	AB	21 06 31.573	36 44 31.05	0.08	0.08	23.93423	0.11314	307.771	0.271	12.243	0.121	81.49	0.12	2020.64293		
			21 06 29.999	36 44 45.71							12.246	0.121	80.90				
21066+3645	TOB209	BC	21 06 29.999	36 44 45.71	0.08	0.08	19.04704	0.11314	322.395	0.340	12.246	0.121	80.90	0.12	2020.64293		
			21 06 29.032	36 45 00.80							11.946	0.121	92.22				
21067+3554	GRV418		21 06 43.491	35 54 05.54	0.05	0.06	58.07981	0.07810	215.504	0.077	12.512	0.140	97.15	0.14	2020.64284		
			21 06 40.715	35 53 18.26							12.738	0.141	86.46				
21082+3628	SEI1410		21 08 09.358	36 28 19.26	0.08	0.08	20.29305	0.11314	170.420	0.319	10.802	0.150	162.65	0.15	2020.64294		
			21 08 09.638	36 27 59.25							12.392	0.151	77.18				
21088+3707	SEI1416		21 08 43.018	37 07 10.34	0.07	0.07	5.99482	0.09899	59.307	0.946	11.603	0.140	116.19	0.14	2020.64294		
			21 08 43.449	37 07 13.40							12.535	0.141	68.96				
21092+3635	GRV425		21 09 14.459	36 35 06.58	0.06	0.07	32.61486	0.09220	266.238	0.162	11.994	0.100	138.31	0.10	2020.64285		
			21 09 11.757	36 35 04.44							14.110	0.103	42.91				
23317+1956	WIR1	AD	23 31 53.024	19 56 12.98	0.04	0.04	5.28554	0.05657	73.287	0.613	10.258	0.100	242.77	0.10	2020.56388	4,8	
			23 31 53.383	19 56 14.50							12.404	0.101	74.73				
23317+1956	LMP24	AB	23 31 53.024	19 56 12.98	0.04	0.04	30.21266	0.05657	12.644	0.107	10.258	0.100	242.77	0.10	2020.56388	6,8	
			23 31 53.493	19 56 42.46							12.283	0.100	130.73				
23317+1956	LMP24	AC	23 31 53.024	19 56 12.98	0.04	0.04	38.05930	0.05657	337.451	0.085	10.258	0.100	242.77	0.10	2020.56388	6,8	
			23 31 51.989	19 56 48.13							13.684	0.101	70.35				

Table 1: Results for measured WDS objects

Notes
1) SNR B <20
2) SNR B <10
3) Measurement very different from WDS data
4) Similar proper motion and parallax (EDR3) suggest physical pair
5) SNR A and B <20
6) Rather different EDR3 parallax suggests optical pair
7) Very fast and very different proper motion
8) Stack of 5 images with 10s exposure time each
9) Stack of 2 images with 20s exposure time each
10) No EDR3 parallax data available

Objects of specific interest

WDS 13465+3443 (CBL 597) is listed in the WDS catalog with only one observation with very different parameters compared to the processed image as well as other sources like Gaia EDR3. This suggests either a position error for CBL 597 or a mix-up with another object. The object at the given position is according to EDR3 parallax and proper motion data potentially a wide physical pair

WDS 23317+1956 (WIR 1) is listed in the 6th orbit catalog with a grade 5 orbit (Izmailov[1]) with a period of ∼234 years and a semi major-axis of ∼5.33 arcseconds. EDR3 gives for WIR 1 parallaxes of 159.6634 and 159.9085; DR2 values of 159.7098 and 160.0598 are slightly higher but very similar and the error range is in both cases reasonably small. The Hipparcos parallax for A is 161.76 mas with an error range of 1.66 mas. EDR3 RUWE values are with ∼1.3/1.6 not perfect, but they suggest no duplicity issues. The Izm2019 orbit gives with the average EDR3 parallax of 159.78595 mas, a dynamical mass of 0.68 – this value is very close to the STARHORSE (Anders *et al.*[2]) median system mass of 0.70.

The new 2020 measurement allows with inclusion of Gaia DR1 and EDR3 measures so far not included in the WDS observation history for the calculation of a new preliminary orbit using the set of programs published by Izmailov 2019 (`http://izmccd.puldb.ru/vds.htm`) resulting in a period of ∼270 years and a semi-major axis of ∼5.5 arcseconds. Several obvious outliers (measures from 1950.0, 1952.66, 1959.78, 1962.959, 1964.819, 1981.640, 2006.818, and 2013.9264) had to be eliminated. Together with the average EDR3 parallax of 159.8848 mas these orbital element values give a dynamical mass of 0.58 – this means that the Izm2019 orbit offers a clearly better match with STARHORSE median mass values making it the seemingly better proposition.

However, a closer look at the available mass data for WIR 1 raises doubts about the reliability of the StarHorse median mass values. Absolute magnitude based system mass estimation gives a significant smaller value about half the STARHORSE data and Cvetkovic *et al.* 2010 reports also significant smaller system mass estimations of 0.39 to 0.43. Ward-Duong *et al.*[4] suggest masses of 0.35 to 0.39 and 0.17 to 0.20. Pearce *et al.*[3] suggests masses of 0.39 and 0.25. This comparison make a system mass of 0.58 look very reasonable, especially as the error range for period and semi-major axis is compared to Izm2019 a bit smaller:

Table 2: Newly calculated orbital element values

Element	Value	Delta to 16th/84th percentile
Period in years	270.016	-45.203/+31.705
Semi-major axis in arcseconds	5.544	-0.464/+0.352
Inclination in degrees	128.716	-1.768/+1.791
Ascending node in degrees	80.295	-5.392/+3.308
Time of periastron passage	2025.905	-83.136/+54.993
Eccentricity [0,1]	0.031	-0.021/+0.187
Longitude of periastron passage in degrees	18.211	+60.011/+313.347

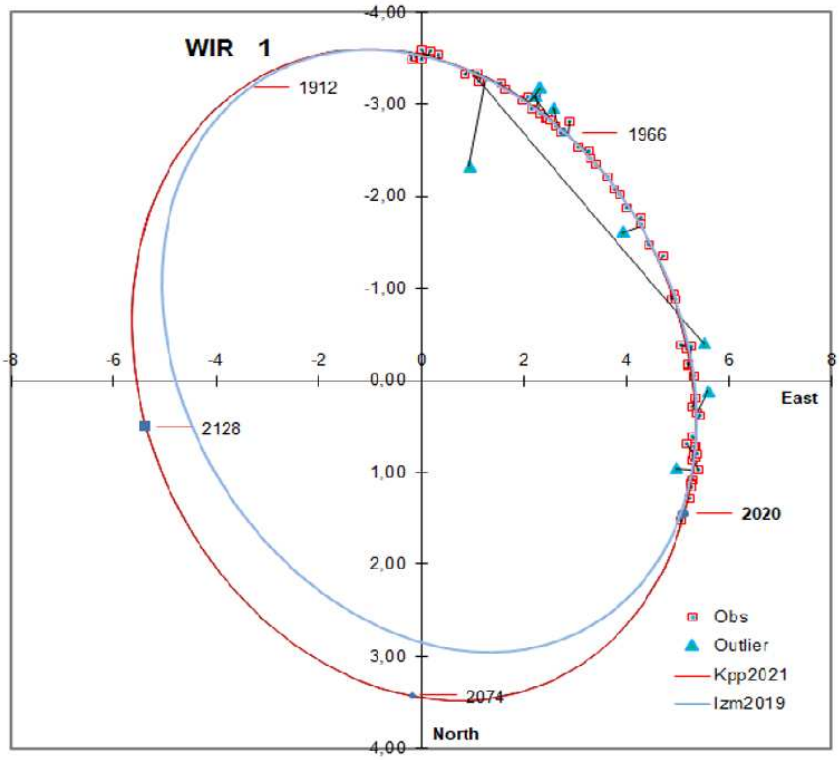

Figure 1: WIR 1 orbit comparison

Measurements in the coming decades should cover one assumed end of the suggested ellipse, which will enhance the quality of then newly calculated orbits.

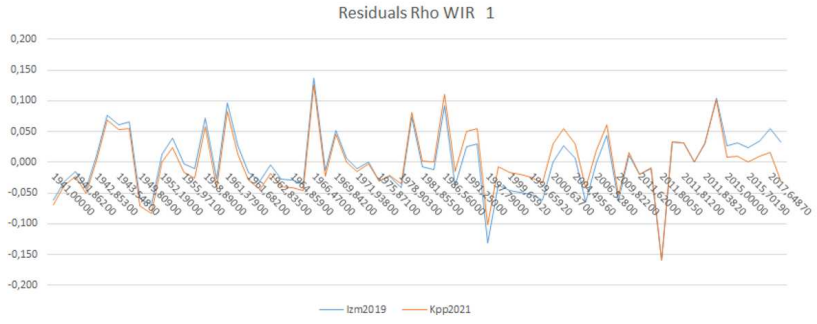

Figure 2: WIR 1 residuals Rho comparison

The RMS residuals for rho in the newly calculated orbit are 0″.04946 which are slightly better compared to 0″.05158 for Izm2019. The latter orbit also shows a systematic bias for the most recent observations (see plot 2), which indicates a somewhat longer period than suggested by Izm2019.

Summary

Many of the objects measured show the expected significant magnitude difference compared to the WDS catalog data, especially for the secondary component, but for a good portion of the objects the given WDS magnitudes are simply confirmed within the stated error range.

Fifty-seven of the objects listed have EDR3 parallaxes and angular distances similar enough to suggest a possible gravitational relationship, while the rest of the objects are most likely optical pairs.

References

1. I. S. Izmailov – 2019, The Orbits of 451 Wide Visual Double Stars, *Astr. Letters*, **45**, 30–38
2. F. Anders, A. Khalatyan, C. Chiappini *et al.* 2019, Photo-astrometric distances, extinctions, and astrophysical parameters for Gaia DR2 stars brighter than $G = 18$. *A & A*, **628**, A94
3. L. A. Pearce, A. L. Kraus, T. J. Dupuy *et al.* 2020, Orbital Parameter Determination for Wide Stellar Binary Systems in the Age of Gaia. *Ap. J*, **894**, Number 2
4. K. Ward-Duong, J. Patience, R. J. De Rosa *et al.*, 2015, The M-dwarfs in Multiples (MINMS) survey – I. Stellar multiplicity among low-mass stars within 15 pc, *MNRAS* 449, 2618–2637

Acknowledgements

The following tools and resources have been used for this research:
- Washington Double Star Catalogue
- 6th Catalog of Orbits of Visual Binary Stars
- GAIA DR1/DR2/EDR3 catalogue
- GAIA DR2 StarHorse catalogue
- URAT1 catalog
- DSS2 and 2MASS images
- iTelescope o iT24: 610-mm CDK with 3962-mm focal length. Resolution $0''.625$ pixel. V-filter. Located in Auberry, California. Elevation 1405m
- Aladin Sky Atlas v11.0
- AAVSO VPhot
- Astrometrica v4.10.0.427
- AstroPlanner v2.2
- MaxIm DL6 v6.08

OBSERVATION OF NEGLECTED DOUBLE STARS - 2

André Debackère, Double Star Commission of the Société Astronomique de France

E-mail: andre.debackere@free.fr

I) TDS 3071

WDS information: RA = 05h 07m 12s.23, Dec = +62° 29′ 11″.5
One observation: 1991, $\theta = 208°.20$, $\rho = 2''.340$, $V_A = 12.23$, $V_B = 13.39$

1. Observation with the FTN

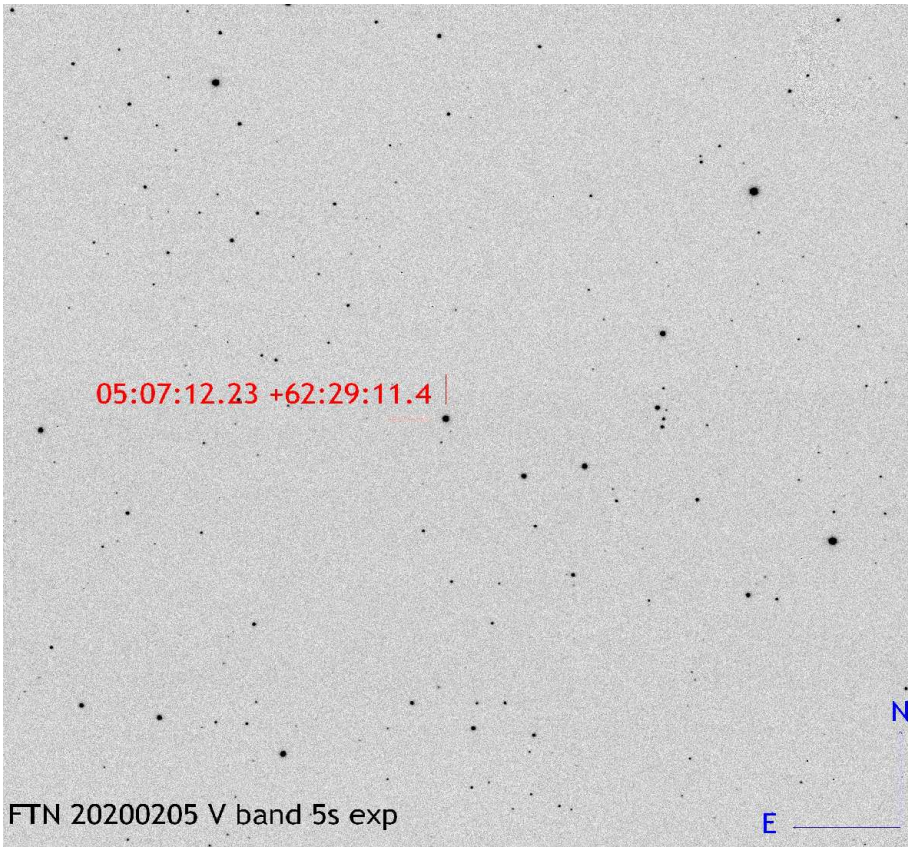

Figure 1: TDS 3071 - FTN field of view (10′ × 10′)

Sampling of FTN images is 0″.3/ pixel. TDS 3071 has a separation of 2″.340 in 1991 which takes about 8 pixels. An observation on one night at FTN on February 5th, 2020 yielded 5 images in the V band.

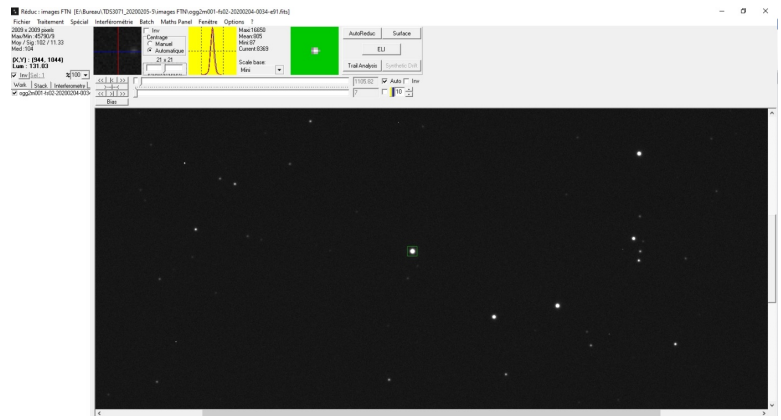

Figure 2: TDS 3071 is seen as a single star with the FTN.

2. Measurements with REDUC (ρ,θ) and Makali'i (photometry) software

a) Stars around the position 05h 07m 12s.23 +62° 29′ 11″.5

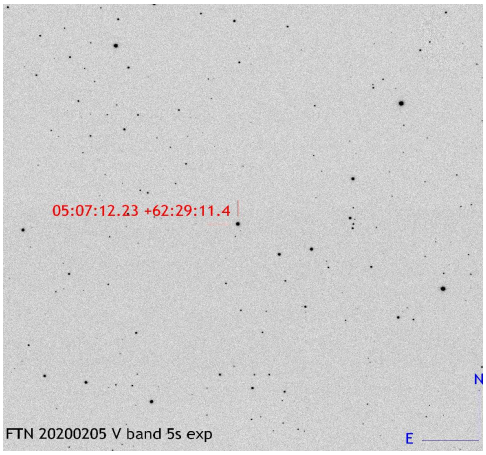

Figure 3: Stars around the position 05h 07m 12s.23 +62° 29′ 11″.5

A: DR2 Name	Gaia DR2 477985329823900160
RA = 05h 07m 12s.2344529673	Dec = + 62° 29′ 11″.429160501
B: DR2 Name	Gaia DR2 477984578207429376
RA = 05h 07m 12s.6448888216	Dec = +62° 28′ 54″.392645305
C: DR2 Name	Gaia DR2 477984578205219238
RA = 05h 07m 11s.7609251936	Dec = +62° 29′ 02″.300346224

Date	Comp	PA	ρ	V_A	$V_{B(C)}$
2020.099	AB	170°.32 ±0.19	17″.206±0.057	12.44± 0.02	17.41±0.05
	AC	199°.71 ±0.72	9″.682±0.083	12.44± 0.02	18.25±0.14

There is no companion with θ = 208 ρ = 2″.3 and V = 13.39

b) Stars around the position 05h 06m 52s.20 +62° 29′ 19″.4

Date	Comp	PA	ρ	V_A	$V_{B(C)}$
2020.099	AB	193°.47±0.09	14″.154±0.032	14.03±0.01	15.29±0.02
	AC	207°.55±0.23	9″.040±0.022	14.03±0.01	15.89±0.02

A has no companion with θ =2°.3 and V = 13.39 but one, called C, with θ = 207°.55 ($\sim$ 208°) ρ = 9″ and V = 15.89.

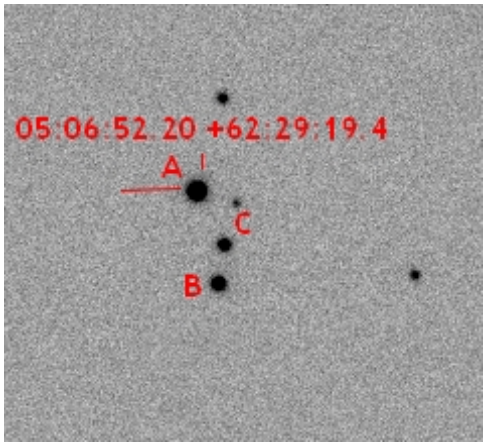

Figure 4: Stars around the position 05h 06m 52s.50 +62° 29′ 19″.4

A: DR2 Name	Gaia DR2 477962003859332096
RA = 05h 06m 52s.2040033356	Dec = + 62° 29′ 19″.397394316
B: DR2 Name	Gaia DR2 477962003859333632
RA = 05h 06m 51s.7187495394	Dec = +62° 29′ 05″.502152726
C: DR2 Name	Gaia DR2 477962003859333376
RA = 05h 06m 51s.5880861722	Dec = +62° 29′ 11″.242527029

II) TDS 1775

WDS information: RA = 01h 07m 00s.23, Dec = +63° 49′ 58″.1 One observation: date 1991, θ = 202°.00, ρ = 2″.650, V_A = 11.13, V_B = 12.03

1) Observation with the Gemini telescope

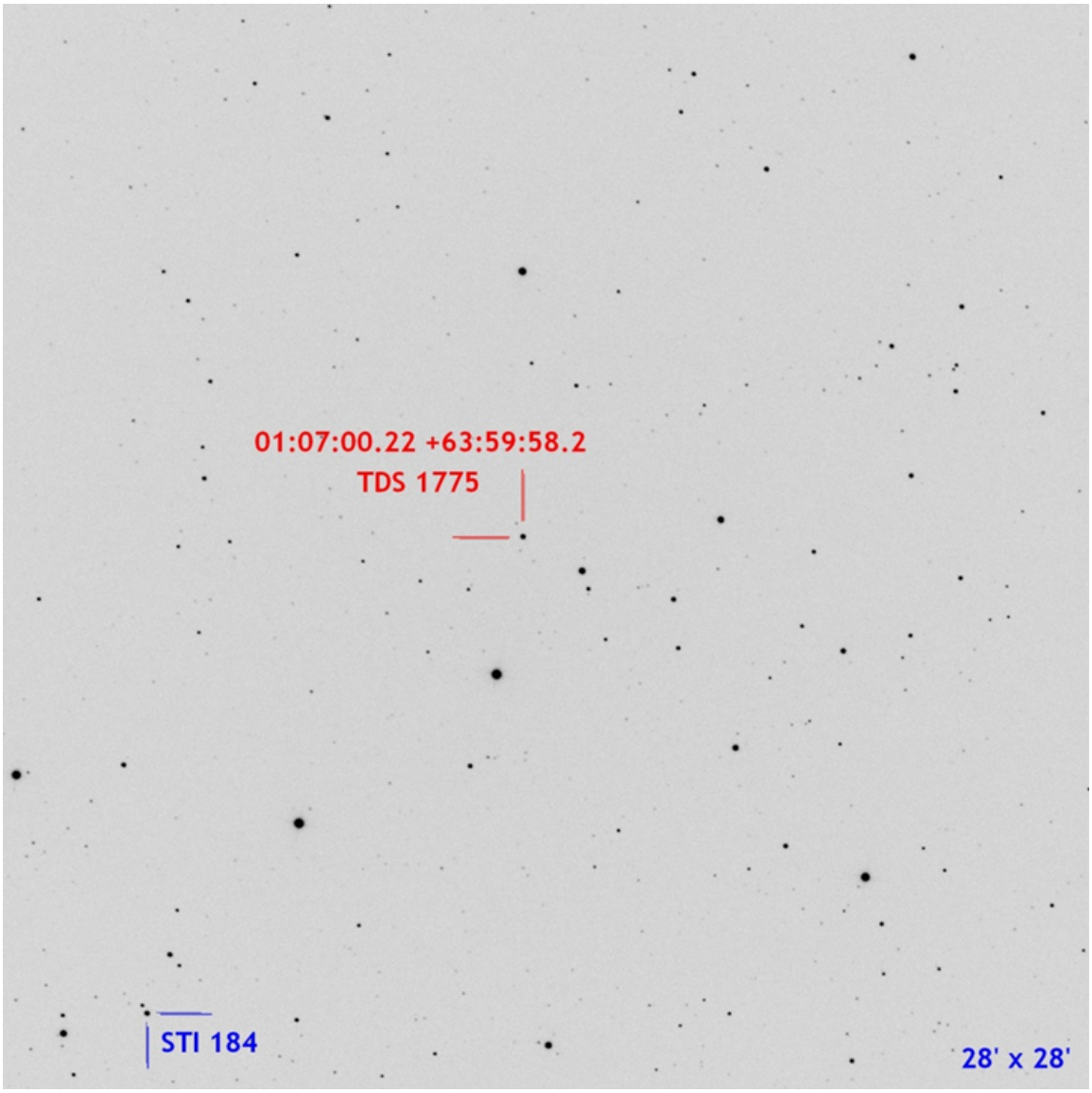

Figure 5: Gemini field of view with ANDOR IKON L-936 back-illuminated CCD camera - - IRO Feb 5,2020, 1 image in V band

Sampling of Gemini images is 0″.81/ pixel. TDS 1775 has a separation of 2″.650 in 1991 which takes about 3.3 pixels. Note : The pair STI 184 is in the field (θ = 43°.1 ρ = 14″.01, 2020.099, measurement with REDUC

2) REDUC software

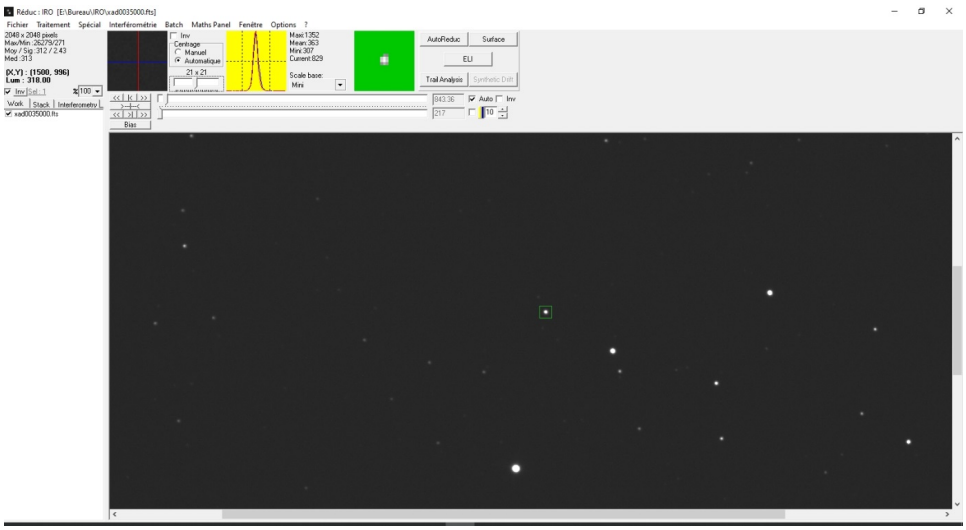

Figure 6:

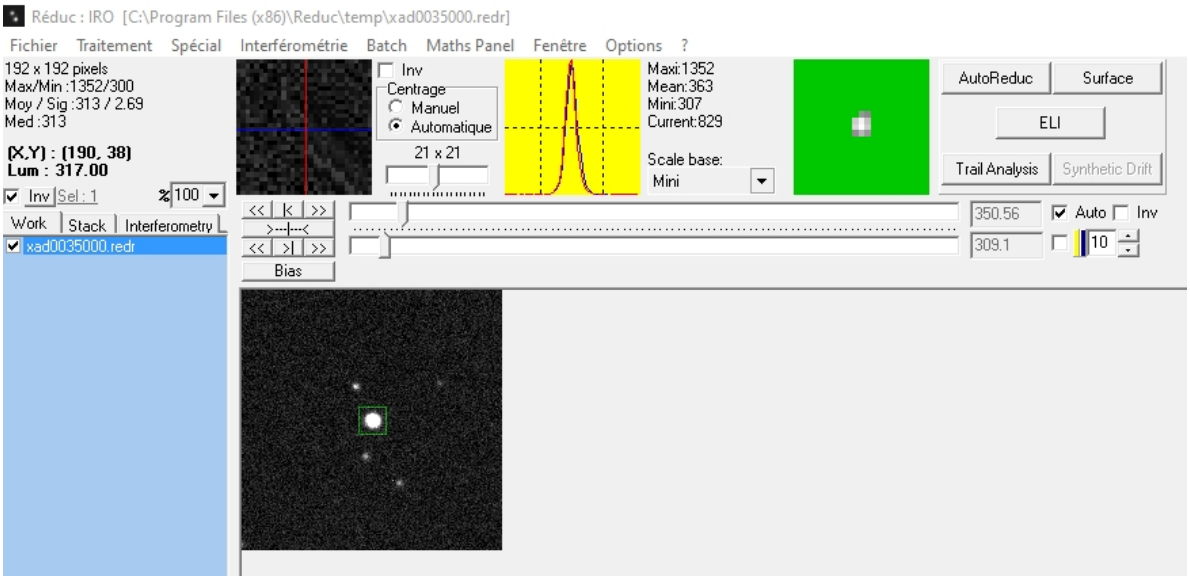

Figure 7: TDS 1775 is seen as a single star with the Gemini telescope. There is no companion with $\theta = 202°$, $\rho = 2.''65$ and $V = 12.03$ (the two nearest faint stars are at about $22'$ away).

III) POU 635

WDS information: RA = 05h 17m 26s, Dec = +24° 23′ 54″
One observation: epoch 1898, $\theta = 227°.40$, $\rho = 16''.300$, $V_A = 12.90$, $V_B = 13.50$

1) Observation with the Gemini telescope

2) REDUC software

1	2	3	4	5	6	7	8	9	10	11	12	13
05171+2423A	No	0.3235	-0.348	-1.976	2020.113	3	268.22	9.599	14.7		IRO	5
		±0.0349	±0.075	±0.047			±1.12	±0.102				
05171+2423B		0.6309	0.033	-3.369						15.2		
		±0.0426	±0.091	±0.057								

Notes: A = Gaia DR2 3417412916589585664 - precise position 05h 17m 13s.51 +24° 23′ 41″.1 ;

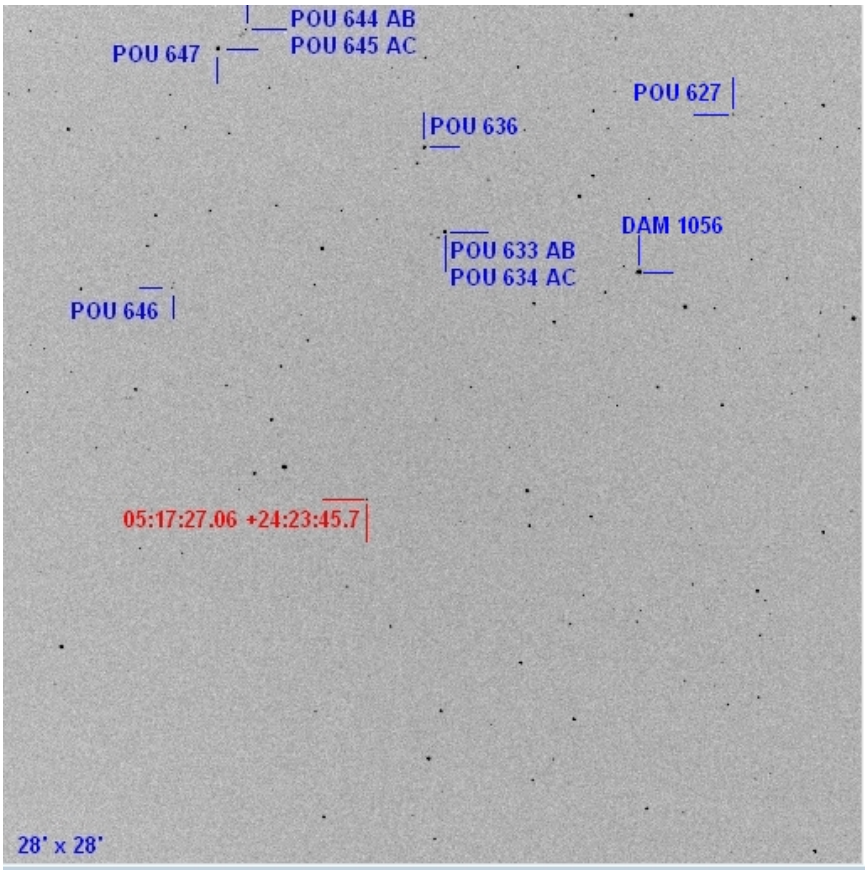

Figure 8: Gemini field of view with ANDOR IKON L-936 back-illuminated CCD camera - IRO Feb 7, 2020, 3 images in V band

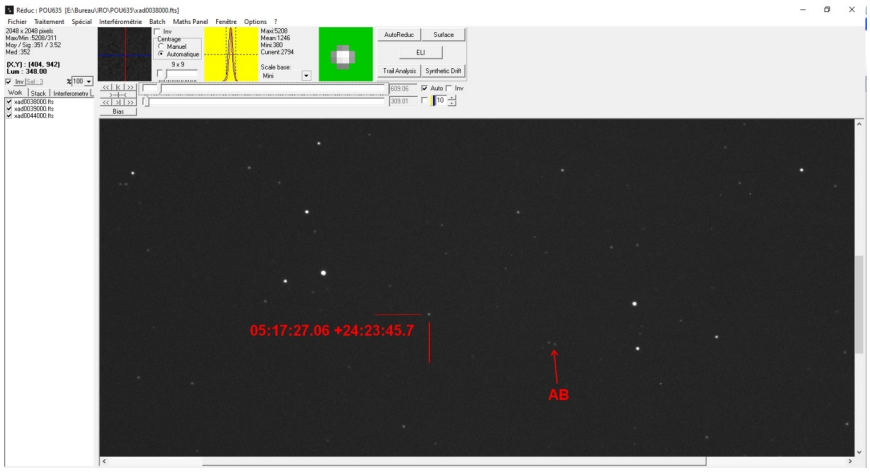

Figure 9: There is no double star at the position indicated in the WDS: 05h 17m 26s and +24° 23′ 54″ . The star closest to this position is Gaia DR2 3417418482867189248, RA 05:17:27.0580148400 and Dec = +24 23 45.716541232, G = 14.4, which is a single star.

B = Gaia DR2 3417412813510371456 - precise position 05h 17m 12s.82 +24° 23′ 40″.6 . This pair does not match POU 635 which is not identified in the GEMINI 28′ × 28′ field.

IV) SLE 481 AB

WDS information: RA = 09h 15m 01s.75, Dec= +28° 16′ 18″.3.
One observation: epoch 1984, $\theta = 129°.60$, $\rho = 4''.330$, $V_A = 12.67$, $V_B = 13.80$

1) Observation with the Gemini telescope

Gemini image scale is 0″.54/pixel. SLE 481 AB has a separation of 4″.330 in 1984 which takes 8 pixels.

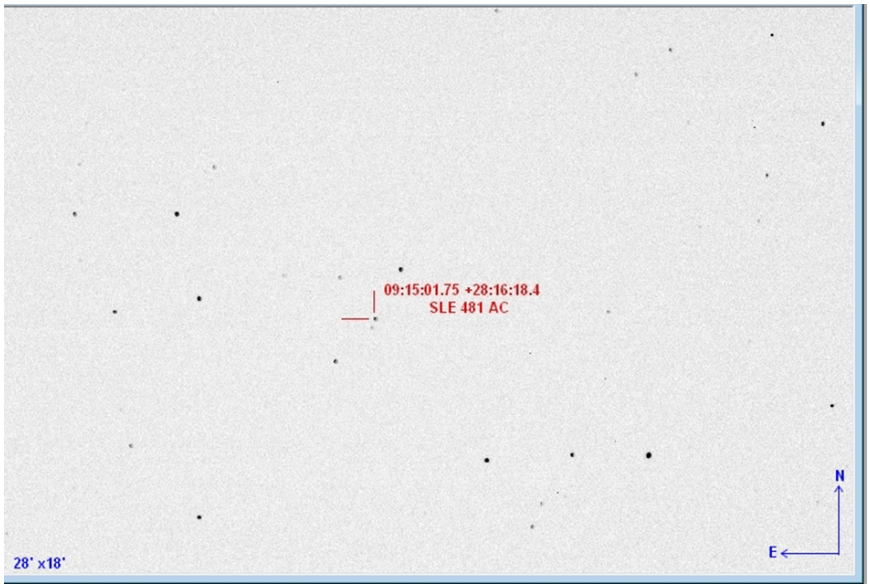

Figure 10: GEMINI field of view with SBIG STXL-6303 3 CCD Camera - IRO, Mar 28, 2020, 1 image in V band

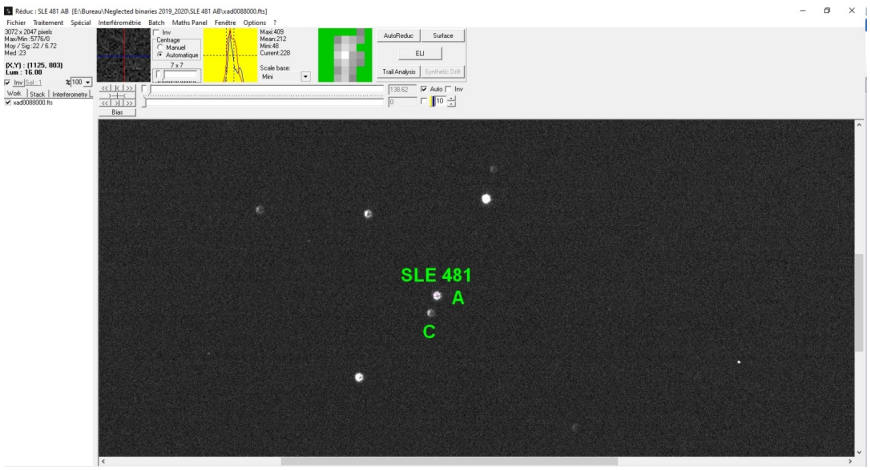

Figure 11: There is no companion with $\theta = 130$ ° , $\rho = 4''.3$ and $V = 13.8$ on our image of SLE 481 with the Gemini telescope. SLE 481 is seen as a single star with the Gemini telescope

2) REDUC software

WDS information: RA = 11h 57m 05s.47, Dec = +28° 55′ 07″.6.
One observation: epoch 1991, $\theta = 309°.90$, $\rho = 3''.750$, $V_A = 12.42$, $V_B = 13.30$

V) TDS 8136

1) Observation with the Gemini telescope

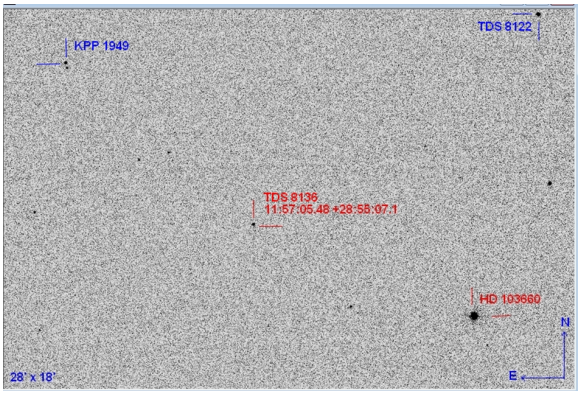

Figure 12: GEMINI field of view with SBIG STXL-6303 3 CCD Camera (the NGC 3984 galaxy near KPP 1949 is not visible on our image). IRO, April 2nd, 2020, 1 image in V

2) REDUC software

There is no double star at the position indicated in the WDS: 11h 57m 05s.47 and +28° 55′ 07″.6. TDS 8136 is seen as a single star with the Gemini telescope.

Note : The neglected binary TDS 8122 can't be observed with Gemini telescope (WDS information: RA = 11h 56m 06s.23, Dec = +29° 06′ 19″.4. One observation: epoch 1991, θ = 110°.00, ρ =0″.450, V_A = 11.22, V_B = 11.52)

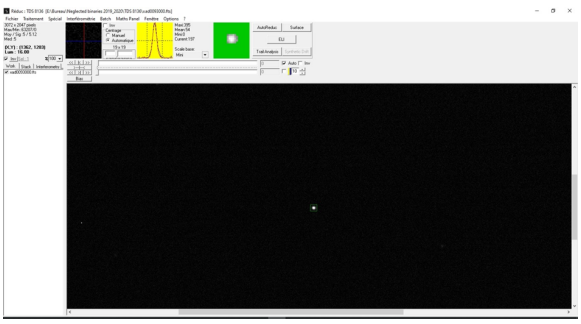

Figure 13: There is no double star at the position indicated in the WDS: 11h 57m 05s.47 and +28° 55′ 07″.6. TDS 8136 is seen as a single star in the Gemini telescope

Explanation of Table

Col.1	WDS designation (based on 2000 coordinates)
Col.2	Discoverer
Col.3	Components and GAIA-DR2 absolute stellar parallax (mas) & standard error of parallax (mas)
Col.4,5	GAIA-DR2 Proper motion in RA direction(mas/yr), Standard error of proper motion in right ascension direction(mas/yr), Proper motion in declination direction(mas/yr), Standard error of proper motion in declination direction(mas/yr)
Col.6	Mean date of observation
Col.7	Number of Observations
Col.8	Position Angle
Col.9	Separation
Col.10	Magnitude of First Component (in G band, GAIA-DR2)
Col.11	Magnitude of Second Component (in G band, GAIA-DR2)
Col.12	Observatory code
Col.13	Nores (see following table)

Notes

Number	Note
1	Neglected couple
2	Orbital
3	Physical pair (same parallax and common proper motion within the errors)
4	Identification uncertain in the WDS
5	Optical pair
6	Inverted quadrant

Acknowledgments

This research has made use of:
- the VizieR catalogue access tool, CDS, Strasbourg, France (DOI: 10.26093/cds/vizier). The original description of the VizieR service was published in A&AS 143, 23
- the Washington Double Star Catalog maintained at the U.S. Naval Observatory
- the REDUC software (Florent Losse)(`http://www.astrosurf.com/hfosaf/uk/tdownload.htm#reduc`)
- the WDSTOOL software (David Chiron)
The author warmly thanks Paul Roche and Robert Mutel who give respectively access to the LCO telescope network and to the Gemini telescope of the IOWA University, USA

MEASUREMENTS OF DOUBLE STARS WITH ROBOTIC TELESCOPES IN 2019/20

André Debackére, Société Astronomique de France

E-mail: andredebackere@orange.fr

Abstract

These observations and measurements were made with the LCO Global Telescope Network. I decided to use the catalog Gaia DR2 which provides a lot of information on a very large number of stars with a high precision until then unequalled, and since December 3rd, 2020 the catalog Gaia EDR3. This is how I added the parallax of the components of the observed pairs when it is known, the G-band magnitude (specific to Gaia), and the precise coordinates of each component. The aim of this work is to measure the polar coordinates of the observed pairs but also to determine whether they are optical or physical couples. In the latter case, when the components have same parallax within the errors, I then see if they have common proper motion to conclude their physicality.

Explanation of Table 1

Col.1	WDS designation (based on 2000 coordinates)/Discoverer & Number
Col.2	Components
Col 3,4	GAIA-DR2 Absolute stellar parallax (mas) & standard error of parallax(mas)
Col.5-8	GAIA-DR2 Proper motion in RA direction(mas/yr), Standard error of proper motion in right ascension direction(mas/yr), Proper motion in declination direction(mas/yr), Standard error of proper motion in declination direction(mas/yr)
Col.9	Mean date of observation
Col.10	Number of Observations
Col.11	Position Angle
Col.12	Error in PA
Col.13	Separation
Col 14	Error in sep.
Col.15	Magnitude component (in G band, GAIA-DR2)
Col.16	Observatory code
Col.17	Notes
Col.18	2000 arcsecond coordinates (GAIA-DR2)

Table 1: Measures

01081+6336	A	3.3842	0.0261	4.324	0.035	-16.335	0.035	2020.099	1	43.14		14.012		10.7	857	5	010802.17+633608.3
STI 184	B	1.1339	0.0285	-6.279	0.041	0.273	0.043							12.7			010803.62+633618.2
01505-2042	A	1.8592	0.2958	12.706	0.568	-3.189	0.349	2020.067	1	89.1		1.05		13.1	E10	1,3,6	015032.85−204223.9
ARA 1257	B	1.4904	0.0503	11.123	0.176	0.201	0.444							13.5			015032.93−204223.9
05168+2439	A	1.0227	0.0378	4.559	0.069	-2.197	0.048	2020.113	2	214.91	0.30	3.040	0.011	14.8	857	3	051647.71+243816.8
POU 627	B	0.9450	0.0448	4.447	0.082	-2.283	0.057							15.3			051647.58+243814.3
05169+2433	A	4.9629	0.0528	-13.888	0.117	-1.914	0.071	2020.105	1	118.4		5.98		10.5	857		051656.04+243242.2
DAM 1056	B	none		none										15.3			051656.44+243238.7
05174+2433	A	1.5226	0.0435	-1.196	0.079	-8.549	0.053	2020.113	3	144.57	0.32	17.282	0.089	12.5	857	5	051724.05+243241.1
POU 633	B	0.6621	0.0326	-0.622	0.058	-6.130	0.039							14.0			051724.78+243227.0
05174+2433	A	1.5226	0.0435	-1.196	0.079	-8.549	0.053	2020.113	3	114.31	0.10	26.900	0.219	12.5	857	5	051724.05+243241.1
POU 634	C	0.6193	0.0359	-2.551	0.063	-4.424	0.043							14.6			051725.85+243230.0
05175+2436	A	1.0314	0.0566	-3.654	0.092	-12.145	0.063	2020.113	3	182.07	0.81	2.554	0.024	12.8	857	3	051729.34+243513.8
POU 636	B	1.0204	0.0376	-3.615	0.062	-12.281	0.043							13.1			051729.33+243511.1
05179+2438	A	2.2370	0.0454	8.487	0.062	-10.981	0.040	2020.113	3	156.40	0.90	9.436	0.084	14.1	857	5	051757.41+243742.9
POU 644	B	5.3806	0.0414	-8.430	0.054	-6.882	0.038							13.8			051757.72+243734.1
05179+2438	A	2.2370	0.0454	8.487	0.062	-10.981	0.040	2020.113	2	146.78	0.10	15.787	0.238	14.1	857	5	051757.41+243742.9
POU 645	C	3.9503	0.2546	-8.489	0.325	-9.327	0.224							13.9			051758.07+243729.6
05180+2430	A	1.8289	0.0352	-1.367	0.062	4.587	0.041	2020.113	3	355.48	1.17	10.409	0.169	14.6	857		051800.08+242906.9
POU 646	B	1.8006	0.0392	3.382	0.069	0.286	0.047							14.9			051800.01+242917.3
05180+2437	A	1.8387	0.0617	-3.814	0.080	-7.970	0.055	2020.113	3	354.53	0.28	3.369	0.032	12.8	857	3	051800.75+243654.9
POU 647	B	1.7430	0.0375	-3.72	0.049	-8.119	0.033							13.1			051800.73+243658.3
09150+2816	A	0.5454	0.6424	-21.095	0.746	-1.834	0.636	2020.242	1	164.80		18.398		12.5	857	5	091501.75+281618.4
SLE 481	C	0.9019	0.0426	6.868	0.057	-5.407	0.039							13.8			091502.08+281600.6
09266-2805	A	1.9026	0.1918	4.425	0.350	-8.287	0.368	2019.472	2	333.32	0.22	4.931	0.038	12.3	F65	5,6	092634.07−280502.7
BRT 2968	B	2.1932	0.0310	4.135	0.051	-8.537	0.052							12.4			092633.90−280458.3
10493-5319	A	-2.759	0.006	0.354	0.006			2020.924	2	308.47	0.59	1.224	0.009	15.6*	E10	2,7	104912.43−531902.8
LUH 16	B													15.7*			104912.33−531902.2
11578+2902	A	3.9044	0.0455	46.170	0.071	-23.468	0.045	2020.256	1	202.10		15.717		11.6	857	3	115749.75+290210.8
KPP 1949	B	3.8536	0.0400	46.609	0.070	-22.966	0.044							13.5			115749.30+290156.5
12425+1311	A	22.2739	0.0580	-261.339	0.112	-212.461	0.066	2019.056	1	243.96		13.031		14.3	F65	1,3	124235.29+131147.8
LDS 1333	B	22.0883	0.1870	-262.026	0.362	-209.634	0.208							18.1			124234.49+131142.1
13372-2957	A	3.8455	0.0394	-26.810	0.088	-24.577	0.078	2019.068	2	206.51	0.19	7.945	0.004	10.5	F65	5	133714.75−295616.3
HJ 4599	B	0.7201	0.0359	-3.062	0.083	-10.953	0.065							11.2			133714.45−295623.5

Table 2: Cross ID between WDS name and Gaia EDR3

Component	Gaia EDR3 number
STI 184A	523314693848011776
STI 184B	523314620826051456
ARA 1257A	513613344976183782
ARA 1257B	5136130494823631872
POU 627A	3417472943052476032
POU 627B	3417472943052476288
DAM 1056A	3417468368910881664
DAM 1056B	3417468373207288320
POU 633A	3417467578636899072
POU 633B	3417467582933286400
POU 634A	3417467578636899072
POU 634C	3417467578637027072
POU 636A	3417469266560451328
POU 636B	3417469266560451712
POU 644A	3417446279895450112
POU 644B	3417446279895450880
POU 645A	3417446279895450112
POU 645C	3417446279895451008
POU 646A	3417417898751591680
POU 646B	3417417898751590528
POU 647A	3417446069439570176
POU 647B	3417446069441853440
SLE 481A	698210911797773440
SLE 481C	698210052804314368
BRT 2968A	5636895193021381888
BRT 2968B	5636895197317021056
LUH 16A	5353626573562355584
LUH 16B	5353626573555863424
KPP 1949A	4008043620698423808
KPP 1949B	4008043624994334976
LDS 1333A	3929166413164009984
LDS 1333B	3929166408868873344
HJ 4599A	6175799071955996416
HJ 4599B	6175799071955995904

Observatory codes

MPC code F65: FTN Faulkes Telescope North T2m, Haleakala, Hawaii, LCO
MPC code E10: FTS Faulkes Telescope South T2m, Siding Spring, Australia, LCO
MPC code 857: T0.51-m GEMINI, Winer Observatory, USA, IRO

Notes to Table 1

1 Neglected couple
2 Orbital
3 Physical pair (same parallax and common proper motion within the errors)
4 Identification uncertain in the WDS
5 Optical pair
6 Inverted quadrant
7 Couple of brown dwarfs, * mag in Sloan SDSS ip band

Explanation of Table 3

Col.1 Usual name
Col.2,3 Difference between our measures of θ° and ρ'' called 'O' and the oldest measures of θ° and ρ'' listed in the WDS catalogue
Col.4 date of the first reliable measurement into the WDS
Col.5 Interval (in years) between the earlier reliable measures and our measures

Table 3 - residuals in ρ and θ between WDS and this paper

Name	Comp.	θ (O-WDS)	ρ (O-WDS)	Date	Interval (in years)
STI 184		+0.04	+0.085	2015	5
ARA 1257		+19.20	+5.803	1920	100
POU 627		-0.39	-0.051	2015	5
DAM 1056		-3.80	-0.634	2015	5
POU 633	AB	+0.17	-0.031	2015	5
POU 634	AC	+0.11	-0.101	2015	5
POU 636		+0.27	-0.056	2007	13
POU 644	AB	+0.4	-0.119	2015	5
POU 645	AC	+0.18	-0.113	2015	5
POU 646		+0.58	+0.020	2015	5
POU 647		-0.17	-0.044	2015	5
SLE 481	AC	+0.10	-0.052	2015	5
BRT 2968		+0.32	+0.003	2015	4
LUH 16		+122.27	+0.931	2016	4
KPP 1949		-0.40	+0.318	2015	5
LDS 1333		-0.04	+0.029	2015	4
HJ 4599		-0.09	+0.165	2019	0

Acknowledgments

This research has made use of:
- the Washington Double Star Catalog maintained at the U.S. Naval Observatory.
- the VizieR catalogue access tool, CDS, Strasbourg, France. The original description of the VizieR service was published in A&AS 143, 23
Special thanks to Herbert Raab, ASTROMETRICA[1] software and Florent Losse, REDUC[2] software

References

1. http://www.astrometrica.at/
2. http://www.astrosurf.com/hfosaf/uk/tdownload.htm#reduc

Index of previous Circulars

DSSC1: Measurements of 232 double stars by five observers between 1971 and 1979 (Double Star Section). Pp.18, 1979

DSSC2: Measures of the 7th hour of RA of Pourteau's Carte du Ciel double stars from POSS (D. Gellera) Pp.26, 1982

DSSC3: Measures of the 18th hour of RA of Pourteau's Carte du Ciel double stars from POSS (D. Gellera)
Micrometric measurements of double stars 1975.0 - 1983.0 (Double Star Section)
A colour catalogue of double and multiple stars based on human colour perception (J. J. Kaznica *et al.*) Pp.55, 1984

DSSC4: Photographic measures of 50 white dwarf pairs discovered by Luyten from POSS plates (D. Gellera)
Micrometric measurements of double stars 1983.0 - 1988.0 (Double Star Section) Pp.35, 1989

DSSC5: Micrometric measurements of double stars 1988.0 - 1992.0 (Double Star Section) Pp.47, 1992

DSSC6: Micrometric measurements of double stars 1992.0 - 1995.0 (Double Star Section)
Photographic measurements of 383 double stars of Pourteau's Catalogue (D. Gellera) Pp.101, 1996

DSSC7: Micrometric measurements of double stars 1995.0 - 1998.0 (Double Star Section)
Catalogue of measurements of 182 double stars made with a CCD camera and 4−cm SCT (G. A. Elliott) Pp.43, 1998

DSSC8: Micrometric measurements of double stars 1998.0 - 2000.0 (Double Star Section) Pp.23, 2000

DSSC9: Micrometric measures of double stars from 2000.0 - 2001.0 (Double Star Section)
Measures of 10 double stars made with a CCD camera and 20-cm Schmid-Cassegrain telescope (J. D. West)
Σ889 : an optical double star (F. Rica Romero)
The PPM and HIPPARCOS Catalogues from a double star observer's point of view (J.-F. Courtot) Pp.37, 2001

DSSC10: Micrometric measures of double stars from 2001.0- 2002.0 (R. W. Argyle & J−F. Courtot)
The nature of the double star Σ2259 (Francisco M. Rica Romero)
Measures of double stars with a CCD camera and 35.-cm Newtonian telescope in 2001 (T. Ladányi & E. Berkó)
Recent measures of double stars made with a CCD camera (J. Doug West & M. Gallo)
Measures of double stars using eyepiece micrometers (M. Tollefsen & E. T. H. Teague) Pp.47, 2002

DSSC11: Micrometric measures of double stars from 2002.0- 2003.0 (R. W. Argyle & J.-F. Courtot)
Micrometric measures of double stars from 1998.02 to 2002.92 (A. Alzner)
An astrometric survey of 250 double stars- Paper I (M. Nicholson)
An astrometric survey of 250 double stars- Paper II (M. Nicholson)
An astrometric survey of 142 double stars- Paper III (M. Nicholson)
An astrometric survey of 187 double stars- Paper IV (M. Nicholson)
New double stars from the Daventry Double Star Survey (M. Nicholson)
Possible quadrant reversals in the Catalog 2001. 0 (R. Harshaw)
CCD measues of double stars 2002 (J. D. West)
Measures of double stars made with an eyepiece micrometer (M. Tollefsen)
A new component in the pair CHE 138 (T. Ladányi)
Measures of double stars with a CCD camera and 35.−cm Newtonian telescope in 2002 (Ernő Berkó, Tamás Ladányi, and György Vaskúti)
Pp. 94, 2003

DSSC12: Micrometric measures of double stars from 2003.0 to 2004.0 (J- F. Courtot & R. W. Argyle)
Measures of double stars made with an eyepiece micrometer (Magne Tollefsen)
Measures of double stars made with an eyepiece micrometer (Tim Leese)
CCD measures of double stars 2003 (Doug West)
Measures of double stars with a CCD camera and 35.-cm reflector from 2002.953 to 2003.394 (Ernő Berkó, Tamás Ladányi, and György Vaskúti)
Data mining the Two Micron All Sky Survey 2MASS) for double stars (Martin Nicholson)
777 double stars in the Two Micron All Sky Survey (2MASS) (Martin Nicholson)
On double identities, recovered pairs, and optical imposters - investigations into some neglected double stars of the Washington Double Star Catalog (Richard Harshaw)
New measures for some neglected double stars of the Washington Double Star Catalog (Richard Harshaw)
Measures of some neglected southern double stars using the superCOSMOS database (Richard Jaworski)
Pp. 96, 2004

DSSC13: Micrometric measures of double stars from 2004.0 to 2005.0 (Bob Argyle)
Micrometer measurements from 2002.97 to 2004.94 (Andreas Alzner)
Measures of double stars with a CCD camera and 35.−cm reflector from 2003.934 to 2003.942 (Ernő Berkó, Tamás Ladányi, and György Vaskúti)
Measures of neglected John Herschel southern double stars using o−line databases (Richard Jaworski)
Measures of selected John Herschel pairs between RA 0 h and 6 h using the SuperCOSMOS database (Richard Jaworski)
Suggested additional double stars to the Catalog (Richard Jaworski)
The John Herschel multiple stars HJ 2116, HJ201 and HJ202 (Richard Jaworski)
Measures of neglected John Herschel southern double stars using the SuperCOSMOS database (Richard Jaworski)
Measures of 396 neglected southern double stars (Tòfol Tobal)
Possible anonymous southern visual double stars (Tòfol Tobal)
Measures of 622 neglected northern double star RA 00h− 12h 55m (Tòfol Tobal)
Measures of double stars made with an eyepiece micrometer (Magne Tollefsen)
Common proper motion pairs from the Sloan Digital Sky Survey (John Greaves)
HJ 327AC, HJ 2002 & HJ 9001 (Richard Jaworski and Bob Argyle)
Possible additional components to double stars (Richard Jaworski)
A search for 'missing' Luyten double stars (Richard Jaworski)
Pp. 88, 2005

DSSC14: Micrometric measures of double stars from 2005.0 to 2006.0 (Bob Argyle)
Micrometer measures from 2004.94 to 2005.96 (Andreas Alzner)
Measures of double stars made with an eyepiece micrometer (Tim Leese)
2520 previously unreported double stars (Martin Nicholson & Hannah Varley)
Updated measures of neglected pairs in the Washington Double Star Catalog (Richard Harshaw)
BKO161 in place of STI 1445 (Gyorgy Vaskúti & Tamás Ladányi)
CCD measures of double stars at Palmer Divide Observatory - 2006.112 to 2006.238
(Brian D. Warner)
A modified industrial micrometer project - preliminary report (Morgan Spangle)
Some recent measures using a CCD camera (Morgan Spangle)
A search for 'missing' Luyten double stars - II (Richard Jaworski)
Measures of Luyten double stars using data from the 2MASS survey and SUPERCOSMOS
image database (Richard Jaworski)
Measurement of the positions of Milburn (MLB) pairs from Sky Surveys (Richard Jaworski)
Measures of the neglected double star HJ2302 AB using the chronometric method (Ian Coster)
Pp. 68, 2006

DSSC15: Micrometric measures of double stars from 2006.0 to 2007.0 (Bob Argyle)
Measures of double stars with a CCD camera and 25 - cm Cassegrain reflector in 2006
(Tamás Ladányi)
CCD observations of double stars at Waverley Observatory (Andrew Soon)
An analysis of errors in the measurement of visual double stars using the
Celestron Micr-Guide with an SCT and Al-Azimuth mount (Tim Napie-Munn)
Measures of 1027 neglected northern double stars RA 13h - 24h (Tòfol Tobal)
Measurement of the positions of Milburn (MLB) pairs from Sky Surveys - II (Richard Jaworski)
Some measures of double stars using the chronometric method,
an eyepiece micrometer and the ALADIN database (Ian Coster)
Candidate binary star systems in the Sloan Digital Sky Survey Data Release Five
(Martin Nicholson) Pp. 70, 2007

DSSC16: Micrometric measures of double stars in 2007 (Bob Argyle)
Micrometer measurements from 2006.21 to 2008.12 (Andreas Alzner)
Micrometric measures of double stars in 2007 (Jean - François Courtot)
Measures of double stars with a DSLR camera and 35.5-cm reflector from 2007.109 to 2007.194 (Ernő
Berkó & György Vaskúti)
SDSS Data Release 6 proper motion information (John Greaves)
A trapezium in the field of Chevalier 138 (Thom Gandet)
Measurements of Selected Southern Double Stars - 1 (Richard Jaworski)
Measures of 1024 neglected visual double stars (Tòfol Tobal & Xavier Miret)
Pp. 84, 2008

DSSC17: Micrometric measures of double stars in 2008 (Bob Argyle)
Micrometer measures of the multiple system ES 1089 (Jean-François Courtot)
Measurement of some neglected southern multiple stars in Pavo (Tim Napier-Munn & Graham Jenkinson)
Measures of double stars with a DSLR camera and 35.5-cm reflector from 2008.781 to 2008.844 (Ernő Berkó)
A sequence of algorithms for the determination of binary star orbital elements and construction of the orbit relative to the apparent ellipse (Bill Oliver)
Measurement of ten bright double stars using a Celestron Microguide eyepiece (Ian Coster)
Analysis of six neglected pairs in the (Ian Coster)
A provisional orbit for STF 333 (WDS 02592+2120) (Ian Coster)
Measures of 36 anonymous and neglected southern visual double stars (Tófol Tobal & Xavier Miret)
OAG common proper motion wide pairs survey (Xavier Miret & Tófol Tobal)
Pp. 75, 2009

DSSC18: Micrometric measures of double stars in 2009 (Bob Argyle)
Micrometer measures of double stars in 2009 (Jean-François Courtot)
Measures of double stars with a DSLR camera and 35.5-cm reflector from 2008.852 to 2008.997 (Ernő Berkó)
Measures of double stars with a DSLR camera and 35.5-cm reflector from 2009.200 to 2009.835 (Ernő Berkó)
Measurement of some neglected southern multiple stars in Dorado and Pictor (Tim Napier-Munn & Graham Jenkinson)
Investigation of two anomalies in the (Tim Napier-Munn & Graham Jenkinson)
Five new visual double stars (Abdul Ahad)
Measures of 58 neglected southern visual double stars (Tòfol Tobal)
OAG Common proper motion wide pairs survey - Part II (OAG Supplement No. 24) (Xavier Miret & Tòfol Tobal)
Pp. 67, 2010

DSSC19: Micrometric measures of northern double stars in 2010 (Bob Argyle)
Micrometer measures of wide southern double stars (Bob Argyle)
The triple visual-eclipsing system CHR 175 (Thom Gandet)
High proper motion pairs from the SPM4 Catalog (John Greaves)
Common-motion pairs and other doubles found in spectral surveys - 1. Stephenson dwarfs and PG stars (Brian Skiff)
Measurements of visually discovered double stars between 1985-2007 (György Vaskúti)
Measures of double stars with a DSLR camera and 35.5-cm reflector from 2008.852 to 2008.997 (Ernő Berkó)
Lost Chevalier pairs? (Ernő Berkó)
Three new visual double stars (Abdul Ahad)
A new double star in Cygnus? (Peter Clark)
Second European Pro-Am meeting on double stars (Bob Argyle)
OAG common proper motion wide pairs survey - Part III (X. Miret, T. Tobal, A. Bernal, M. Bernal, I. Novalbos, J. A. Santos, & N. Miret)
Pp. 73, 2011

DSSC20 Micrometric measures of double stars in 2011 (Bob Argyle)
Micrometric measures of double stars in 2011 (Jean-François Courtot)
Astrometric measurements from 2010.7898 to 2011.6113 and six probable new pairs (Guiseppe Micello)
Measures of double stars near M39 (Mike Swan)
A new common proper motion pair in Serpens (Abdul Ahad)
A companion to the pulsating variable V1162 Tauri (Abdul Ahad)
Lost Chevalier pairs - a followup (Bill Hartkopf)

Observations of Visually Discovered Double Stars 1997 - 2011 (György Vaskúti)
Measures of double stars with a DSLR camera and 35.5-cm reflector on 2010.041 (Ernő Berkó)
Common-motion pairs and other doubles found in spectral surveys - 2. HD and miscellaneous stars (Brian Skiff)
Common-motion pairs and other doubles found in spectral surveys - 3. Lowell, Kuiper, Vyssotsky and other low-mass pairs (Brian Skiff)
An uncatalogued double star discovered by Ward (Bob Argyle and Ernő Berkó)
The wide triple system 14 Ari (Bob Argyle, Brian Skiff and Robert Kerr)
Measures of 74 equatorial neglected visual double stars RA: 00h00m to 05h59m - OAG Common proper motion survey - Supplement 26 (Tòfol Tobal)
Pp. 89, 2012

DSSC21 Micrometric measures of double stars in 2012 (Bob Argyle)
Micrometric measures of double stars in 2012 (Jean-François Courtot)
Orbit and astrophysical study of 12392-4022 = B1215 (Fernando Rica Romero)
Measures for 24 pairs in Capricornus (Abdul Ahad)
Three new cpm pairs in Capricornus (Abdul Ahad)
Measures of wide double stars using a webcam (Axel Tute)
Common-motion pairs and other doubles found in spectral surveys - 4. Faint M-dwarf doubles from the Sloan Digital Sky Survey (Brian Skiff)
Common-motion pairs and other doubles found in spectral surveys - 5. Miscellaneous pairs (Brian Skiff)
Common-motion pairs and other doubles found in spectral surveys - 6. Measures for known pairs (Brian Skiff)
Twenty one wide double stars in Aquila (Giuseppe Micello)
Pp. 107, 2013

DSSC22 Micrometric measures of double stars in 2013 (Bob Argyle)
Micrometric measures of wide southern double stars in 2013 (Bob Argyle)
The system J 868 (00152+2722) - a new optical double star with orbital parameters (F. M. Rica)
A new visual binary system in Cetus (Abdul Ahad)
A new visual double star in Orion (Abdul Ahad)
Measurement of 24 southern multiple stars (Graeme Jenkinson and Tim Napier-Munn)
Common-motion pairs and other doubles found in spectral surveys: - 7. Miscellaneous new and known pairs (Brian Skiff)
Pp. 54, 2014

DSSC23 Micrometric measures of double stars in 2014 (Bob Argyle)
Micrometric measures of double stars in 2014 (Jean-François Courtot)
Orbital solution and astrophysical parameters for 09005+3225 (= HU 718) and WDS 11137+2008 AB (= STF 1517 AB) (Francisco Rica)
A new double star near Gamma Hydrae (Abdul Ahad)
Two new common proper motion doubles in Virgo (Abdul Ahad)
Measurement of nine neglected southern multiple stars (Graeme Jenkinson)
Common-motion pairs and other doubles found in spectral surveys - 8. One hundred forty new pairs found in the Orion complex (Brian Skiff)
Common-motion pairs and other doubles found in spectral surveys - 9. Survey work for 2014 (Brian Skiff)
New astrometric catalogue available from USNO (Brian Skiff)
Pp. 100, 2015

DSSC24 Micrometric measures of double stars in 2015 (Bob Argyle)
Micrometric measures of double stars in 2015 (Jean-François Courtot)
Measures of double stars at the Winer Observatory and discovery of new pairs (Andrè Debackére)
Discoveries of new pairs with the LCOGT network telescopes (T2M Faulkes Telescope North, Hawaii and T1M McDonald, Texas) (Andrè Debackére)
Five new common proper motion double stars (Abdul Ahad)
Measures of 17 southern multiple stars) (Graeme Jenkinson)
Measurement of neglected southern multiple stars - two listed pairs and a possible new pair (Graeme Jenkinson)
Measures of multiple stars in Norma (Graeme Jennkinson)
A new visual double star in Aquila (Ian Coster)
Common-motion pairs and other doubles found in spectral surveys: - 10.
Survey work for 2015 (Brian Skiff)
Pp. 92, 2016

DSSC25 Micrometric measures of double stars in 2016 (Bob Argyle)
Micrometric measures of southern double stars in 2016 (Bob Argyle)
Micrometric measures of double stars in 2016 (Jean-François Courtot)
Some 2016 measurements of wide and faint double stars (Wilfried Knapp)
Double stars measurements with an astrometric eyepiece in 2016 (Neil Webster)
Two new visual common proper motion pairs (Kasper Wierzchos)
Measures of wide double stars with a webcam - II (Axel Tute)
Common-motion pairs and other doubles found in spectral surveys: - 11.
Survey work for 2016 prior to Gaia (Brian Skiff)
Measures of double stars with robotic telescopes (A. Debackére)
Study of the double star DBR 89 (A. Debackére)
Pp. 102, 2017

DSSC26 Micrometric measures of double stars in 2017 (Bob Argyle)
Micrometric measures of visual double stars (VI list) (Marco Scardia)
Micrometric measures of double stars in 2017 (Jean-François Courtot)
An improved technique for measuring the separation of close binary stars with a filar micrometer (Grant Morris)
Astronomical Association of Queensland 2016 programme. Measurements of nine neglected southern double stars (Graeme Jenkinson)
Measurements of double stars with robotic telescopes in 2017 (André Debackére)
Double star measurements with a Meade 12mm astrometric eyepiece in 2017 (Neil Webster)
Astrometric and photometric measurements of the double star J 703 (07106+1543) (André Debackére)
2017 measurements of some wide and faint double stars (Wilfried Knapp)
Pp. 63, 2018

DSSC27 Micrometric measures of double stars in 2018 (Bob Argyle)
Measurements of double stars in 2018 Jean-François Courtot
Double star measures (2016-18) made with Reticle and Maksutov at f/30 (Rob Moseley and Martin Grahn)
Double star measurements made with a Meade 12-mm astrometric eyepiece in 2018 (Neil Webster)
Measurements of double stars with robotic telescopes in 2017-2018 (André Debackère)
Recovery of Skiff objects in Gaia DR2 (Wilfried Knapp)
Physical pairs found in Gaia DR2 (Wilfried Knapp)
Recovery of KPP objects in Gaia DR2 (Wilfried Knapp)
Photographic measurements of wide double stars (Michael Hayes)
Update on the double star J 703 (07106+1543) (André Debackère)
A serendipitous double star discovery (Stephen Westmoreland)
Blue Star Observatory measurement of twenty neglected southern multiple stars (Peter N. Culshaw, Diane Hughes, John Hughes, Des Janke & Graeme Jenkinson)
Pp. 102, 2019

DSSC28 Micrometric measures of double stars in 2019 (Bob Argyle)
Measurements of double stars in 2019 (Jean-François Courtot)
Micrometric measurements of double stars in 2019 (Andreas Alzner)
Nearby stars with evidence of orbital motion (John Greaves)
Double star measurements performed with a 12-mm astrometric eyepiece during 2019 (Neil Webster)
On the Lowell Proper Motion Survey double stars listed in Simbad but unnoted in WDS (John Greaves)
A miscellany of double stars not in WDS (John Greaves)
A new common proper motion binary in Leo (Abdul Ahad)
Catalog access and new lists of neglected doubles (Brian Mason)
Astronomical Association of Queensland 2018 programmes: Blue Star Observatory measurement of 16 neglected southern multiple stars (Peter Culshaw, Daine Hughes, John Hughes, Des Janke & Graeme Jenkinson
Observation of neglected double stars (Andre Debackére)
Pp. 64, 2020